TEMPERATURE MEASUREMENTS AND INTERNAL WAVES IN SENECA LAKE, NEW YORK

Myron H. Fliegel

Lamont-Doherty Geological Observatory

Prepared for:

Office of Naval Research
Advanced Research Projects Agency

October 1973

i AD-769227

SECURITY CLASSIFICATION OF THIS PAGE (When Data Entered)

REPORT DOCUMENTATION PAGE

READ INSTRUCTIONS BEFORE COMPLETING FORM

1. REPORT NUMBER: Technical Report #9	2. GOVT ACCESSION NO.
3. RECIPIENT'S CATALOG NUMBER	
4. TITLE (and Subtitle): Temperature Measurements and Internal Waves in Seneca Lake, New York	5. TYPE OF REPORT & PERIOD COVERED: Technical Report
6. PERFORMING ORG. REPORT NUMBER	
7. AUTHOR(s): Myron H. Fliegel	8. CONTRACT OR GRANT NUMBER(s): N00014-67-A-0108-0016
9. PERFORMING ORGANIZATION NAME AND ADDRESS: Lamont-Doherty Geological Observatory of Columbia University, Palisades, N. Y.	10. PROGRAM ELEMENT, PROJECT, TASK AREA & WORK UNIT NUMBERS: Task Number NR 307-320/1-6-69 (415)
11. CONTROLLING OFFICE NAME AND ADDRESS: Office of Naval Research and Advanced Research Projects Agency	12. REPORT DATE: October, 1973
	13. NUMBER OF PAGES: ~~143~~ 149
14. MONITORING AGENCY NAME & ADDRESS (if different from Controlling Office): Office of Naval Research and Advanced Research Projects Agency	15. SECURITY CLASS. (of this report): Unclassified
	15a. DECLASSIFICATION/DOWNGRADING SCHEDULE

16. DISTRIBUTION STATEMENT (of this Report)

Reproduction of this document in whole or in part is permitted for any purpose of the U. S. Government.

17. DISTRIBUTION STATEMENT (of the abstract entered in Block 20, if different from Report)

Reproduction of this document in whole or in part is permitted for any purpose of the U. S. Government.

18. SUPPLEMENTARY NOTES

19. KEY WORDS (Continue on reverse side if necessary and identify by block number)

Seneca Lake
internal waves
lake temperatures
lake dynamics
non-linear waves
heat budget
temperature measurements

20. ABSTRACT (Continue on reverse side if necessary and identify by block number)

Temperatures were measured near the center of Seneca Lake with thermistors and bathythermographs during four different years. Seneca Lake is a long, narrow, deep lake in the Finger Lakes region of western central New York State, with a temperature structure similar to that of many oceans. The bathythermograph records, which were used to reconstruct the annual temperature cycle of the lake, indicate that it is freely cir-

DD FORM 1 JAN 73 1473 EDITION OF 1 NOV 65 IS OBSOLETE
S/N 0102-014-6601

SECURITY CLASSIFICATION OF THIS PAGE (When Data Entered)

20
Abstract (cont.'d)

culating throughout much of the winter although its temperature is below 4°C. The annual heat budget was estimated to range between 40,000 and 47,000 cal./cm.^{2} for most years.

Thermistor chains with probes at five depths revealed large amplitude internal waves. Wave amplitudes of 25 feet were commonly seen and 50 foot amplitudes were occasionally seen. These internal waves are characterized by a general decrease in temperature at several levels for tens of hours followed by a very rapid rise that restores temperatures to earlier values within a few minutes, followed by oscillations of periods of tens of minutes lasting for several hours thereafter. The form of these waves is very similar to that of non-linear surface undular surges investigated theoretically using the Korteweg-de Vries equation and with tank models by various authors. The internal waves seen in Lake Seneca are therefore considered to be non-linear internal undular surges.

A direction of travel was determined for 12 surges seen in 1971 when two thermistor chains, 190 feet apart, were in operation. In all 12 cases, the disturbance was travelling north. Five of the surges were seen at a third chain 2.4 miles away and enabled phase velocities, which ranged from 19 to 50 cm./sec., to be determined. Wind speed and direction data were collected for 78 days in 1970 and 1971. No clear relationship between wind patterns or atmospheric pressure patterns and surges could be determined. It is concluded that the surges are generated by a resonant interaction between the winds or pressure systems and weak internal seiches already travelling through the lake.

ABSTRACT

TEMPERATURE MEASUREMENTS AND INTERNAL WAVES IN SENECA LAKE, NEW YORK

Myron Harvey Fliegel

Temperatures were measured near the center of Seneca Lake with thermistors and bathythermographs during four different years. Seneca Lake is a long, narrow, deep lake in the Finger Lakes region of western central New York state, with a temperature structure similar to that of many oceans. The bathythermograph records, which were used to reconstruct the annual temperature cycle of the lake, indicate that it is freely circulating throughout much of the winter although its temperature is below 4°C. The annual heat budget was estimated to range between 40,000 and 47,000 cal./cm.^{2} for most years.

Thermistor chains with probes at five depths revealed large amplitude internal waves. Wave amplitudes of 25 feet were commonly seen and 50 foot amplitudes were occasionally seen. These internal waves are characterized by a general decrease in temperature at several levels for tens of hours followed by a very rapid rise that restores temperatures to earlier values within a few minutes, followed by oscillations of periods of tens of minutes lasting for several hours thereafter. The form of these waves is very similar to that of non-linear surface undular surges investigated theoretically using the Korteweg-de Vries equation and with tank models by

various authors. The internal waves seen in Lake Seneca are therefore considered to be non-linear internal undular surges.

A direction of travel was determined for 12 surges seen in 1971 when two thermistor chains, 190 feet apart, were in operation. In all 12 cases, the disturbance was travelling north. Five of the surges were seen at a third chain 2.4 miles away and enabled phase velocities, which ranged from 19 to 50 cm./sec., to be determined. Wind speed and direction data were collected for 78 days in 1970 and 1971. No clear relationship between wind patterns or atmospheric pressure patterns and surges could be determined. It is concluded that the surges are generated by a resonant interaction between the winds or pressure systems and weak internal seiches already travelling through the lake.

TABLE OF CONTENTS

INTRODUCTION

Introductory remarks

During the summer of 1968, the Arctic group at Lamont-Doherty Geological Observatory installed a string of five thermistors connected to a chart recorder near the center of Seneca Lake. The initial purpose of the installation was to test instrumentation to be used in the Arctic Ocean on ice island T-3. Lake Seneca is a deep fresh-water lake with strong temperature stratification during the summer that models that of many oceans. In addition, the Naval Underwater Systems Center, Systems Measurement Branch at Dresden, New York, maintained a barge moored near the center of the lake which provided an excellent platform from which to conduct experiments. For these reasons, the excellent logistics provided by the NUSC, SMB and the short distance from Lamont (less than five hours away by automobile) it was felt that instruments could be field-tested at this location rather inexpensively before being sent to the Arctic. However, it became apparent soon after the thermistors were installed in the lake, that the temperature data obtained were very unusual and extremely interesting in themselves. Large amplitude temperature fluctuations, with periods of tens of minutes, were seen at various times on the original records. When the records were digitized at one-hour intervals and then plotted it became evident that the lake was in continual motion.

Temperature measurements were continued and expanded during the following three years. By the fall of 1971, 17 thermistors on three chains at two separate barge sites were in operation. This report presents the results obtained from the four years

of data collection on the lake.

Regional setting and water characteristics

The Finger Lakes of western central New York State lie in an area of gentle relief underlain by beds of limestone, shale and sandstone with a total thickness of 8000 feet and dipping gently to the south. These rocks are Paleozcic, the surface beds in the region being Devonian. Physiographically, Seneca Lake lies principally in the New York Limestone Belt, with only the southern end extending into the Northern Appalachian Plateau.

The deep and elongated basins of the Finger Lakes were formed from previously existing river basins by glacial erosion during the Pleistocene Epoch. Von Engeln (1961) separates the region into east and west provinces according to the preglacial drainage patterns. In the west the rivers flowed south and the glaciers followed the valleys downslope in a manner analogous to that which created the fiords of Norway. In the eastern province of which Seneca is the western-most lake, the preglacial rivers flowed north. Glaciers, entering from the north, had to flow up the river valleys which narrowed to the south. This funnelling effect enhanced the erosive powers of glaciers in the eastern province with the result that these lakes are deeper than those in the western province, Seneca and Cayuga having bottoms below sea level.

Seneca Lake, with a surface area of 67.7 square miles and a volume of 15 x 10^9 m^3 is the largest of the Finger Lakes. It is 35 miles long with a maximum width of 3.25 miles and a drainage area (including that of Keuka Lake which drains into Seneca Lake) of 707 square miles. The maximum depth is 618 feet, which is 174 feet below sea level, and the mean depth is

290 feet. The lake surface is 444 feet above sea level. Drainage is north into Lake Ontario by a devious route through the Seneca and Oswego Rivers.

Chemically, Seneca Lake belongs to the Northern Appalachian Plateau because its major inlets flow primarily through that region (Berg, 1963). Both Seneca and Cayuga Lakes have much higher concentrations of sodium and chloride than the other Finger Lakes. Berg (1963) considers the possibility that this results from discharges by salt mining operations on the shores of these lakes and dismisses this hypothesis on the basis of the volume of salt involved. Salt strata underlie all of the Finger Lakes region with a few of the purest and most extensive being commercially extracted. The Seneca and Cayuga lake basins intersect beds lower than any of the other Finger Lakes. Berg (1963) contends that impure salt beds in contact with the lakes are responsible for the abnormally high sodium and chloride concentrations.

A temperature profile taken with a bathythermograph near the southern end of the lake (J. Gorman, personal communication) showed a temperature maximum at a depth of 70 feet that was 4°F greater than the surface temperature. This implies a high concentration of salt at that depth. It was not determined whether this was due to leaching of salt from a bed or was due to discharges from a nearby commercial salt plant.

An account of the geology of the Finger Lakes region can be found in Von Engeln (1961) and an account of the general limnology of the region in Berg (1963).

DATA COLLECTION AND HANDLING

Temperature probes

Temperatures were measured using Fenwal glass probe thermistors. Thermistors possess a negative temperature coefficient of resistivity, i.e., increased temperatures produce decreased resistance. The equation relating temperature and resistance may be expressed in the form:

$$R = Ae^{\beta/T} \qquad (1)$$

with A and β constants for a particular thermistor, R the resistance in ohms and T the temperature in degrees absolute.

The probe's leads were connected to the male leads of an underwater connector and then sealed in either a brass or plastic cylinder, using a potting compound in such a way that at one end of the cylinder the temperature-sensitive part of the probe was exposed. A water-tight seal was made by connecting this to the female connector and then through cable to the recording instrument. The time constant of the thermistors used was 25 seconds.

The thermistors used had a nominal resistance of 2000 ohms at a temperature of 25°C and 5800 ohms at 0°C. Each thermistor was calibrated individually by accurately measuring the resistance of the potted thermistor and its temperature while immersed in an isothermal bath. The temperature standard was a Dymec quartz crystal thermometer which had been calibrated

against a triple-point bath. Values were determined for at least 12 different temperatures for each probe. A least-square method was used to determine the constants in equation (1) and the RMS deviation. In no case was the RMS deviation greater than 0.25 degrees centigrade and in most cases it was less than 0.05 degrees centigrade.

The recording instrument used was an Esterline Angus 12-channel Wheatstone bridge servo recorder. Each channel was sampled every fifteen seconds. A chart speed of 8 inches per hour was used. The charts were digitized and converted to temperature before analysis.

The recorder was calibrated according to the linear equation

$$R = C_0 + C_1 U \qquad (2)$$

with R the resistance in ohms, C_0 and C_1 constants and U the reading in recorder units. Resistance between about 2000 and 6000 ohms could be recorded without going off-scale. The recorder was calibrated a number of different times using a decade resistance box. A least-square method was used to determine the constants in equation (2) for each calibration. The RMS values ranged between 2.5 and 7.0 ohms for the various calibrations. Because of the non-linear relationship between temperature and resistance in the probe, a small uncertainty in the resistance will result in a larger uncertainty in temperature for temperatures near 25°C than for temperatures near 0. An RMS deviation of 7 ohms in resistance corresponds to an RMS deviation of 0.09 degrees for temperatures near 25°C and about 0.027 degrees for temperatures near 0.

Calibrations performed at various times yielded consistent values for the constant C_1, but significantly different values for the constant C_0. This implies that while the slope of resistance versus recorder reading remained stable, the instrumental zero shifted. Since at least one of the twelve channels was always shorted out with a constant resistor of known value, the value of C_0 in equation (2) could be determined for any time between calibrations.

As a further check on the reliability of the temperature data, comparisons were made with 23 BT's taken in 1969 by the personnel of the Naval Underwater Systems Center, Systems Measurement Branch at Dresden, N.Y. The RMS deviations between temperatures obtained from thermistors and from BT's ranged between 0.2 and 0.8°C for the five thermistors in use at the time. When a second set of five thermistors was emplaced 190 feet from the original string in 1971, discrepancies were noted between pairs of thermistors at the same depths (Figures 23 through 27). It was determined that the absolute temperatures obtained from the newer thermistors were in error although relative temperatures from any single thermistor were reliable.

It was decided that the difficulties of obtaining a good absolute calibration for data obtained in the field from thermistors which had shown consistently reliable calibrations in the laboratory were due to leaks in both the material of the potting compound and the conducting cable. A new set of thermistors was built, using a different potting compound and heavier cable. These thermistors were emplaced in September of 1971. Comparison with BT's showed these new thermistors to

be much more reliable. It can be seen from Figures 31, 32, 34, 36, 44, 46, 51 and 53 that pairs of thermistors at similar depths give consistent results.

Temperature profiles at both barge sites were obtained at various times during the four years of the experiment using a bathythermograph. The instrument used had a temperature range of -2 to +30°C and could record to a depth of 275 meters. A temperature versus depth profile was etched on a glass slide in the instrument as it was lowered and raised through the water. The glass slide was then removed from the instrument, inserted in a viewer and the profile was redrawn on graph paper.

Experimental set-up

The Naval Underwater Systems Center, Systems Measurement Branch (NUSC, SMB) at Dresden, has, as its primary function, the testing and calibration of transducers developed and used by the U.S. Navy. Seneca Lake was chosen as the site for this facility because of its great depth. Until 1970, tests were conducted on a facility composed of two barges, the Transducer Calibration Platform (TCP) and the WFNX-22 lighter, which were tied together and moored near the center of the lake at site 1 on the map in Figure 1

A thermistor string with five probes at depths of 25, 50, 75, 100 and 150 feet was installed in August, 1968. A steel cable with a 60-pound weight at the end was used to hold the string vertical. Each probe with its conducting cable was taped to the steel wire, commencing at the proper depth and continuing up to the surface. The support wire was tied to a cleat on the east side of the TCP and the five conducting cables

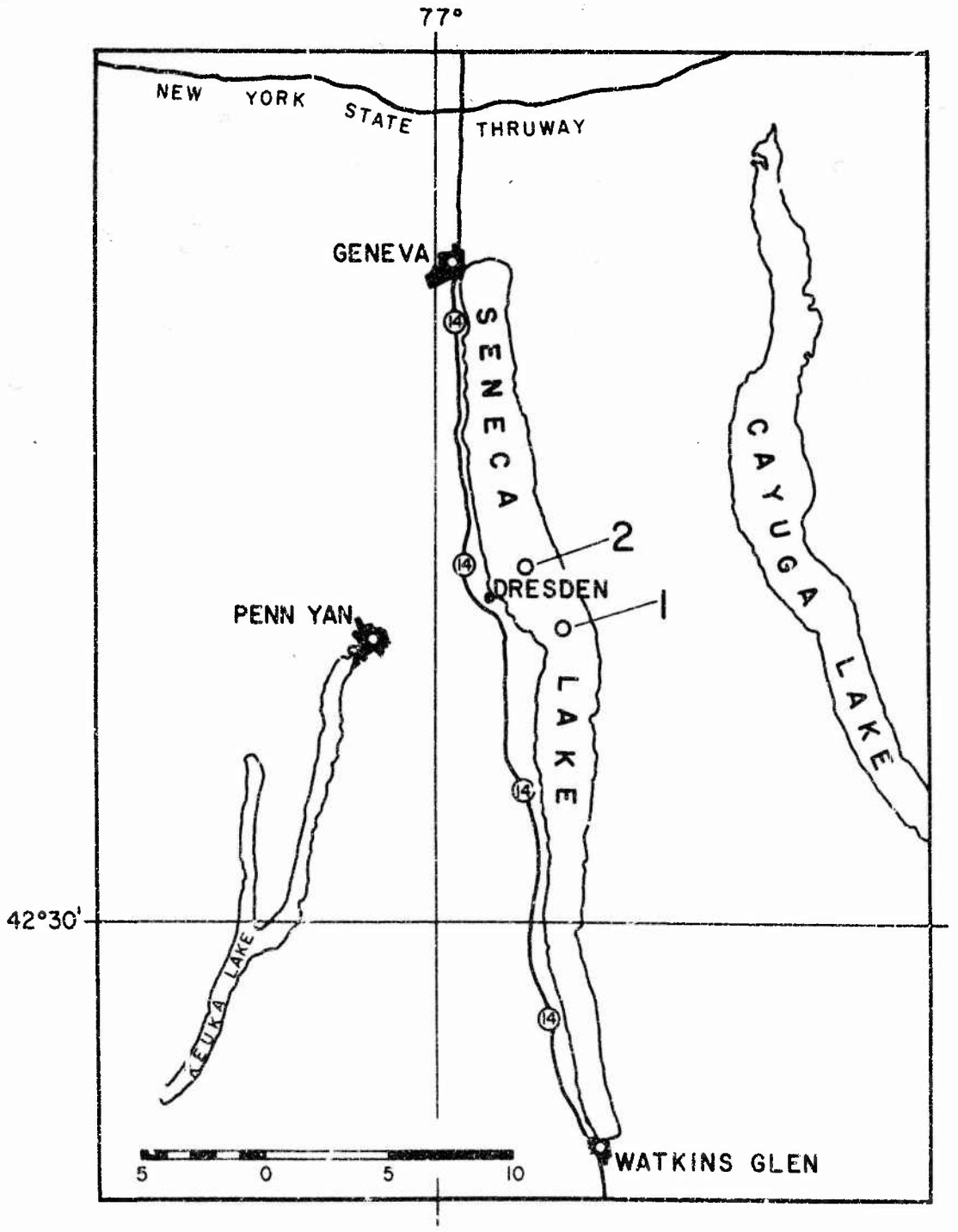

Figure 1. Location map of Seneca Lake and Facilities. No. 1 is the site of the TCP and no. 2 is the site of the SMP. The scale is in miles.

were run into the laboratory on the barge where they were connected to the recording instrument. Temperatures were continuously recorded in this manner until the beginning of February, 1969, when the instruments were removed. The thermistor chain was installed again in May, 1969 and removed in November of that year. It was installed once more in May, 1970.

In August, 1970, a new facility, the Systems Measurement Platform (SMP), was completed and the NUSC,SMB moved their base of operations to it. It is a large, floating facility composed of two barges connected by a superstructure and shaped like the letter "H". It is permanently moored at its four corners at a location near the middle of the lake about 2.4 miles north of the TCP (see map, Fig. 1). The SMP is oriented with the two hulls parallel to each other and the bows pointing north. The thermistor string was hung at the north end of the east hull and cables were run along the deck and into the laboratory which was located on the superstructure connecting the barges. In September, 1970, a second thermistor chain was installed at the south end of the east hull which is 190 feet long. Originally consisting of three probes at 25, 100 and 150 feet it was completed by the addition of two more probes at 50 and 75 feet in November. Both of these strings were removed in January, 1971, and installed again in May.

Because of the problems of obtaining absolute temperatures from the data obtained from these thermistors (especially those on the south chain) a new set was built, using a different potting compound and heavier cable that included a strength member, eliminating the necessity of an extra wire. Each thermistor

was hung separately with its own 15-pound lead weight. This much simplified the problem of checking on an individual thermistor and permitted the probes to be lowered to the proper depth much more accurately (on the old strings, the steel wire with the weight had a tendency to slip past the thermistor cables as the string was lowered into the water). These new probes were installed at the two ends of the east hull of the SMP at the same depths as the old ones, in September, 1971. In October, a sixth probe, consisting of an old thermistor connected to the new, heavier cable, was hung from the north end of the SMP at a depth of 225 feet. The installation was again disassembled and removed in December.

The instruments were removed every winter because the lake is nearly isothermal throughout most of the winter and early spring, so very little useful data would be obtained with the instruments used. During this time the thermistors and the recorder were calibrated and if it needed to be, the recorder was serviced.

In the summer of 1971, thermistors were installed at site 1 (Figure 1) with the purpose of measuring the speed of propagation of internal waves between the two sites. In July a Rustrak 2-channel temperature recorder was installed on the TCP. The thermistor depths were 50 and 100 feet. In laboratory calibrations it had become evident that the thermistors used with this recorder had considerable drift. The data obtained were therefore used only to obtain times for internal waves. This recorder was in operation for three weeks in July and

August, after which the TCP was removed from this site and the lighter was moored there. For one week in the middle of September and then from late October until December, temperatures were recorded at site 1 using a thermistor arrangement similar to that employed on the SMP. The recording instrument was an Esterline-Angus 24-point chart recorder with a scale running from 0 to 1 millivolt. The thermistors were connected through bridge circuits to provide voltage outputs.

Because the thermistors used were old ones and because of problems with the bridge circuits used (there was some crossover between channels) the data cannot be used to obtain reliable temperatures. However, internal waves can be seen and used to determine propagation velocities between the two sites.

In Figure 2 are shown all the intervals when useful data was obtained during the four years the instruments were in operation.

Data handling

In 1968 data was digitized from mid-August to the end of November. Each record had at least two time marks that had been put on by hand while the data was being recorded. From the time marks and the known chart speed, marks were put on the record at hourly intervals. Values were then read off the record for each of the five probes and for one channel shorted with a resistor. These were then punched on IBM cards and eventually put on tape. The data is continuous except for a few gaps when the paper on the recorder wasn't changed in time and for some power failures. The longest segment of no data was in mid-

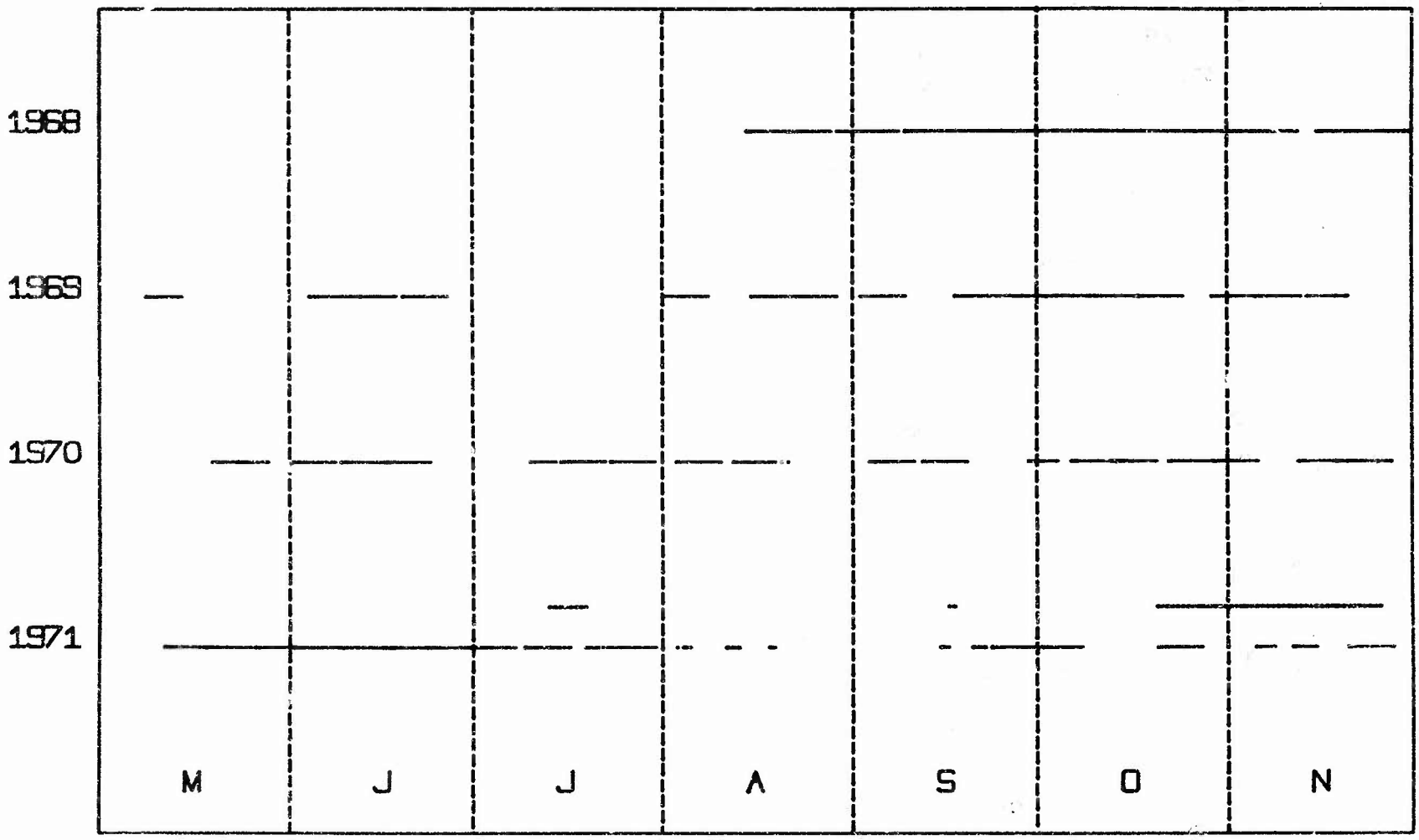

Figure 2. Times at which thermistor data was obtained during the four years of the experiment. For 1971, the lower line represents data obtained at site 2 and the upper dotted line is for data obtained at site 1. The vertical dashed lines delineate months, beginning with May.

November and amounted to 69 hours. Eight segments of data at times of short-period internal wave activity were later digitized directly from the records to IBM cards using a digitizing machine. These segments were digitized at one-minute intervals.

The 1969 data from May to November was digitized directly from the records using the digitizing machine. Rather than digitizing at any fixed time interval, a point was digitized on a channel whenever a change in slope occurred. The times of all the digitized points was later calculated by computer for all records that contained at least two time marks. Unfortunately, there are a few records from 1969 that contain only one or no time marks. Thus, while the records digitized span an interval of 188 days between May 8 and November 5, there are less than 108 days of usable data. Of the 81 days of missing data, 56 occur in May, June and July.

The data obtained during 1970 was similar to that obtained in the previous two years and was not digitized. The 1971 data was digitized only during times of short-period internal wave activity using the same method employed with the 1969 data. Because of difficulties encountered with the recorder, there were only a few short intervals of reliable data between July 30 and October 20.

Once digitized, the data was converted into resistance using equation 2 and the reading from a channel shorted by a resistor. Equation 1 was used to convert the data to temperature. The final form of the data are time series of temperature for specific depths.

GENERAL FEATURES OF THE TEMPERATURE DATA

Yearly temperature cycle

Temperature at all levels in the lake fluctuates over a large range of time scales, from climatic changes extending over centuries to turbulence with periods of only a few seconds. Two prominent time scales in Seneca Lake are the seasonal one and one due to internal surges with periods of ten minutes to a few days.

Seasonal changes in the temperature structure of lakes have been observed and discussed by many authors. A comprehensive summary and bibliography was given by Hutchison (1957). In his classification, Seneca Lake should be temperate or dimictic, circulating twice a year. In late autumn or early winter and again in mid-spring, the lake is isothermal at the temperature of maximum density, 4°C (39°F), and mixing throughout. In between, the surface water should cool (and freeze if the winter were long enough or cold enough), the lake should become stratified with a negative temperature gradient and should not mix until the surface warmed to 4°C. However, the few winter profiles obtained, although showing a weak negative temperature gradient, indicate that Seneca Lake does not conform to this simple model. Figure 3 shows the typical temperature structure of the lake at various times of the year. The curves shown were selected from the bathythermograph records.

In late autumn or early winter the lake is isothermal above 4°C (Figure 3, December 31, 1969). Later in the winter there is an inverse temperature structure (Figure 3, February 16, 1968)

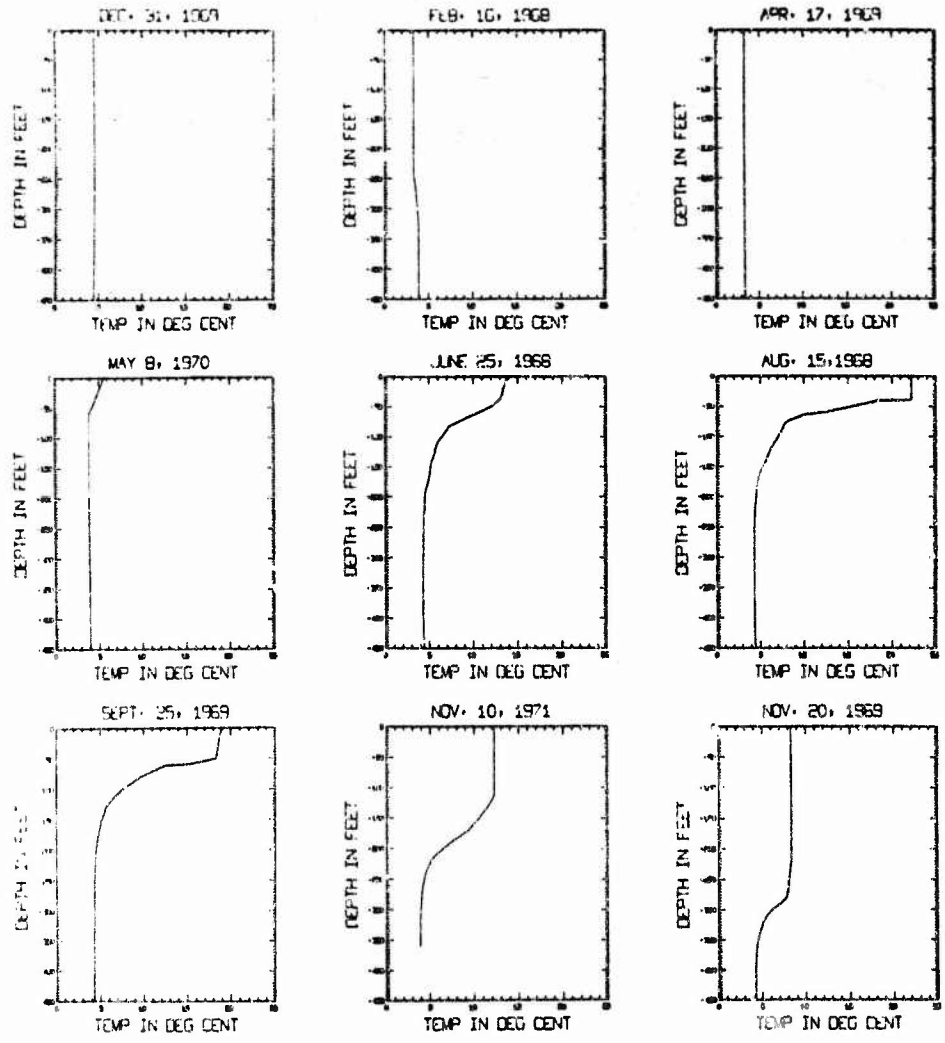

Figure 3. Vertical temperature structure of Seneca Lake at various times of the year. Bathythermographs from 1968, 1969 and 1970 were taken at barge site 1; from 1971 at barge site 2.

but the surface layer is very thick (over 200 feet) and not much colder than the deep layer. By early spring, the lake is again isothermal but below 4°C (Figure 3, April 17, 1969). This pattern of the lake becoming isothermal at a temperature above 4°C in early winter, cooling and developing two thick layers with a very small temperature difference in mid-winter and becoming isothermal below 4°C in late winter and early spring is seen in other winter profiles. Berg (1963) in discussing nearby Cayuga Lake, which is very similar to Seneca Lake, maintains that except during unusually cold winters that lake circulates completely throughout the winter. He refers to data obtained by other workers, especially Henson et al. (1961), to support his conclusion and proposes that the term warm monomictic, with a change in the definition given by Hutchinson (1957), be used to classify lakes such as Cayuga (and possibly Seneca) that have one circulation period annually.

It is uncertain whether Seneca Lake should be considered as dimictic or warm monomictic in Berg's sense. The inverse temperature structure seen in the few profiles taken in mid-winter indicate that the lake is dimictic but the stratification is weak. In any case, the lake is isothermal and freely circulating for a good part of the winter and early spring with temperatures both above and below 4°C. Seneca Lake may be a borderline case between dimictic and monomictic; some winters the inverse stratification may be strong and the lake would behave more like the classical dimictic model, while in other years the stratification might not develop at all and the lake would be monomictic.

In late April or May, the surface warms, the lake becomes stratified and a thermocline begins to develop (Figure 3, May 8, 1970). By the end of June the lake consists of two isothermal layers, a warm upper layer, the epilimnion, and a cold lower layer, the hypolimnion, separated by a strong thermocline with an approximately exponential temperature gradient (Figure 3, June 25, 1968). Throughout most of the summer, the epilimnion warms, reaching a maximum temperature in August (Figure 3, August 15, 1968) and then begins to cool (Figure 3, September 25, 1969). Throughout most of the fall the upper layer continues to cool and thicken (Figure 3, November 10, 1971 and November 20, 1969). By late December or early January, the lake is once again isothermal and mixing throughout. The lake need not be at 4°C when this occurs. Berg (1963) points out that Cayuga Lake becomes isothermal at a temperature appreciably above 4°C.

Heat budget

Another way of looking at the yearly temperature cycle in a lake is to consider the heat budget. A mean temperature can be determined for the lake at any time that the thermal structure is known. The mean temperature is the temperature that the lake would be at if it were to be completely mixed without any gain or loss of heat. To determine the mean temperature the lake is divided into a number of layers, the average temperature in each layer is calculated and multiplied by the volume of that layer. The results for all the layers are summed up and divided by the total lake volume. Birge and Juday (1914) made the first attempt to obtain mean temperatures and heat budgets in the Finger Lakes from data collected from 1910 through 1912.

They obtained temperatures in Seneca Lake on five days at the beginning of August, 1910 and on February 10 and September 1, 1911. Data was also obtained on September 5, 1914 and on August 29, 1918. Only a single temperature profile was used for each determination of a mean temperature. A mean temperature determined in this fashion will be valid only if the temperature profile used is representative of the average conditions of the whole lake and not only of the point where it was obtained. For this to be the case, either the isotherms in the lake cannot be tilted or if they are, the temperature profile must be taken at a point in the lake where "average" conditions prevail. Birge and Juday were well aware of internal waves in lakes (they called them "temperature seiches") and endeavored to make their measurements near the "center of oscillation" of the lake. They obtained their measurements near the center of Seneca Lake, assuming that the internal waves were linear, first mode oscillations with maximum amplitude at the ends of the lake and a node near the center. It will become evident from the data presented in this paper that the internal waves in Seneca Lake are non-linear and travel through the lake as a surge. Therefore, temperature profiles obtained even near the center of the lake may not represent a true picture of the complete thermal structure.

Figure 4 shows the variations in the mean temperature of the lake over the course of three different years. The data is from BT's taken at site 1 in 1968 and 1969 and site 2 in 1971 (Figure 1). Again it must be emphasized that because of the distortions of the thermal structure caused by internal

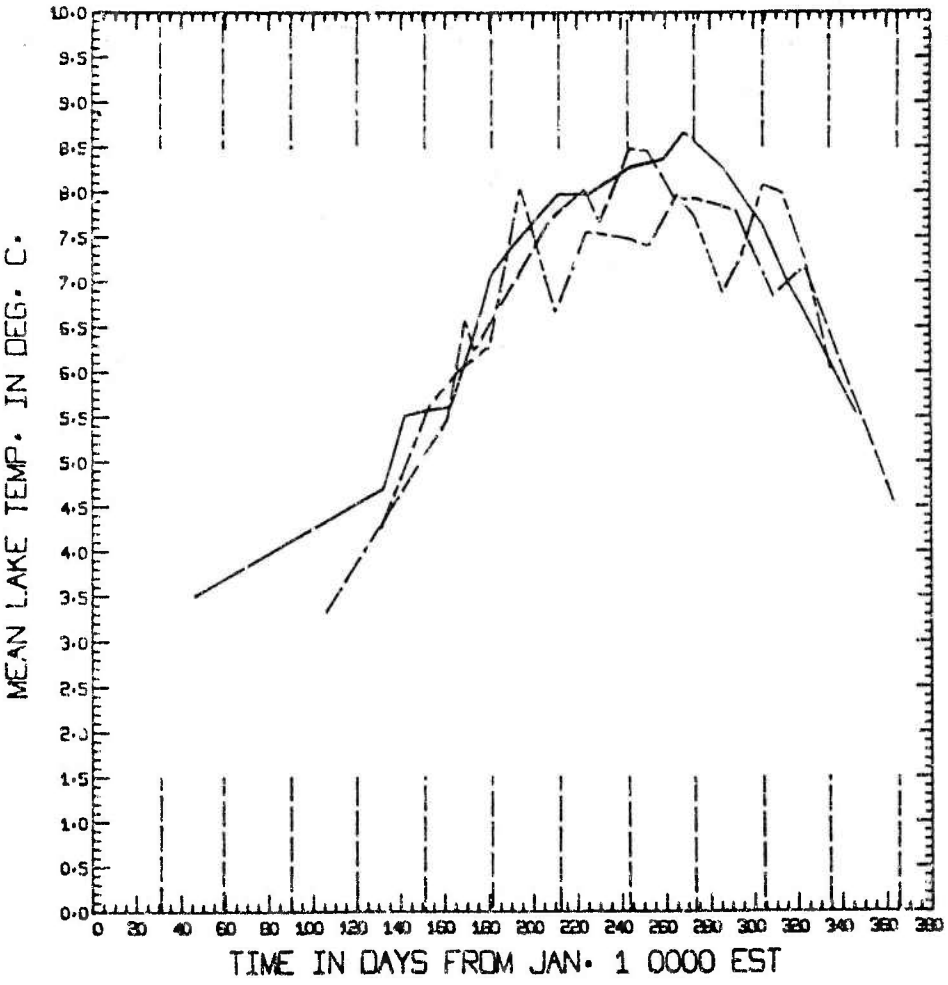

Figure 4. Mean temperature of Seneca Lake for three different years. The vertical dashed lines separate the months. The solid curve is for 1968. The dashed curve with a long line and a short space is for 1969. The dashed curve with a long and short line separated by a short space is for 1971.

surges, any individual mean temperature plotted in Figure 4 must not be considered very reliable (for example, the temperatures plotted for July 14 and 30, 1971; the former is probably too high while the latter is too low). However, the general pattern of the lake's thermal cycle can be seen in the figure. The lake warms throughout the spring and early summer, the temperature increasing most rapidly in June. By the end of July the temperature is increasing at a very moderate rate, reaching a peak in September or October. There is then a moderate decline in temperature followed by a more rapid loss of heat in November and December. This general pattern is seen for all three years plotted. The 1968 and 1969 data are very similar but the 1971 data appears erratic throughout the summer and early fall. For comparison, Birge and Juday (1922) obtained summer temperatures ranging from 7.34 to 8.27°C from data obtained during four different years.

The data shown in Figure 4 can be represented in a few other ways. If the mean temperature is multiplied by the total volume of water in the lake, the total heat content in calories above 0°C will be obtained. This is a less useful figure than the mean temperature because it cannot readily be compared with other lakes (the heat content of a large, cold lake can be greater than that of a smaller, warmer one). However, if we then divide the total heat content by the surface area of the lake, we obtain the Birgean heat budget, θ_b, which is the heat per unit surface area necessary to bring the lake from 0°C to its mean temperature. Since almost all of the heat gains and losses of the lake occur at its surface, this is a very useful

figure. Subtracting the Birgean heat budget at the time of the lowest mean temperature in winter from that of the highest in summer, results in the annual heat budget, θ_{ba}, which is the total amount of heat per unit area that must enter the lake as it warms or leave as it cools. The summer heat income, θ_{bs}, is the amount of heat per unit area that enters the lake between the time when the lake is isothermal at 4°C and when it is at its warmest. The term wind-distributed heat is sometimes used for this quantity. Because the lake is normally stratified above 4°C and solar radiation can only heat the upper few meters of water directly, most of this heat is delivered to the lower layers of the lake by mixing of water with the energy coming from the wind.

Birge and Juday (1914) obtained only one winter mean temperature for the lake, 3.39°C on February 10, 1911. From the summer temperatures measured in 1910 and 1911, they calculated two annual heat budgets and obtained 38,300 and 35,100 cal./cm.^{2} Two winter mean temperatures have been calculated from BT data; 3.52°C on February 16, 1968 and 3.34°C on April 17, 1969. Assuming the maximum summer temperature to be between 8.0 and 8.5°C and the minimum winter temperature between 3.2 and 3.5°C, the annual heat budget will be between 40,000 and 47,000 cal./cm.^{2} for most years (the results of Birge and Juday are low because the summer temperatures they used, 7.71°C in 1910 and 7.35°C in 1911 are low; they probably are not the maximum temperatures achieved by the lake during those summers). The summer heat income for Seneca Lake was estimated to be between about 35,500 and almost 40,000 cal./cm.^{2} The four values

obtained by Birge and Juday (1922) ranged from less than 30,000 to almost 39,000 cal./cm.^{2}

A simple calculation shows, that if we assume that the maximum and minimum temperatures occur six months apart, the average heat flow through the lake surface is between 220 and 255 cal./cm.^{2} per day. From Figure 4 it is seen that the heat flow through the surface is not constant but varies throughout the year. It is maximum in the spring and fall and near zero in summer and, presumably, in winter. The heat flow during any time interval between two observed mean temperatures can also be calculated. Unfortunately, because of the large error bounds of the individual temperature points, a graph of heat flow versus time would look very erratic. Instead, the curves in Figure 4 were smoothed by eye and a composite smooth curve, representing an "average" year was drawn. This curve was then used to determine heat flow for various months. The heat gain is greatest during June, exceeding 400 cal./cm.^{2} per day. This can be compared with the total solar radiation in June at the latitude of the lake which is about 600 cal./cm.^{2} per day. This value is augmented by the scattered light of the sky and is diminished whenever the sun is obscured by clouds.

The heat flow diminishes throughout the summer reaching zero in September, after which there is a heat loss that continues to grow throughout the fall. It is over 300 cal./cm.^{2} per day in November. Because of the paucity of winter data, the time and value of the maximum heat loss could not be estimated.

In addition to the total heat in the lake, the heat in

each ten-meter layer has been calculated for a number of points in 1968, 1969 and 1971. Figure 5 shows the total heat in the upper 20 meters of the lake for the three years. It can be seen that, like the total heat (Figure 4), the heat content of the upper layer increases rapidly for most of the spring and early summer, reaching a maximum in August or September. The BT records (Figure 3) show the same behavior; that most of the heat entering the lake during this period remains in the upper 20 meters. In October and early November, however, at a time when the lake as a whole is in thermal equilibrium or losing heat at a slow rate, the upper layer is rapidly losing heat. Figure 6, in which the total heat between 20 and 40 meters has been plotted, shows that some of the heat lost by the upper 20 meters has been transported down. This layer gains heat slowly throughout the spring and early summer until September or October when there is a rapid heat gain followed by a rapid heat loss. Figure 7 shows the total heat in the 40 to 70 meter layer. In this layer there is almost no heat gain from June through October. In October, the layer begins to warm, the rate becoming maximum in November, after which the layer cools. A similar pattern is seen in the bottom region of the lake. Figure 8 shows the total heat between 70 meters and the bottom of the lake at 188.4 meters.

In summary, the five sets of curves plotted in Figures 4 through 8 and the yearly BT cycle (Figure 3) illustrate the annual thermal cycle of the lake. In May and early June, the upper region of the lake warms, with an isothermal upper layer, the epilimnion, and a thermocline forming. The epilimnion is

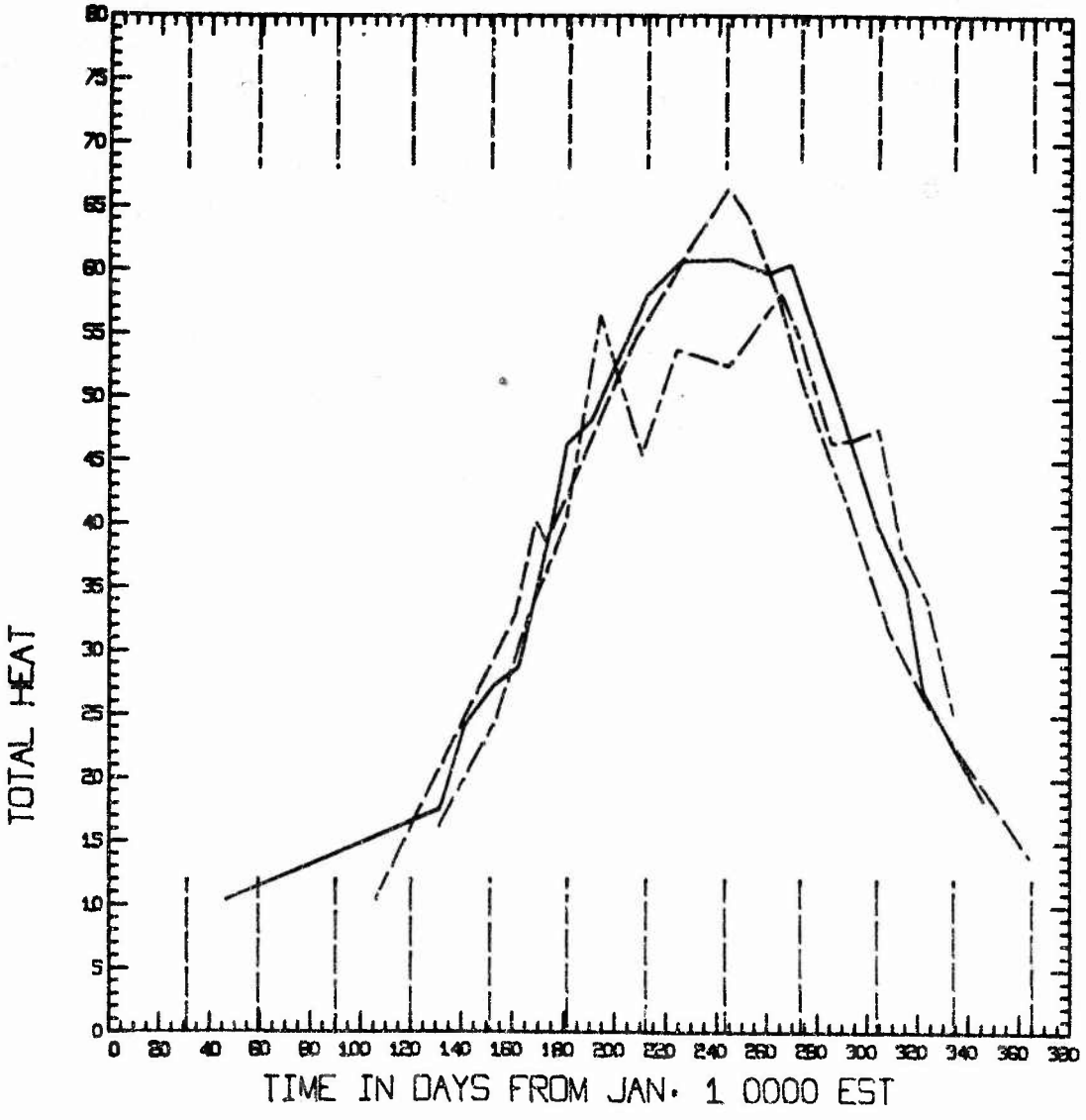

Figure 5. Total heat above 0°C between the surface and 20 meters in Seneca Lake during the years 1968, 1969 and 1971.

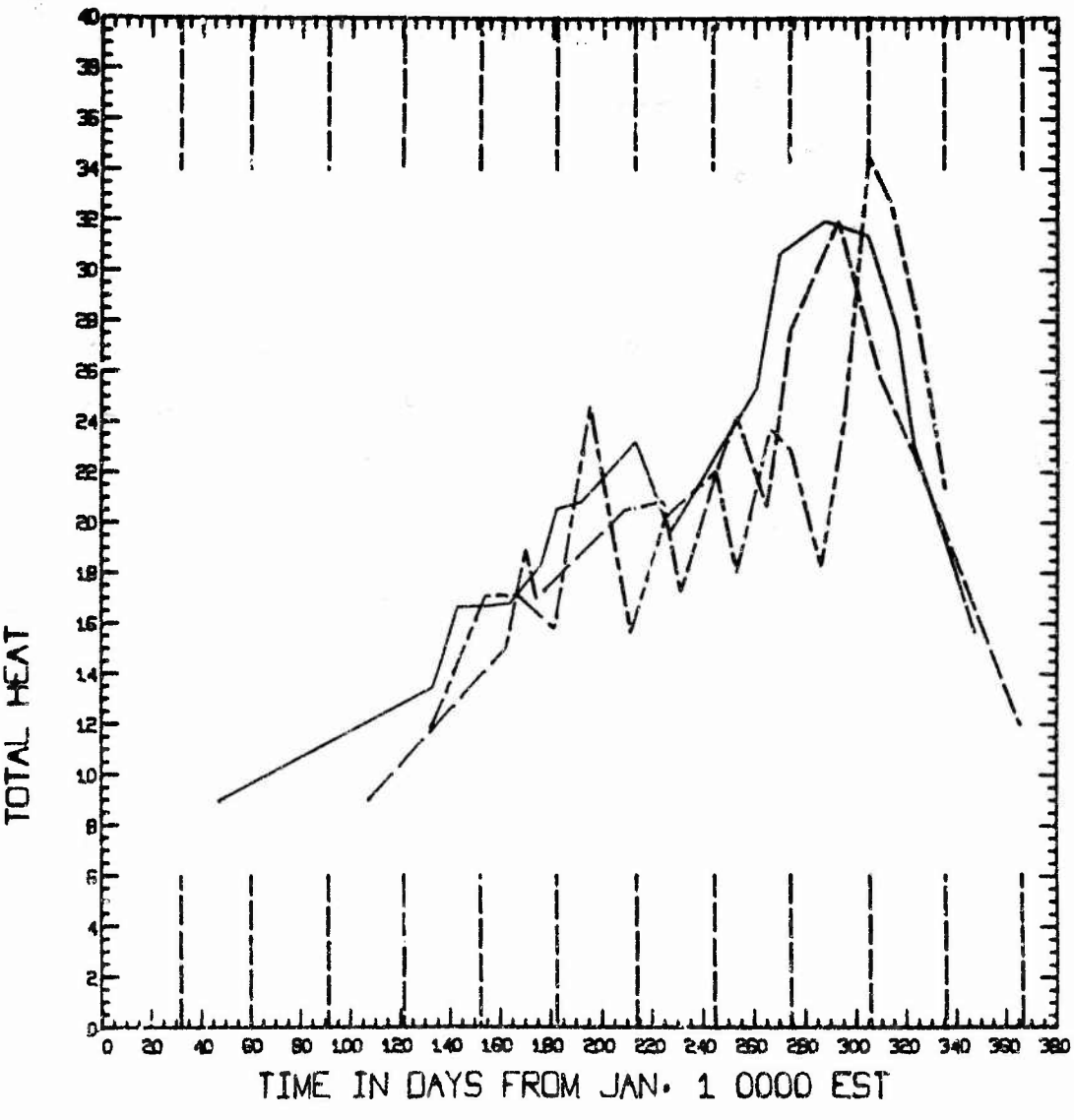

Figure 6. Total heat above 0°C between 20 and 40 meters in Seneca Lake during the years 1968, 1969 and 1971.

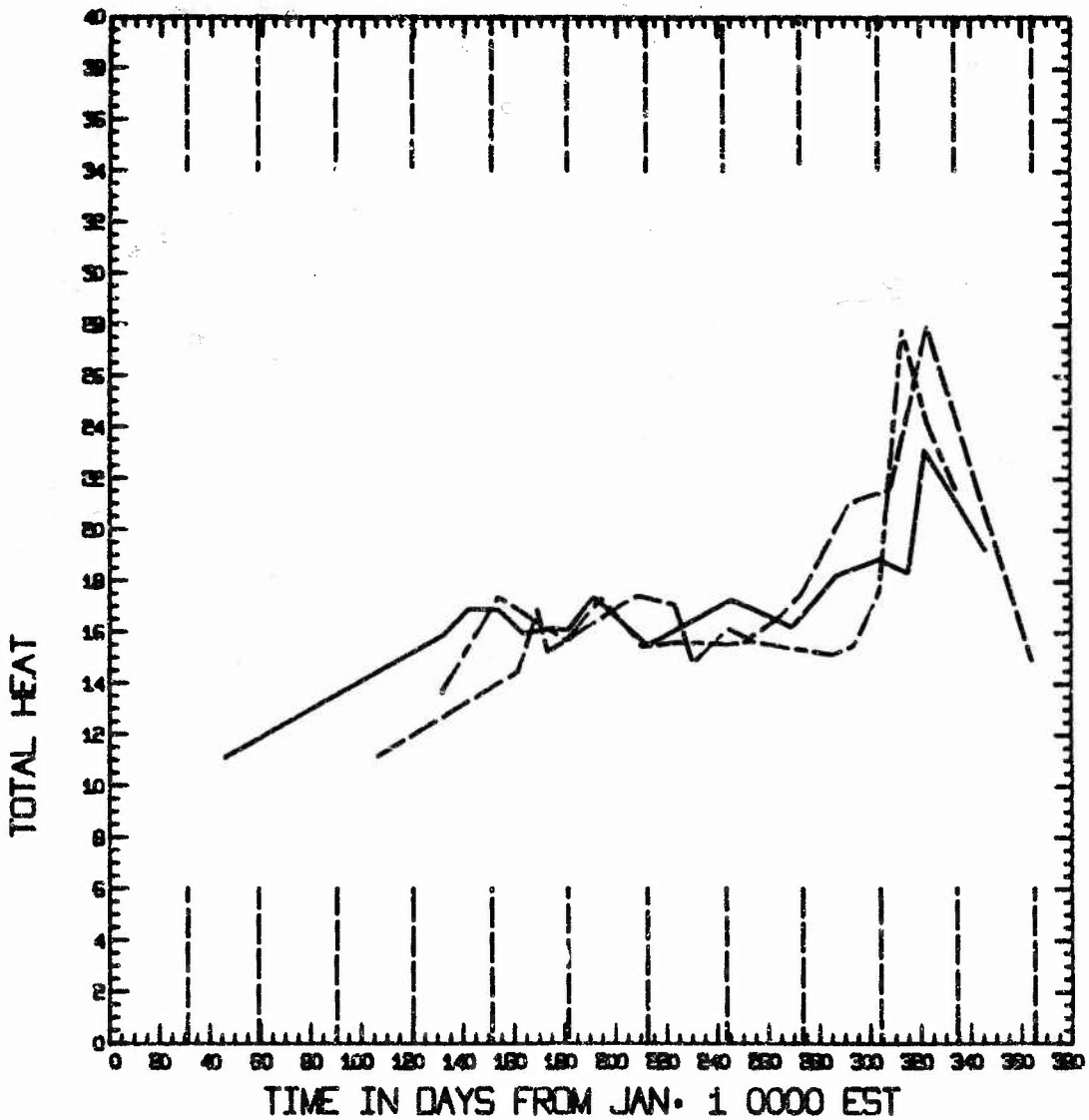

Figure 7. Total heat above 0°C between 40 and 70 meters in Seneca Lake during the years 1968, 1969 and 1971.

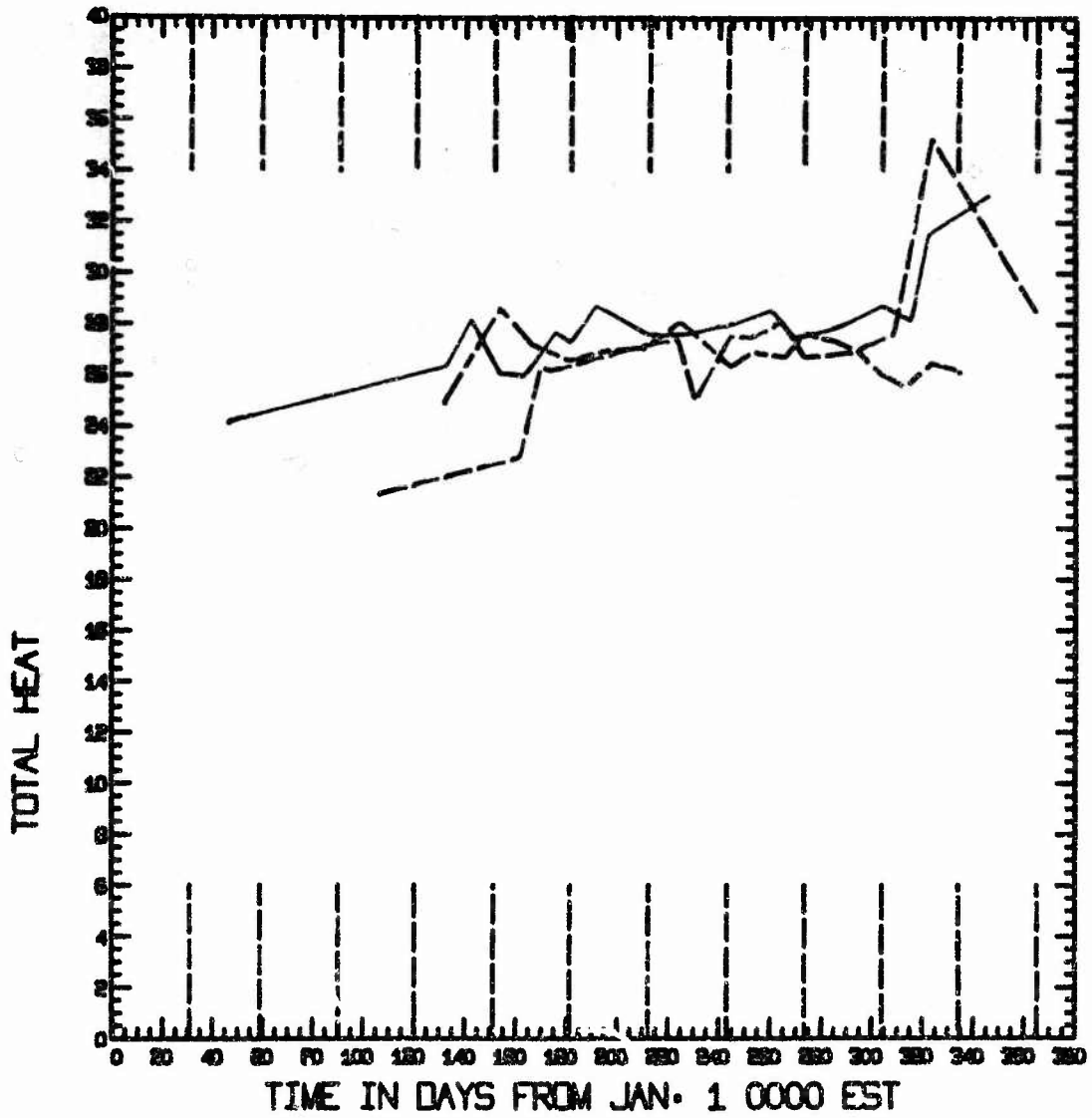

Figure 8. Total heat above 0°C between 70 meters and the deepest part of Seneca Lake (188.4 meters) during the years 1968, 1969 and 1971.

confined within the upper 20 meters while the water below 70 meters feels little of the effects of this warming of the lake. When the epilimnion is at its highest temperature, most of the heat that has been added to the lake is still confined to the upper 70 meters. It is only after the epilimnion begins to cool that it thickens, and considerable amounts of heat are carried to the lower regions of the lake.

LONG PERIOD INTERNAL WAVES

Introduction

An examination of the data reveals that, in addition to the yearly temperature cycle, there are large-scale temperature oscillations with periods of tens of hours to a few days. Figure 9 shows the temperature at five levels in the lake from mid-August to the end of November, 1968. The data was digitized at one-hour intervals. In many instances it is seen that a minimum temperature recorded at one depth is below the preceding and succeeding maximum temperatures recorded by the next deepest thermistor. Since the top four thermistors were spaced at 25-foot intervals, this implies water motions with vertical amplitud of at least 12-1/2 feet. There are a few cases where a maximum or minimum temperature moves past what would be considered the mean temperature of the thermistor above or below it, indicating 25-foot amplitudes.

The oscillations seen in Figure 9 cannot be attributed to actual changes in the thermal structure of the lake as a whole because the periods seen are much too short. It was shown in the sections on the seasonal changes in the lake and on the heat budget that these changes have time scales of weeks and months and not days. It is therefore evident that these large temperature fluctuations recorded by the thermistors cannot be due to warming and cooling of water but must be due to different water masses of fairly constant temperature moving past the thermistors, which is one of the criteria of wave motion. The motion also appears to be periodic, although the period is not

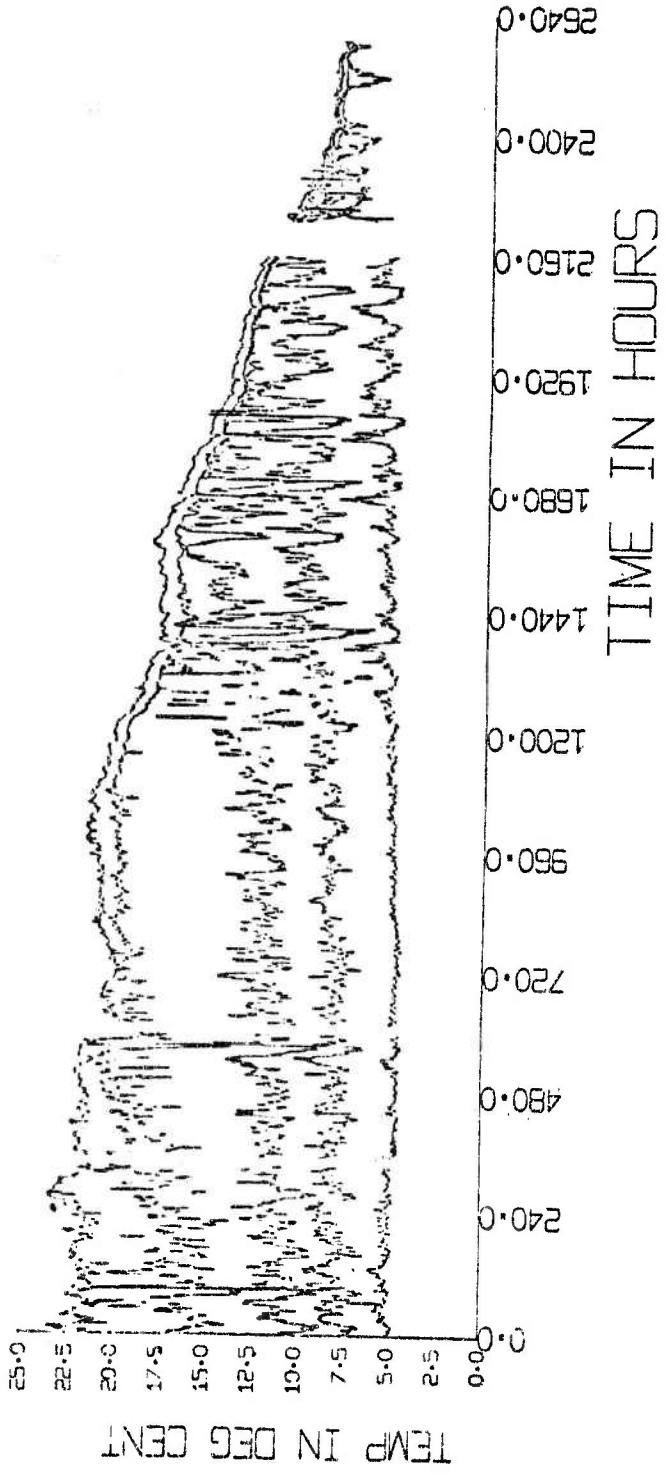

Figure 9. Temperatures recorded at five depths at barge site 1. The thermistors were at 25, 50, 75, 100 and 150 feet. The data were digitized at one hour intervals. The abscissa is in hours from August 14, 1968 at 1600 EST.

constant. Other criteria of wave motion such as energy transport cannot be determined from measurements made at one location. Because they have been seen in other lakes, it will be assumed here that the temperature oscillations are due to internal waves although some of the motion is undoubtedly turbulent.

Internal waves in narrow lakes have been well known for more than half a century. Most of the early investigators (Watson, 1904; Wedderburn, 1907, 1909, 1911 and 1912; Wedderburn and Williams, 1911) could not obtain continuous recordings of temperature and thus could only analyze internal waves with periods of hours or days. Mortimer (1953) gives a good summary of the work done up to the middle of this century, showing that the assumption of internal seiches in two-layered basins gives good agreement between theory and the observed data in most cases. (Henson (1959) gives evidence of internal seiches with a 57-hour period in nearby Cayuga Lake in August, 1951. The amplitude was over 20 meters at his station which was about 10 miles from the southern end of the lake which is 38 miles long.) It would appear that the first attempt to understand the long-period oscillations observed in Seneca Lake should be along these lines.

Theory of internal waves in a two-layered fluid

Internal waves can be defined as waves in which the maximum amplitude occurs within the fluid rather than at the surface. They are an inherent characteristic of a stratified fluid that has been disturbed from equilibrium and are analogous to surface waves (indeed, surface waves can be considered to be a special case of a two-layered fluid with the density of the

upper layer taken as equal to zero). A period equation for internal waves in a two-layered fluid can be derived (see, for example, Neumann and Pierson, 1966). In the derivation, the Coriolis force has been ignored; this is justified for narrow bodies of water like Seneca Lake.

$$w^4(\rho \coth(kh)\coth(kh')+\rho') - w^2k\rho g(\coth(kh)+\coth(kh')) + g^2k^2(\rho-\rho') = 0 \quad (3)$$

In equation 3, w is the frequency, k the wave number ($=2\pi/\lambda$, with λ the wave length), ρ the density, h the thickness of the layer and g the acceleration of gravity. The primed symbols refer to the upper layer, the unprimed to the lower.

Equation 3 is quadratic in w^2 and can easily be solved for w^2 in terms of k. However, for waves of wavelengths on the order of the length of Seneca Lake, the expressions kh and kh' will be very close to zero and the terms coth(kh) and coth(kh') can be replaced by $(kh)^{-1}$ and $(kh')^{-1}$. Making this simplification and replacing w by kc (c is the phase velocity), equation 3 can be rewritten:

$$c^4 - c^2g(h+h') + g^2hh'\left(\frac{\rho-\rho'}{\rho}\right) = 0 \quad (4)$$

This equation has two roots which are, approximately:

$$c_1^2 \approx g(h+h')$$

$$c_2^2 \approx g\frac{hh'}{h+h'}\left(1 - \frac{\rho'}{\rho}\right) \quad (5)$$

The first root is the familiar long wave velocity of a surface gravity wave. The second root corresponds to the internal wave. The phase velocity of the surface waves on Seneca Lake (whose mean depth is 290 feet) will be about 100 feet per second. For the internal waves the phase velocity will be on the order

of 1 foot per second for the summer and early fall stratification, the exact value depending on the lake structure at the time.

An expression for the ratio of the amplitudes of an internal wave at the interface and the surface can also be determined:

$$\frac{\eta}{\eta'} = -\frac{\rho(h+h')}{h(\rho-\rho')} \tag{6}$$

with η the amplitude at the interface and η' at the surface. The conditions in Seneca Lake yield values of this ratio on the order of 1000. Thus, internal waves with amplitudes of tens of feet can have associated surface waves with amplitudes of less than an inch.

The natural period of the lake, also called the seiche period, can be determined for both the surface and internal waves. The seiche period of order (or mode) n is that period that will allow exactly n/2 wavelengths to fit the length of the lake:

$$(\frac{n}{2})\lambda = L$$

with λ the wavelength and L the length of the lake. The period can be determined from:

$$T = \frac{\lambda}{c} = \frac{2L}{n}\frac{1}{c}$$

Substituting for the phase velocity, c, from equation 5, the surface and internal wave seiche periods are:

$$T_1 = \frac{2L}{n}\left[g(h+h')\right]^{-\frac{1}{2}}$$
$$T_2 = \frac{2L}{n}\left[\frac{\rho(h+h')}{ghh'(\rho-\rho')}\right]^{\frac{1}{2}} \tag{7}$$

The fundamental seiche period (n=1) is about one hour in Lake Seneca for the surface wave. For the internal wave it will be between 45 and 95 hours, depending upon the thermal structure at the time.

The non-linear characteristics of the observed long-period waves

It is at this point that the earlier investigators would measure the period of the internal waves and compare it with the period predicted from equation 7. Mortimer (1953) did this for a number of lakes and showed that the observed period was very close to the theoretical uninodal seiche period in most cases (see his Tables 1 and 2). This approach presents problems when it is attempted with the data obtained from Seneca Lake. Figure 10 shows the temperature data obtained during October 1968. This figure is similar to Figure 9 but only 30 instead of 110 days of data have been plotted with an appropriate expansion of the time axis.

It is clearly seen that there are no sinusoidal oscillations with periods of a few days. There are a number of large amplitude variations in which temperatures decline slowly for some tens of hours and then return to their former level within an hour (see arrows in Figure 10). It will be shown later in this report that this rapid increase in temperature is accompanied by large-amplitude oscillations with periods of tens of minutes (which do not appear in the data presented in Figures 9 and 10 because a digitizing interval of one hour has been used. They can, however, be seen in Figures 18 through 22)

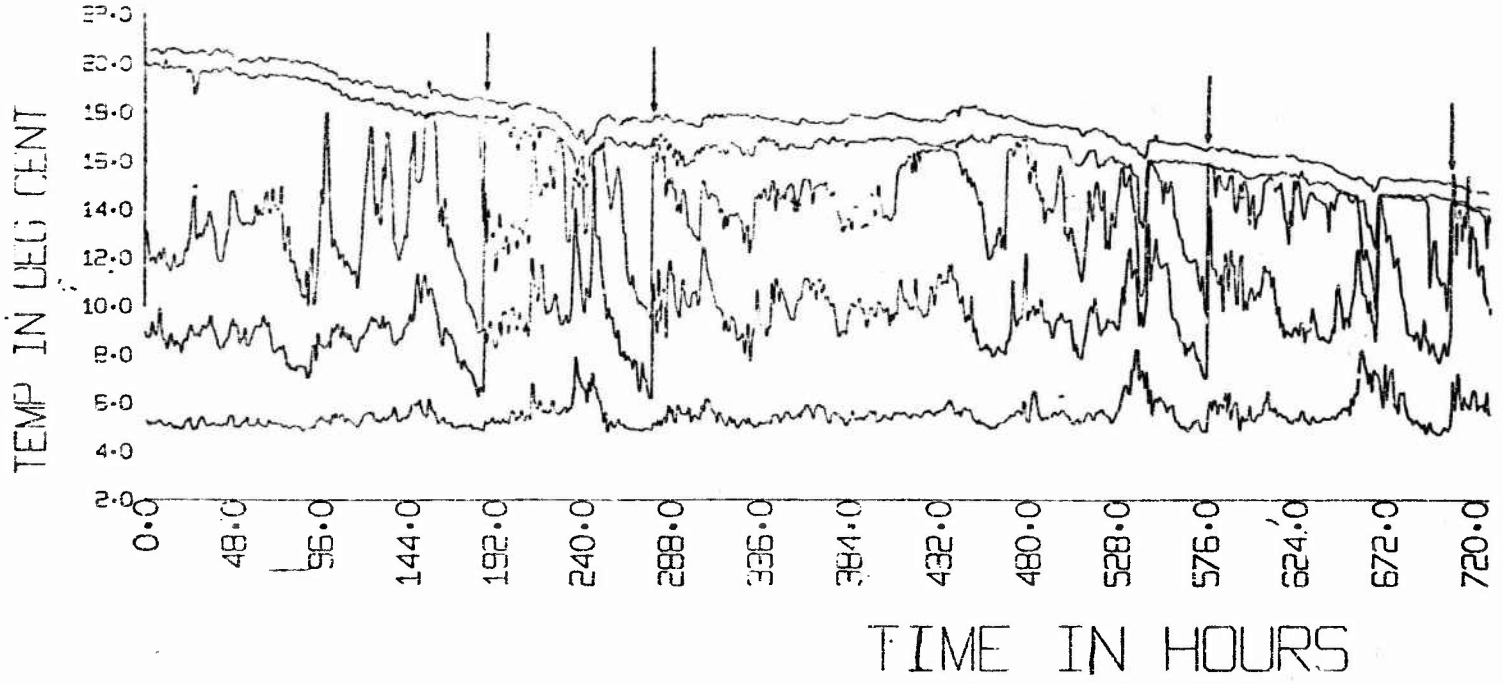

Figure 10. Temperature recorded at five depths at barge site 1. The thermistors were at 25, 50, 75, 100 and 150 feet. The data were digitized at one hour intervals. The abscissa is in hours from October 1, 1968 at 0000 EST. The arrows mark times when high frequency oscillations were recorded.

and that they are non-linear phenomena.

Before discussing non-linear waves it will be instructive to look at temperature data that has been filtered to reduce the amplitude of short-period oscillations. Figure 11 shows the 1968 and 1969 data after having been put through cosine filters with widths of 12 and 25 hours. The cosine filter reduces the energy of those oscillations with a period equal to the filter width by 50%. Periods twice the filter width are reduced only 15% while periods half the filter width are completely lost. It is seen that the filtered data looks smoother and less non-linear than the original data. The data filtered with a 12-hour filter (Figure 11, bottom) is particularly interesting. If, instead of being recorded every 15 seconds (the sampling interval of the Esterline-Angus recorder), the temperature had been recorded every three hours (for instance by lowering thermometers, a technique used before thermistors had been developed) and a smooth curve drawn between the points, the result would look very much like this graph. The filtered data also show that the upper layers of the lake cooled more rapidly in the fall of 1969 than they did in the previous fall. This was also seen in Figure 5.

Power spectra were obtained for the 1969 hourly data and are shown for the five thermistor depths in Figures 12 through 16. There are very few peaks that depart from the spectra background by more than the 90% confidence band and those that do, just barely do so and in many cases are not sharp peaks. It is apparent that there are no predominant frequencies in the data. This was also seen in Figures 9 and 10 which showed large tem-

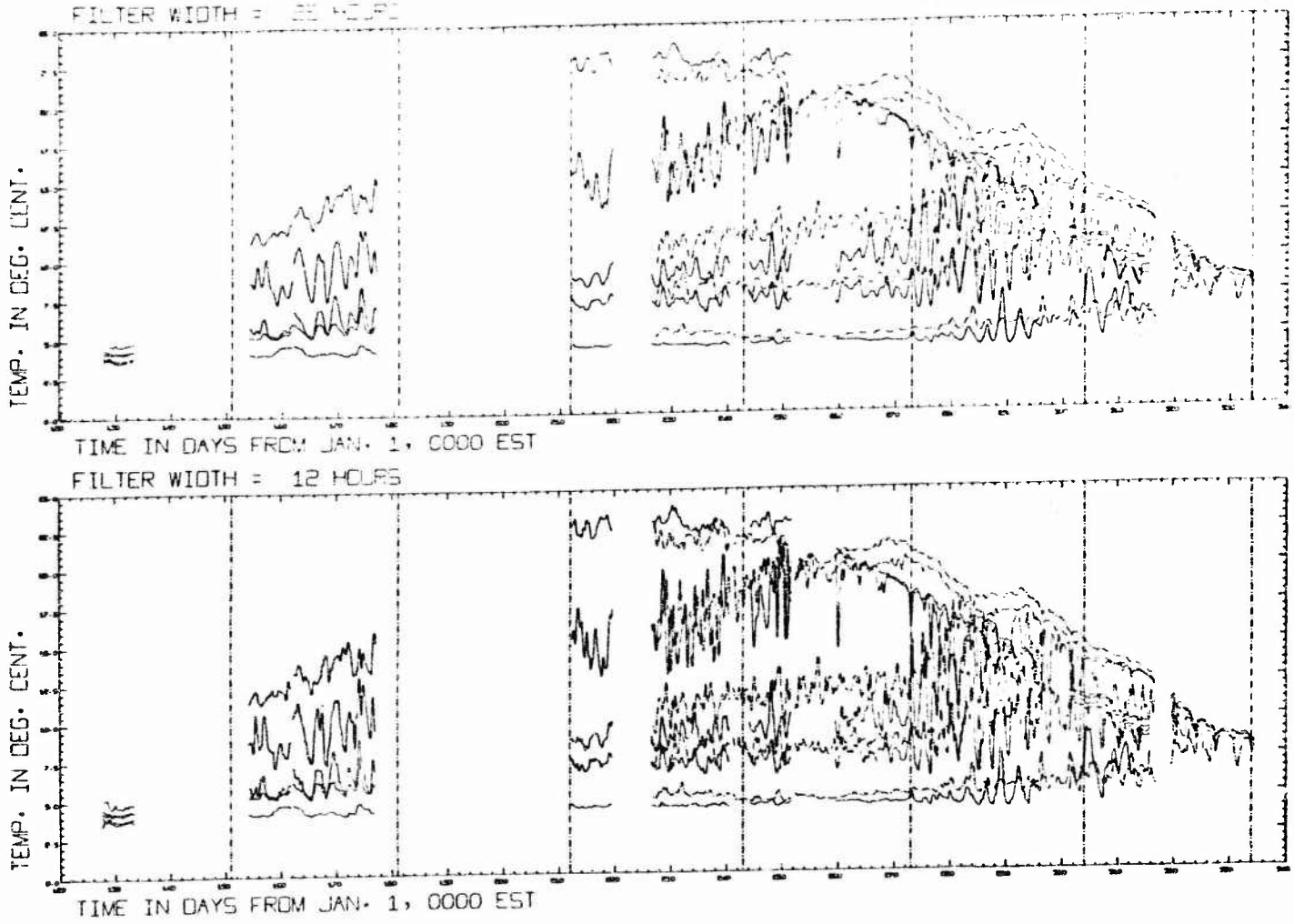

Figure 11. Filtered temperature data recorded in 1968 and 1969 at barge site 1. Depths of the thermistors are 25, 50, 75, 100 and 150 feet. The data for 1968 are drawn with a broken line, for 1969 with a solid line. The vertical broken lines delineate separate months. The first month shown is May and the figure runs through the beginning of December.

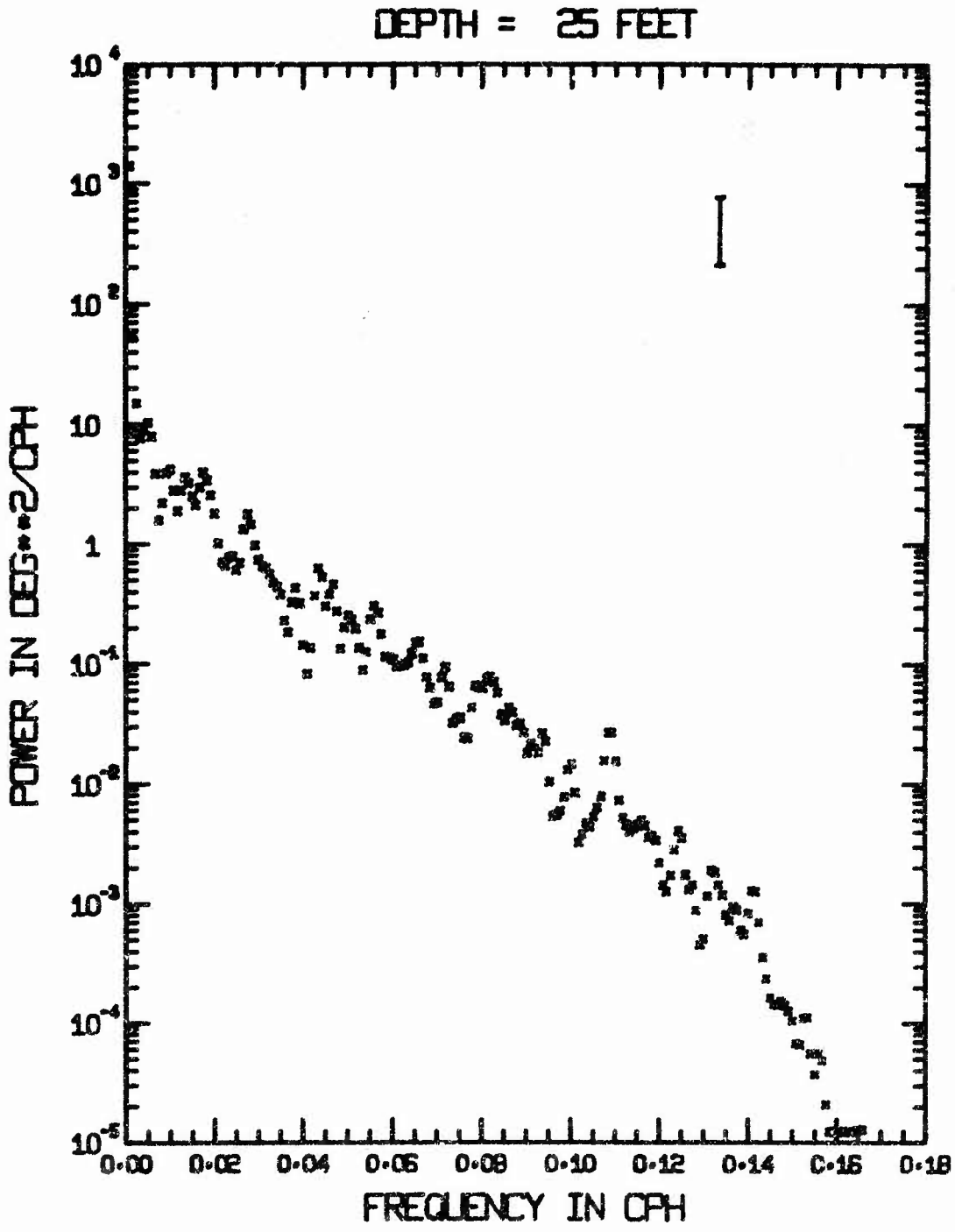

Figure 12. Power spectrum of the 1969 hourly data. The data were from May 8 to November 12. The 90% confidence band is shown in the upper right hand corner. Thermistor depth is 25 feet.

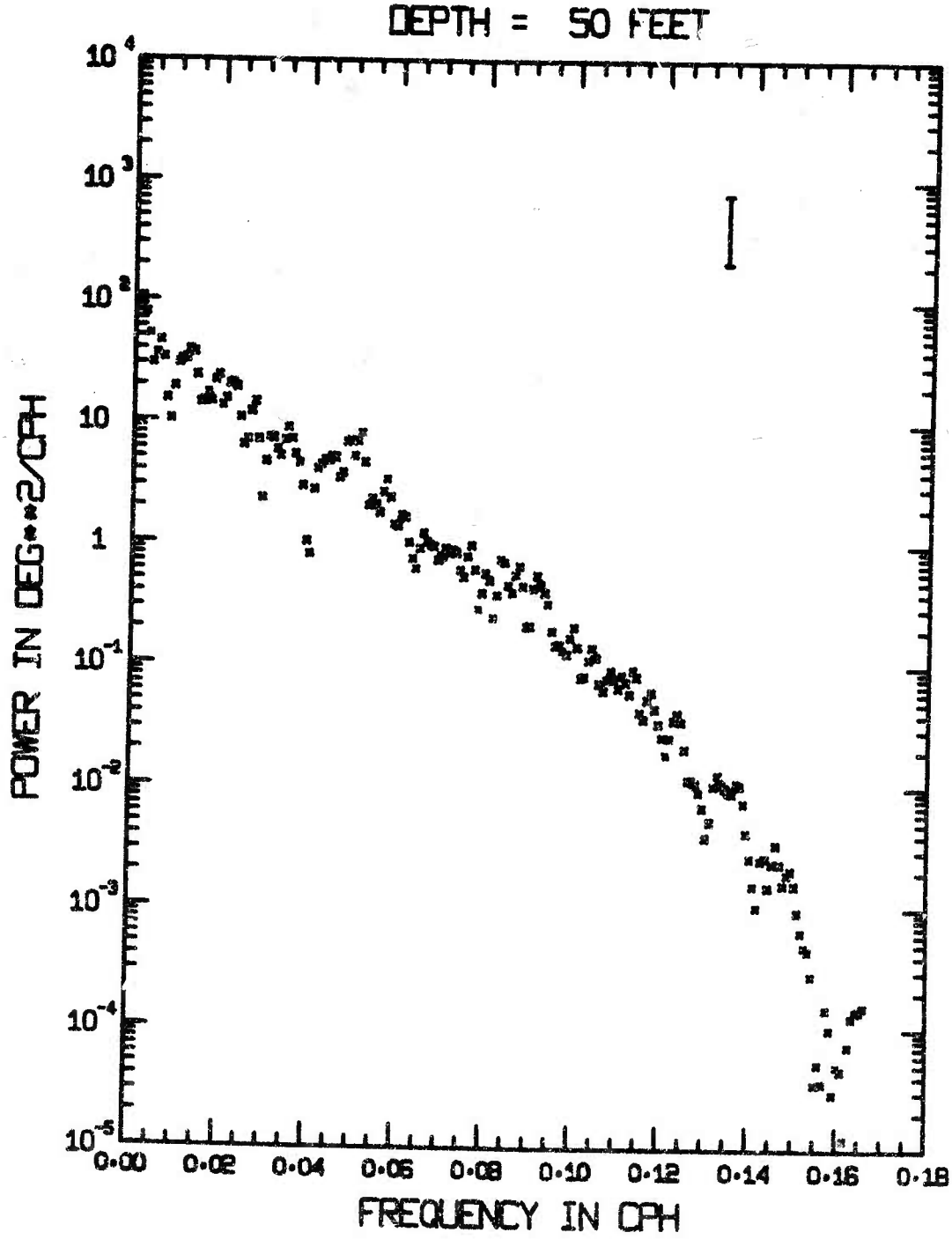

Figure 13. Similar to Figure 12. Thermistor depth is 50 feet.

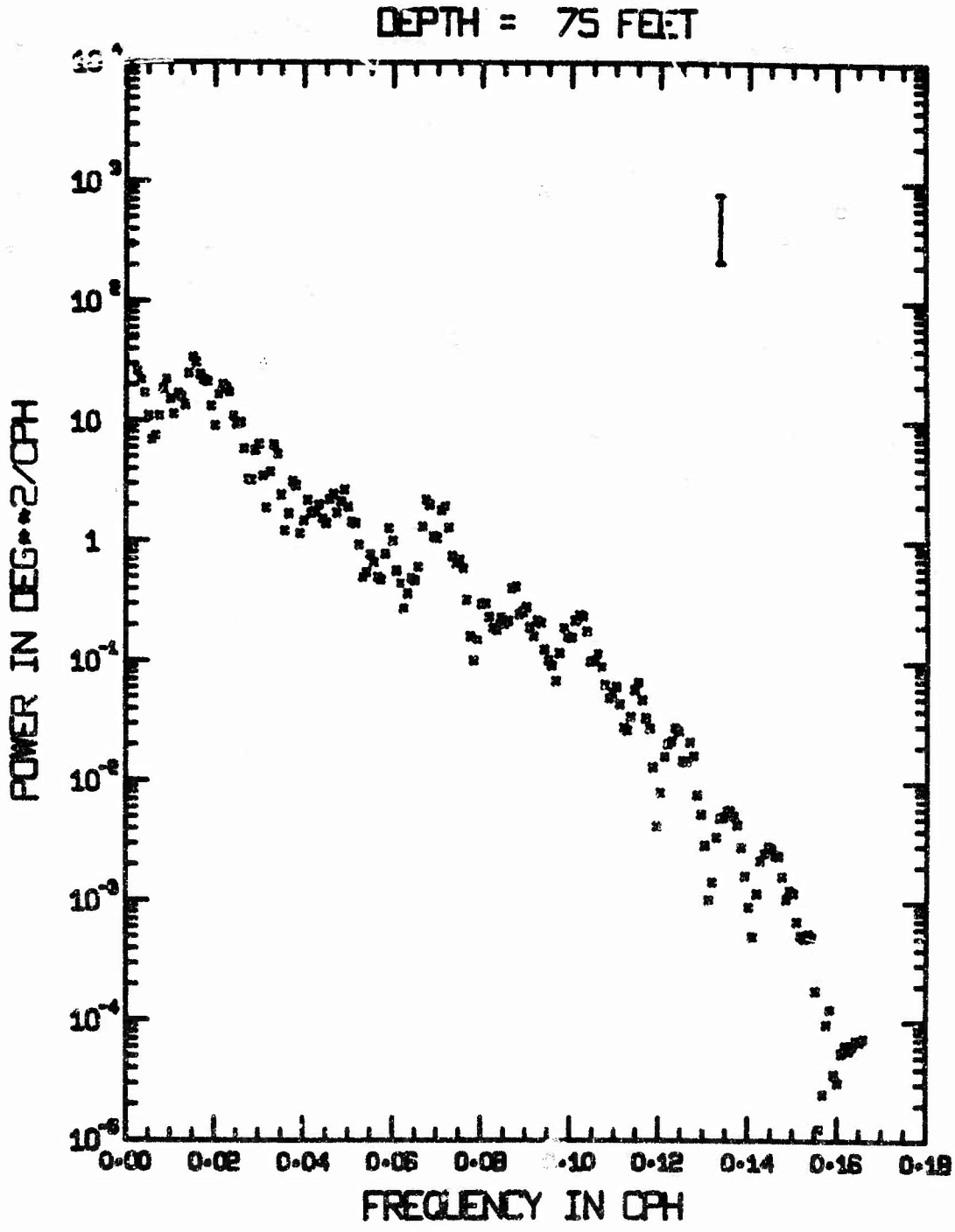

Figure 14. Similar to Figure 12. Thermistor depth is 75 feet.

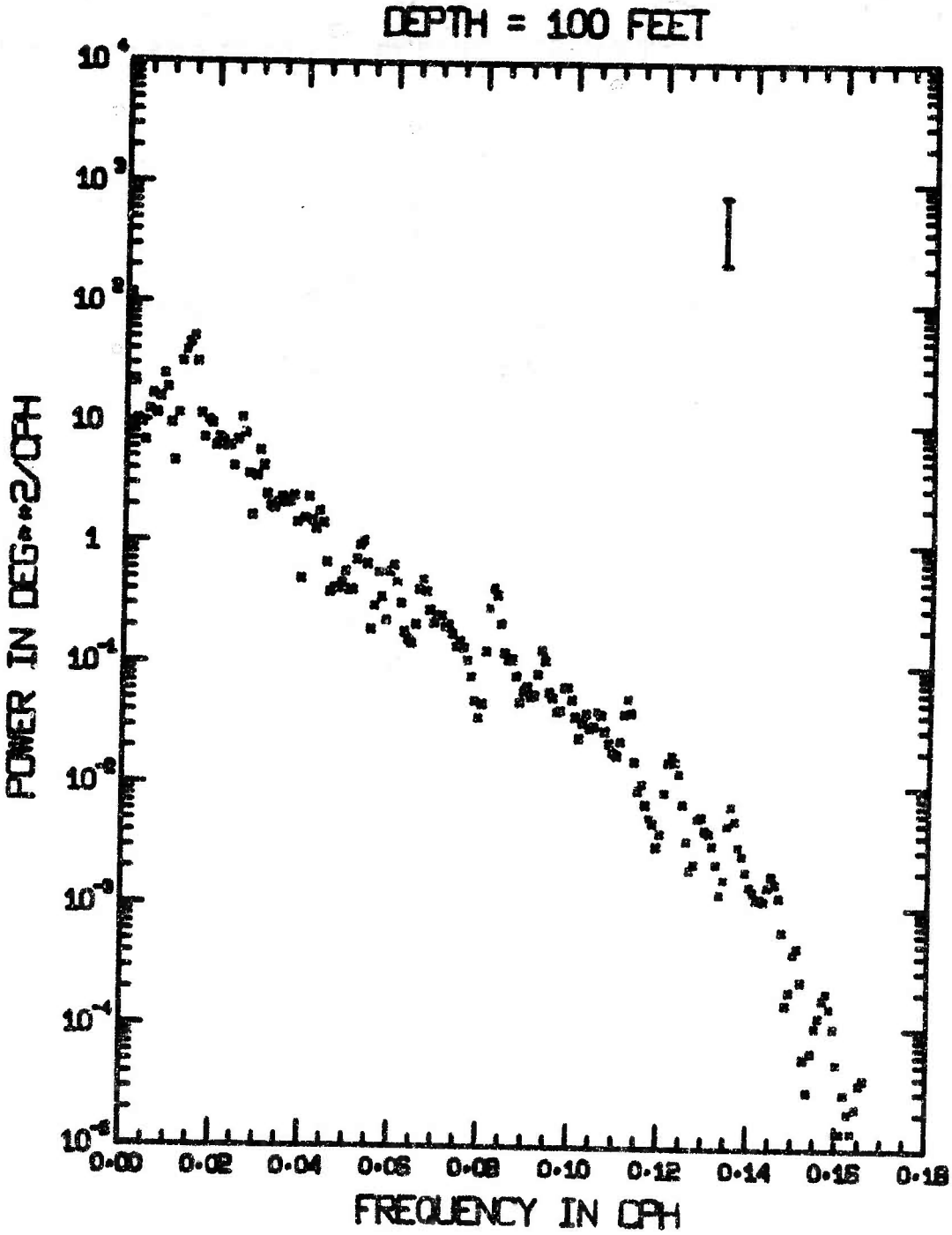

Figure 15. Similar to Figure 12. Thermistor depth is 100 feet.

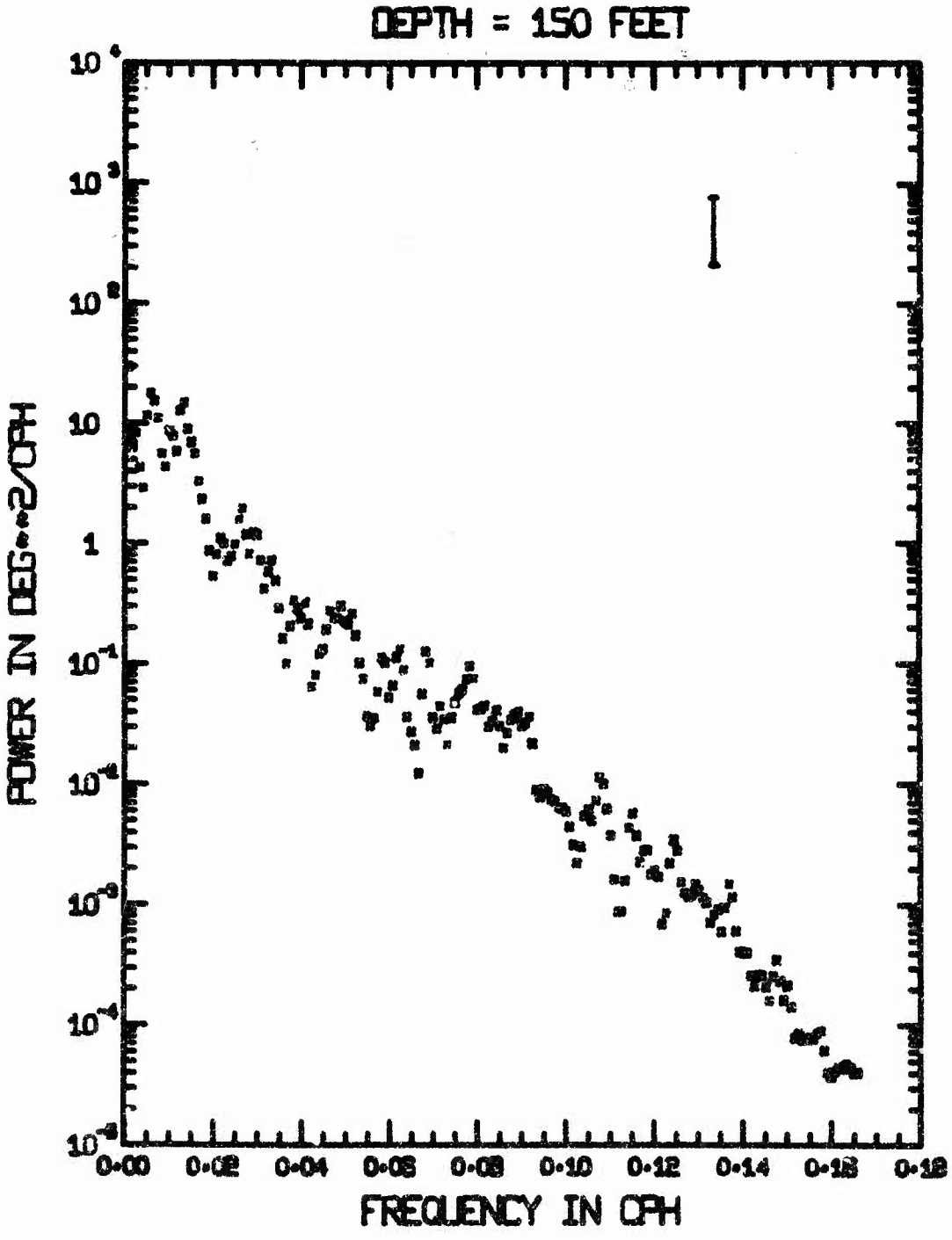

Figure 16. Similar to Figure 12. Thermistor depth is 150 feet.

perature fluctuations with periodicities of a few days but the periods were not constant and there were many other frequencies superimposed.

The most striking aspect of the large-scale temperature fluctuations seen in Figure 10 is its asymmetry. Mortimer (1955) measured temperatures in Loch Ness in 1952 by means of a thermistor chain. He found that the main internal seiche was characterized by a sudden rise in temperature similar to that seen in Seneca Lake. Thorpe (1971) made temperature observations at a different point in Loch Ness in 1970 and confirmed the asymmetrical shape of the seiche. He ruled out as a cause of the asymmetry the effects of the thermocline and its microstructure, the breaking of the seiche wave as it approaches the end of the Loch and the effects of the wind. It was his conclusion that the main cause of the asymmetry observed in Loch Ness was non-linear effects. To show this, he introduced an expansion parameter, δ (which is a function of the amplitude of the seiche motion, the length of the lake, and the thickness and densities of the two layers), which must be much less than 1 in order for linear theory to be applicable. For Loch Ness in September, he found δ to be $126\underline{a}$, with $\underline{a}$ (the half amplitude of the seiche motion whose wavelength is twice the lake length) measured in meters. He thus concluded that a non-linear approach must be used to explain the seiches observed.

A qualitative examination of the temperature data shown in Figures 9 and 10 indicates that the seiche period internal waves seen in Seneca Lake are non-linear. Amplitudes of over 25 feet are seen near the top of the thermocline when the

epilimnion is only about 50 feet thick. These waves cannot be considered small amplitude, so simple linear theory does not apply. To show this quantitatively, the expansion parameter, δ, was calculated for the typical stratification found in Seneca Lake in mid-July and mid-October. The July value was found to be over 1000$\underline{a}$ and the October value about 500$\underline{a}$, with $\underline{a}$ measured in feet. Since the amplitudes seen in Seneca Lake are usually well over ten feet, the expansion parameter will be much greater than unity and non-linear theory must be used.

Thorpe calls these non-linear seiches internal undular bores or surges. It is suggested that the term internal surges be used to describe the non-linear seiches as the term bore is usually associated with tides. Thorpe gives a solution for the case of a simple harmonic body force applied to the upper layer. He states that if parameter $\gamma = \frac{\rho_1 h_2^2}{\rho_2 h_1^2}$ is less than 1, the surge will be a rise in the level of the interface and if γ is greater than 1 it will be a fall in the level. Throughout most of the summer and fall, γ will be greater than 1 in Seneca Lake and the records do show a fall in the level of the interface (this is just what the sharp temperature rises seen in Figure 9 mean; a moving disturbance with a sharp front in which the thermocline is lower behind the front will cause a stationary thermistor to show a sharp temperature rise as the level at which the thermistor is changes from being below the thermocline to being above it as the front goes by).

Thorpe (1968A, 1968B and 1971) did model experiments using a rectangular tank filled with two fluids of different densities.

By rocking the tank (modelling a harmonic body force) or tilting it and then bringing it to rest horizontally (modelling the relaxation of a wind stress) he was able to produce surges.

A long, narrow plastic rectangular tank with inner dimensions of 6.5, 15.25 and 60.0 cm. was constructed and filled with alcohol and turpentine. The tank was tilted, causing the interface to be at an angle with the top and bottom of the tank. This might be the situation in a long narrow lake after a wind had been blowing parallel to the length of the lake for some time. The tank was then restored to the horizontal as an analogy to the lake wind dying off or reversing direction. The resulting surge can be seen in Figure 17 in which it is travelling to the left. In the figure a train of waves can also be seen to be travelling with the surge front although these might not be analogous to wave trains seen in Seneca Lake. In the tank the waves have sharp crests and broad troughs while in the lake the reverse is seen. Thorpe (1971) found similar wave trains associated with surges produced in his tank experiments. He was unable definitely to identify similar wave trains in his records of surges in Loch Ness.

The temperature records from Seneca Lake clearly show these wave trains; indeed their amplitudes in many cases are greater than that of the surge itself (see Figures 18 through 52).

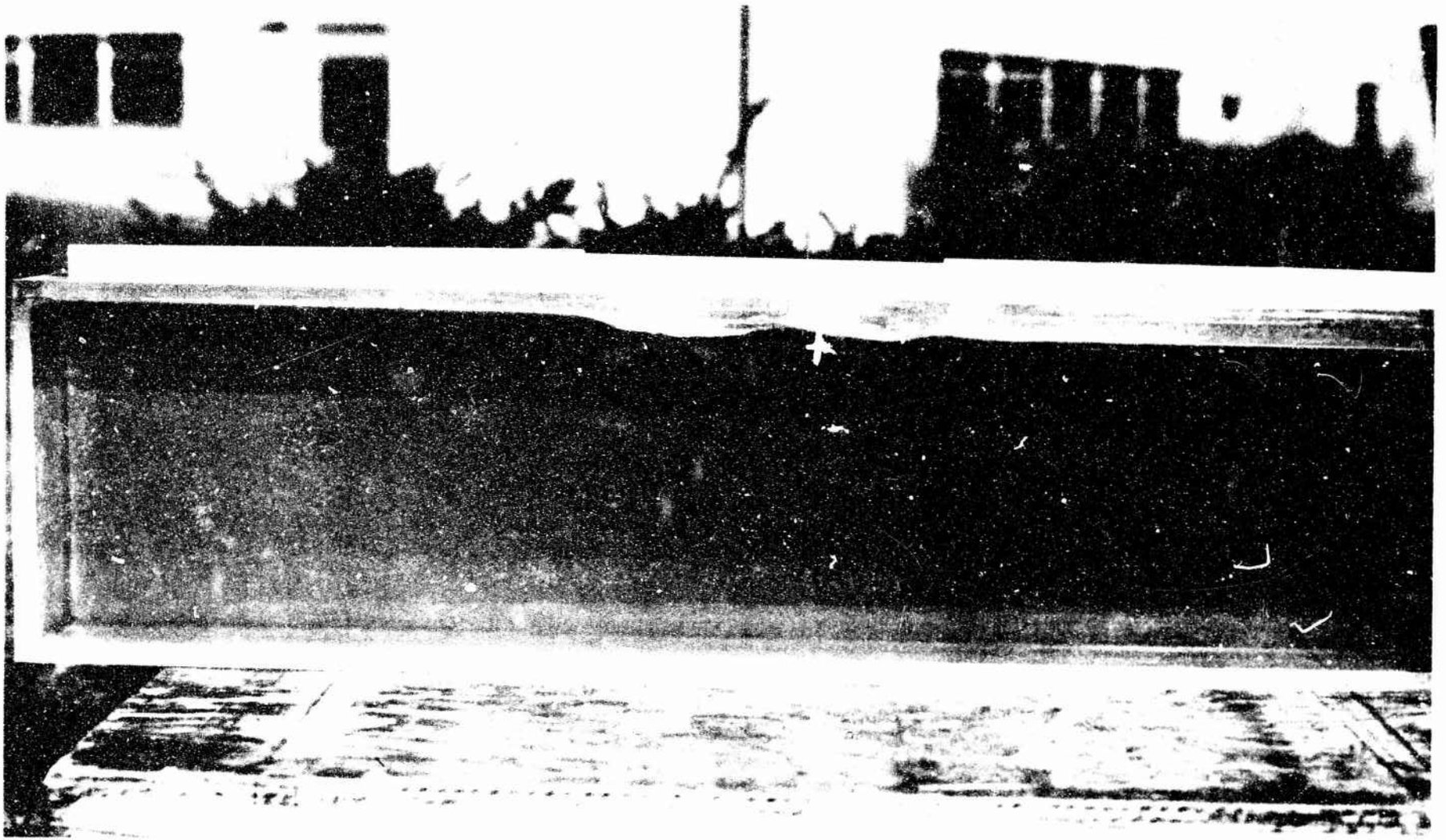

The surge is moving to the left. What appears to be a second interface about one-third of the way from the top of the tank is actually only a shadow of the true interface against the background.

SHORT-PERIOD INTERNAL WAVES

Introduction

The wave train seen travelling with the surge in the tank model in Figure 17 and similar wave trains seen by Thorpe (1971) in his model experiments are very predominant in Seneca Lake. The equations governing similar wave trains associated with non-linear surface bores have been investigated by a number of authors. Theoretical profiles of these waves are given by Peregrine (1966), Kadomstev and Karpman (1971) and Witting (1972) who also showed photographs of model experiments.

The large-amplitude oscillations with periods of tens of minutes seen in Seneca Lake are always associated with the internal surges seen in the lake. The occur only after the water temperatures have fallen to relatively low values (i.e., the thermocline has risen) and after they pass, water temperatures are higher (the thermocline has shifted downward). This can be seen in Figure 10 in which the temperature data obtained during October 1968 and digitized at one-hour intervals is shown. Four periods of large-amplitude oscillations were seen that month and the initial times are shown by arrows in the figure. Figures 18 through 22 show short-period oscillations recorded in 1969. It can be seen from these figures that although the short-period oscillations occur only in association with a long-period surge, not all of the surges have short-period wave trains associated with them (e.g., the surge seen at about 470 hours in Figure 10 and the one seen at about 5462 hours in Figure 18. The latter has one sharp spike at 50 feet; it may

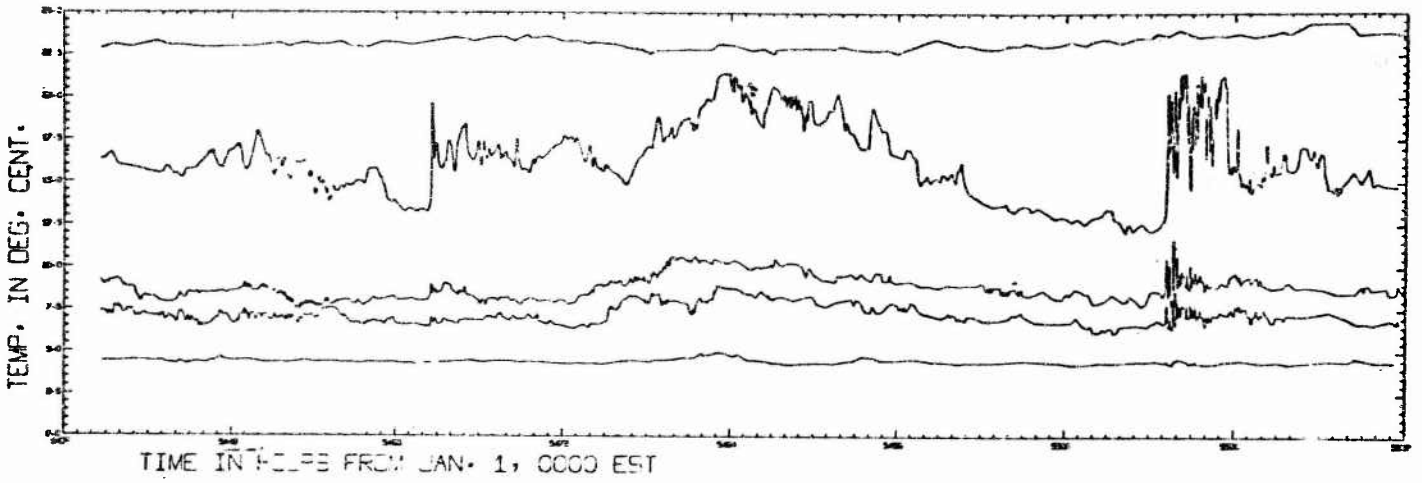

Figure 18. Temperatures recorded at five depths (25, 50, 75, 100 and 150 feet) at barge site 1 from August 15, 1969, 1200 EST to August 19, 1969, 1200 EST.

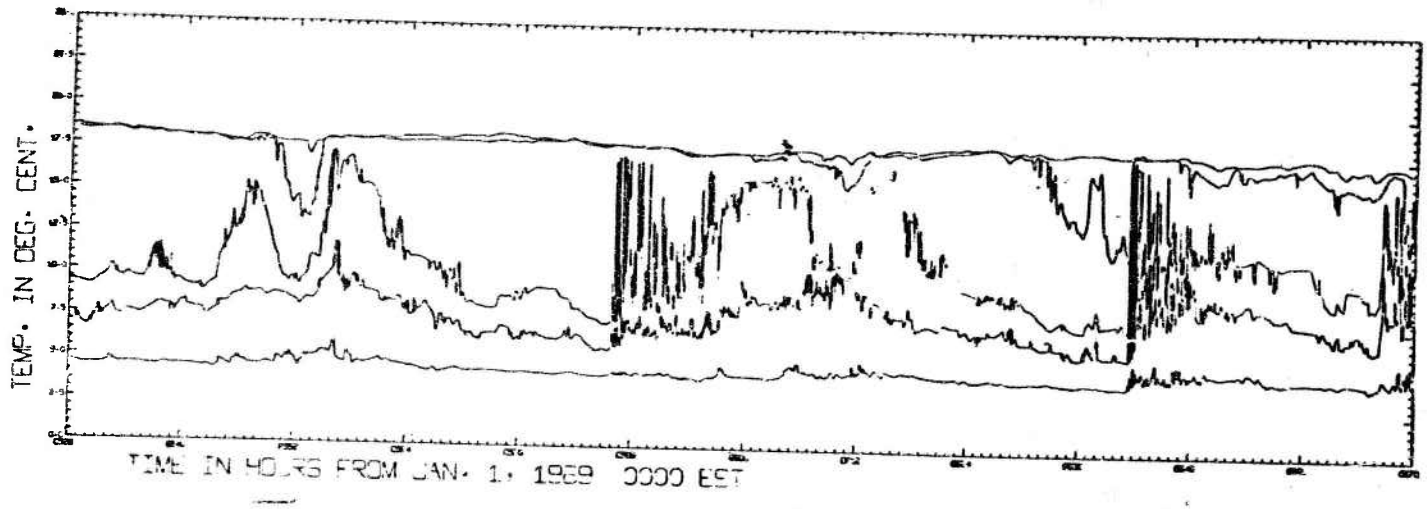

Figure 19. Similar to Figure 18. The data are from September 30, 1969, 0000 EST to October 6, 1969, 0000 EST.

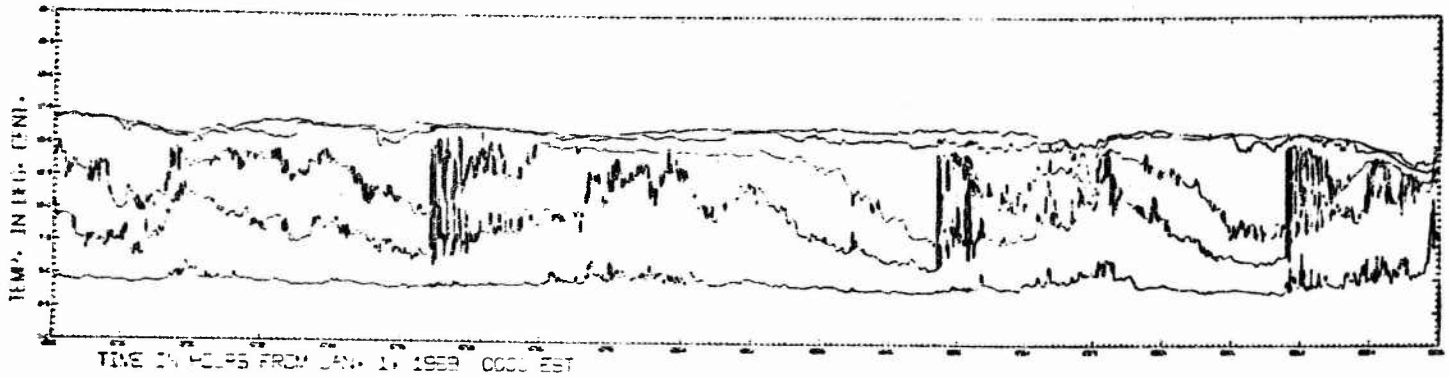

Figure 20. Similar to Figure 18. The data are from October 7, 1969, 0000 EST to October 17, 1969, 0000 EST.

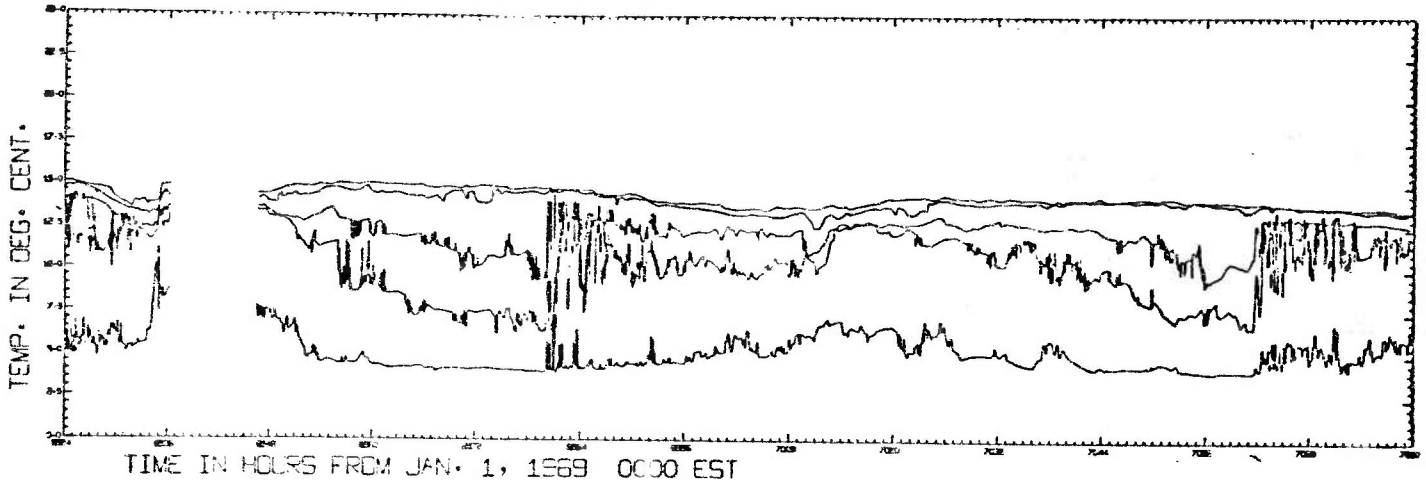

Figure 21. Similar to Figure 18. The data are from October 16, 1969, 1200 EST to October 23, 1969, 0000 EST.

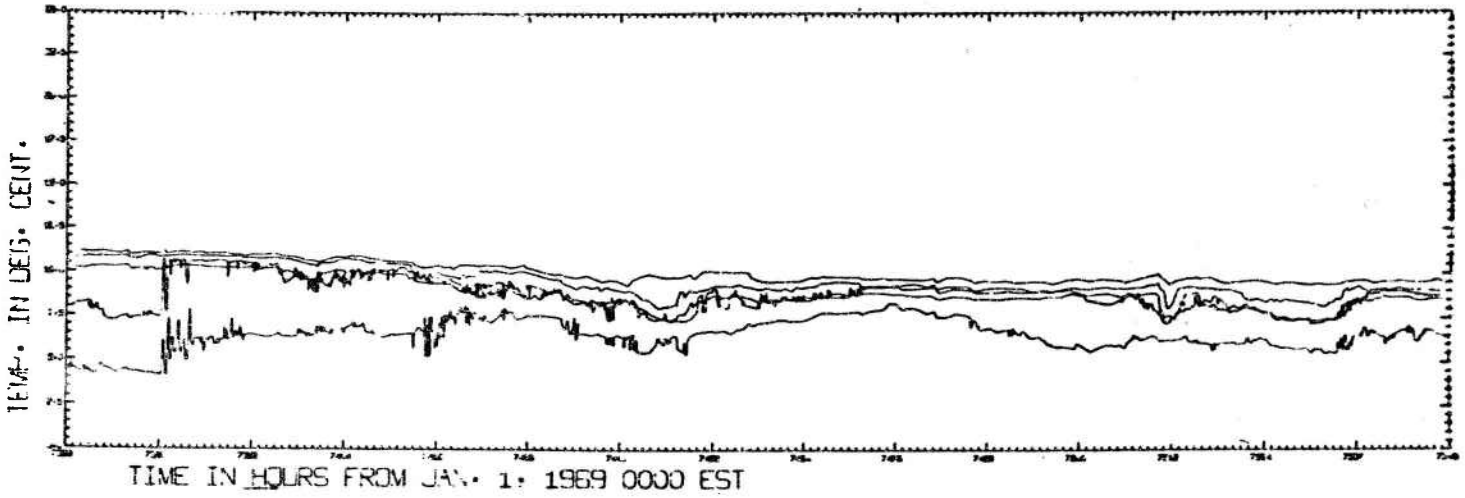

Figure 22. Similar to Figure 18. The data are from November 4, 1969, 0000 EST to November 11, 1969, 1200 EST.

be that the surge was not developed strongly enough to generate a complete wave train).

Survey of the short-period oscillations seen in Seneca Lake

Short-period oscillations were seen in all four years that thermistors were installed on the lake. The earliest recorded oscillations that could be identified with a surge occurred in early July, 1970. The oscillations were observed throughout the rest of each summer and early fall, occurring most frequently in October. In November, as the temperature differences between the epilimnion and the hypolimnion decreases, the surges and the associated wave trains become progressively more indistinct.

Figure 23 shows the surge and wave train of July 15, 1971. The data from the two 25-foot thermistors show large temperature differences due to instrumental effects (see the section on temperature probes). Part of the temperature differences can also be due to discrepancies in the depth of the thermistor pairs. Because it shows more temperature fluctuations it is probable that the 25-foot thermistor on the south string was actually somewhat deeper than its counterpart on the north string. This would partly explain the lower temperature recorded by that probe. Large-amplitude oscillations are seen only at the 50-foot level. The 25- and 75-foot levels show some activity while the lower levels show almost no temperature fluctuations. This does not necessarily mean that there was no internal wave activity at the lower levels; the water was almost isothermal below 75 feet so it would take very large amplitude waves to show any appreciable temperature changes. (This

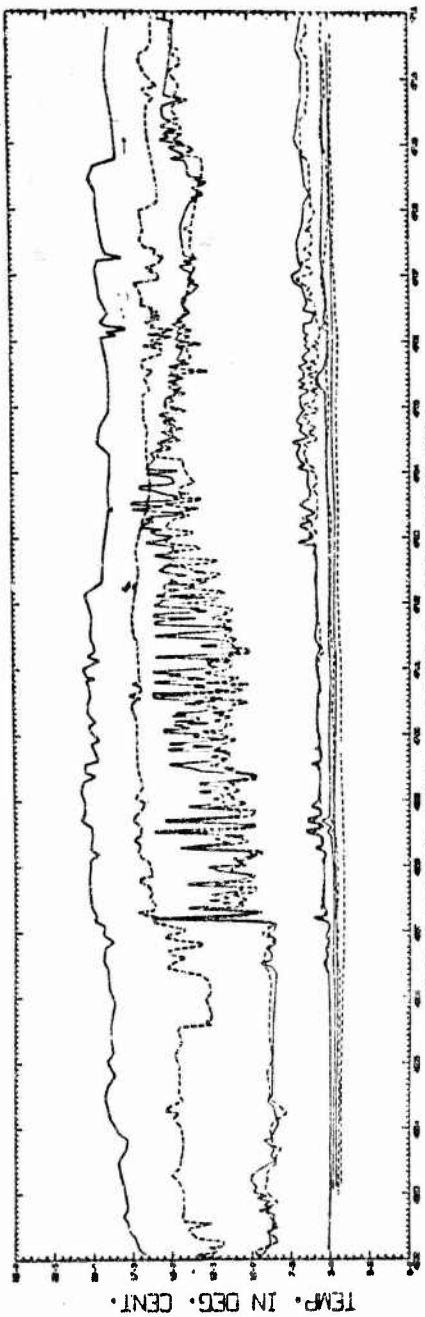

Figure 23. Temperatures recorded in 1971 at barge site 2. The thermistor depths are 25, 50, 75, 100 and 150 feet. The data from the north SMP chain is in solid line, that from the south chain in dashed line. The left margin at 4692 hours is July 15, 1971, 1200 EST.

characteristic limitation of thermistors to indicate much internal wave activity in nearly isothermal water is graphically shown in Figure 24. In this figure, the response of thermistors at five depths (25, 50, 75, 100 and 150 feet) to sinusoidal internal waves with amplitudes linearly increasing from 0 to 25 feet peak-to-peak are shown for four of the temperature structures plotted in Figure 3. The sinusoidal internal waves used to construct this figure had the same amplitude throughout the water mass. This is not the case in the lake where the maximum amplitude will be in the thermocline and amplitudes will decrease both above and below it. The response curves for the structure of September 25, 1969 show flat-topped temperature peaks at the 50-foot level. This is caused by the (hypothetical, in this case) thermistor entering the upper mixed layer and is commonly seen on the records.) There are some small-amplitude oscillations seen before the surge front passes the thermistor chains. The large-amplitude oscillations are initially very coherent between the two thermistor strings (see Table 1) and become progressively less so further from the surge front, indicating increasing turbulence. This was the general pattern seen for all of the 1971 surges analyzed for coherency and presumably is the pattern for all the surges. The amplitude at the 50-foot level is about 25 feet, peak-to-peak. The period of the initial large oscillations was about 9.4 minutes.

Figure 25 shows the surge front of July 28, 1971. There is more activity at 25 and 75 feet than during the previous surge. The beginning of the wave train is not as distinct as

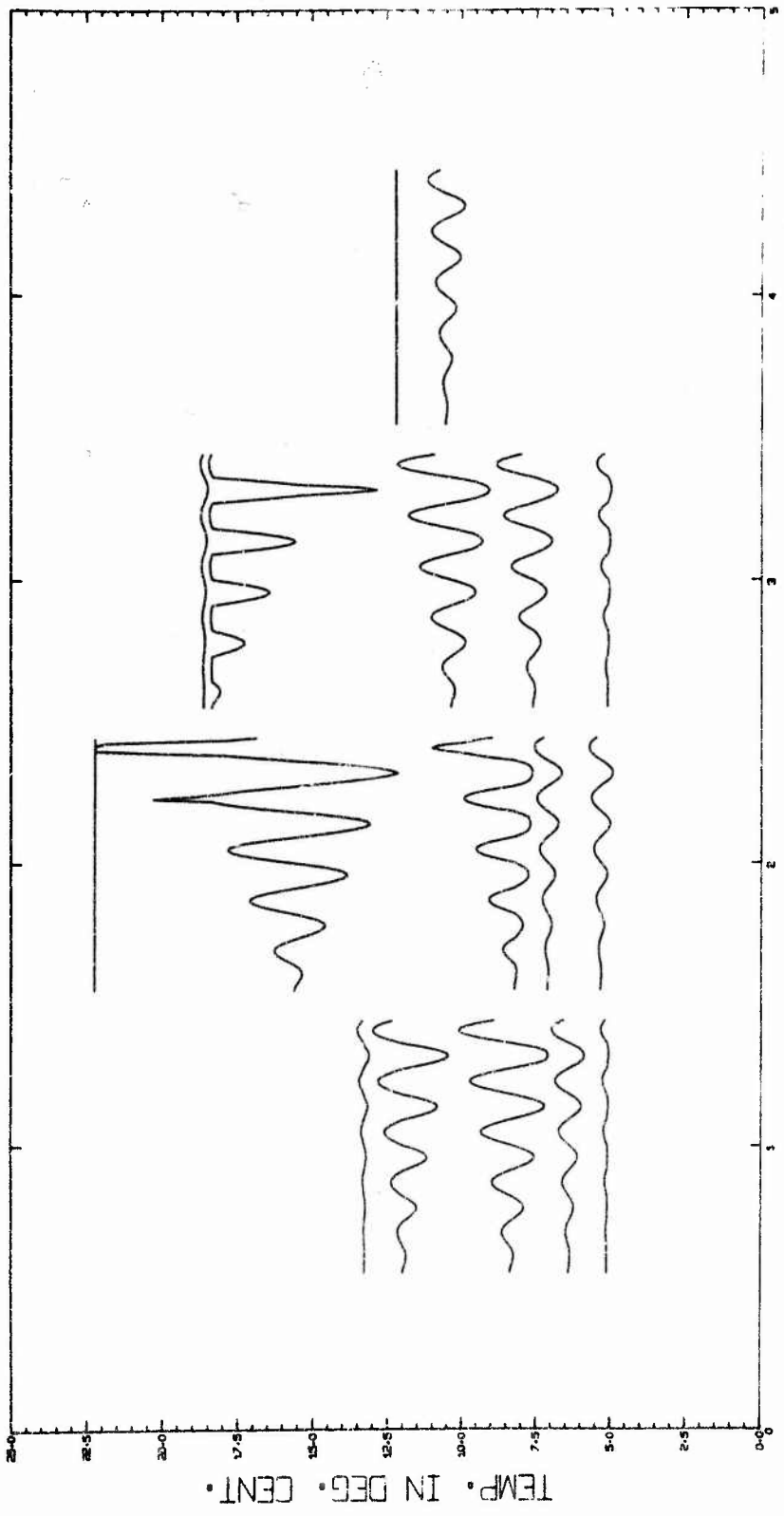

Figure 24. Thermistor response to sinusoidal internal waves. Wave amplitude is linearly increasing from 0 to 25 feet peak-to-peak. Temperature structures used are (from Fig. 3) June 25, 1968, August 15, 1968, September 25, 1969 and November 10, 1971. Thermistor depths are 25, 50, 75, 100 and 150 feet.

TABLE 1: COHERENCY BETWEEN NORTH AND SOUTH THERMISTORS IN 1971

Date	Time (EST)	Depth in feet 50	75	100	150
Jul 15	1700-1750	0.956			
	1800-1900	0.889			
	1700-1900	0.919			
	1900-0000*	0.778			
Jul 28	1200-1500	0.805	0.898		
	1500-2055	0.553	0.908		
Jul 30	2300-2355	0.937	0.964		
Aug 18	1715-2035	0.923	0.924		
	2030-0415*	0.745	0.630		
Sep 22	0400-0730	0.991	0.960	0.958	
	0730-1235	0.919	0.817	0.874	
Sep 24	1210-1800	0.783	0.866		
	1800-2100	0.952	0.950	0.935	
	2100-0140*	0.944	0.865	0.779	
Oct 3	1500-1800		0.976	0.982	
	1800-2340		0.919	0.799	
Oct 6	0800-1100	0.985	0.980	0.975	
	1100-1400	0.840	0.907	0.897	
	1400-1835		0.743	0.838	
Oct 23	1540-1650		0.991	0.986	
	1650-1800		0.978	0.987	0.975
	1500-1900		0.989	0.987	0.952
	1900-0250*		0.904	0.921	
Oct 27	1300-1700	0.958	0.976	0.974	0.916
	1700-2020		0.801	0.914	0.911
Nov 12	1620-2020		0.953	0.989	0.987
	2000-2350			0.795	0.948
Nov 22	0210-0700				0.456
	0700-0900				0.928
	0900-1550				0.847

*of the following day

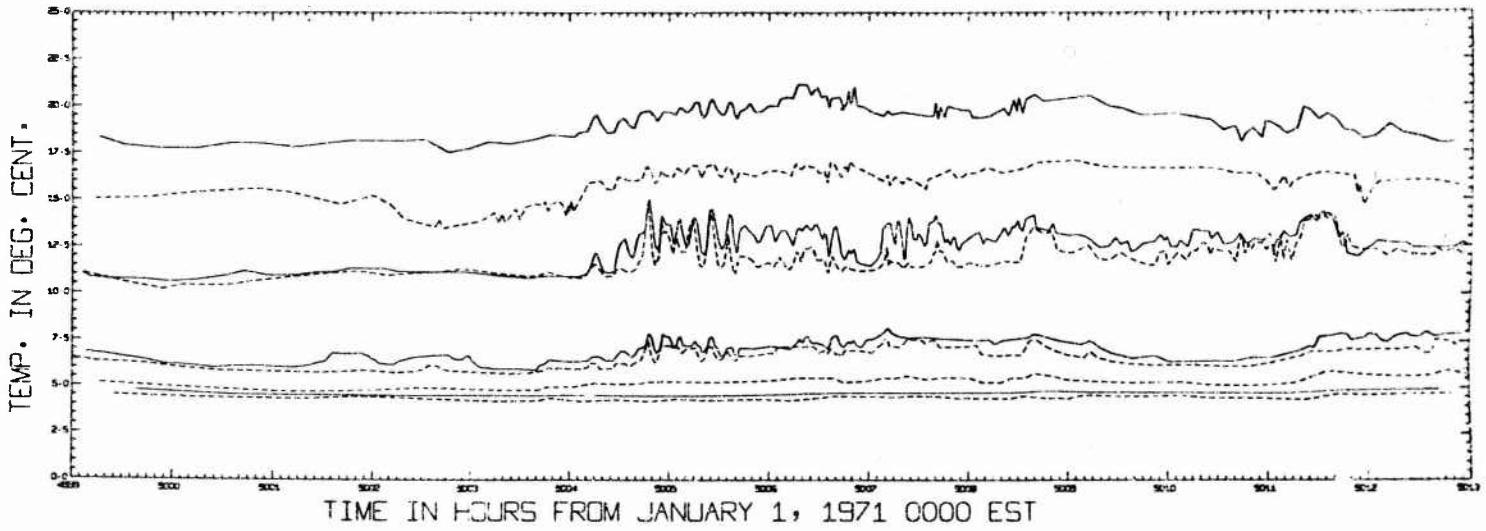

Figure 25. Similar to Figure 23. The 100 foot north thermistor was not recording. The left margin at 4999 hours is July 28, 1971, 0700 EST.

in most cases. The coherency at the 50-foot level is the lowest for any of the 1971 surges analyzed.

Figure 26 shows the surge of July 30, 1971. The drive cord on the recording instrument broke soon after the front passed so only a portion of the wave train was recorded. There was considerable activity at the 75-foot level in addition to that at the 50-foot level. The 25- and 100-foot levels show some oscillations similar to that seen on July 15, 1971 before the front arrives. The period of the initial large oscillations was about 11.3 minutes.

The surge of August 18, 1971 is shown in Figure 27. This one is somewhat different from those seen in July. There is very little activity before the front arrives and it contains three distinct oscillations seen from 25 to 100 feet. Their period was about 13.0 minutes.

The surge of September 7, 1968 is shown in Figure 30. There is some small-amplitude oscillation seen at 50 feet before the surge arrives but the front is sharp. There are five temperature peaks seen from 50 down to 150 feet with the amplitude increasing with each peak. The base of the mixed layer is coming down below 50 feet during these oscillations; this is the explanation of the flat-topped peaks seen. The maximum amplitude of these oscillations is about 50 feet and the period is about 15.9 minutes.

Figure 31 shows the surge of September 22, 1971. The newer thermistor strings were in use at this time and it can be seen that the data from pairs of thermistors at the same depth appear very similar. The wave train of this surge is very

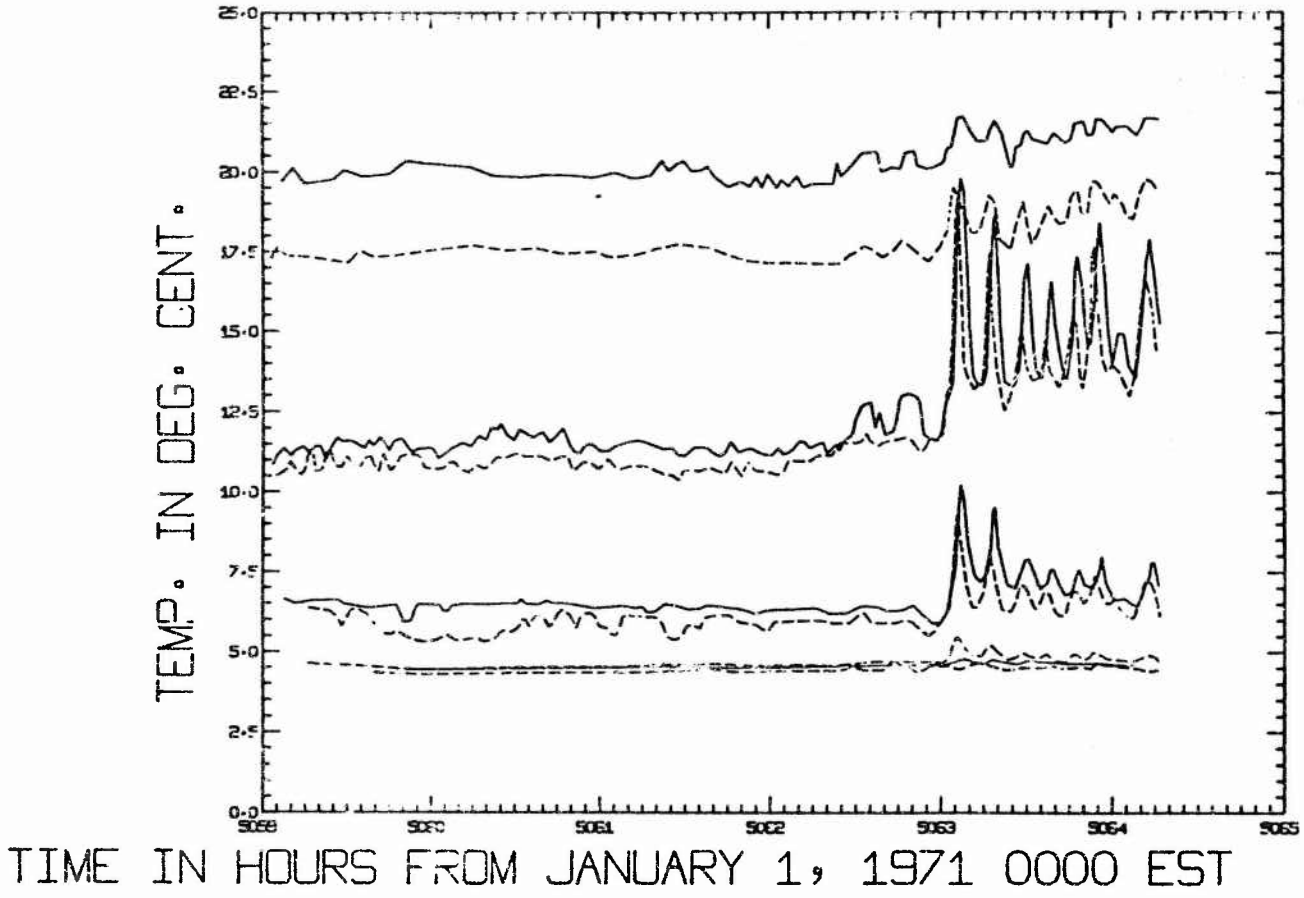

Figure 26. Similar to Figure 23. The 100 foot north thermistor was not recording. The left margin at 5059 hours is July 30, 1971, 1900 EST.

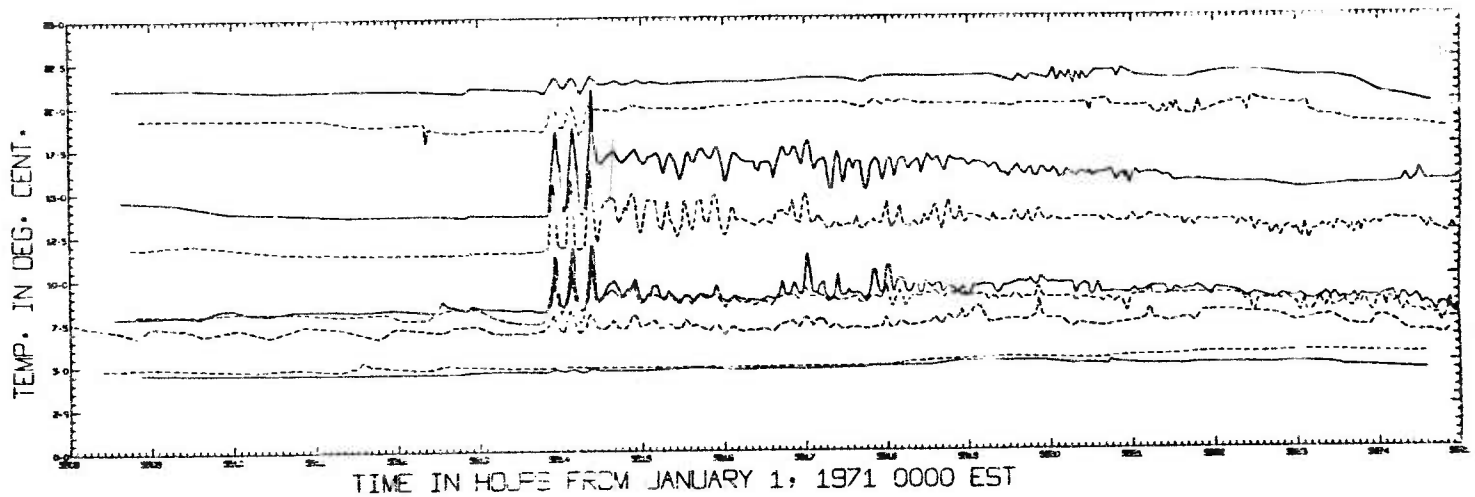

Figure 27. Similar to Figure 23. The 100 foot north thermistor was not recording. The left margin at 5508 hours is August 18, 1971, 1200 EST.

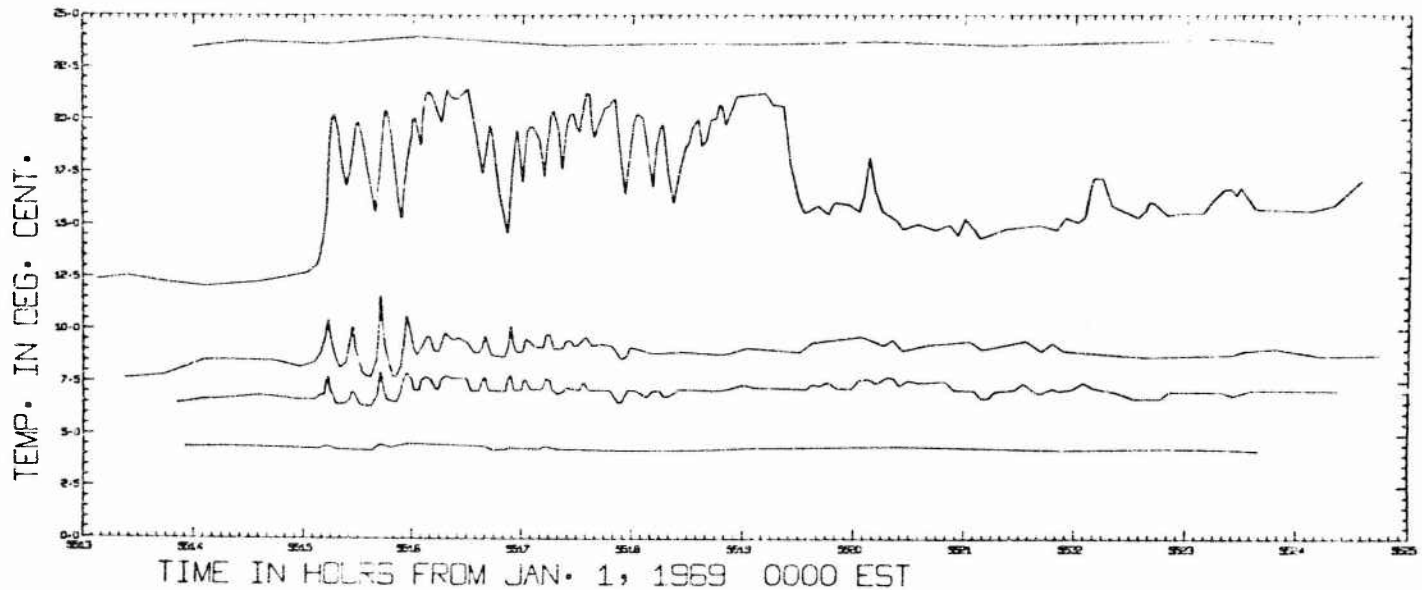

Figure 28. Temperatures recorded in 1969 at barge site 1. The thermistor depths are 25, 50, 75, 100 and 150 feet. The left margin at 5513 hours is August 18, 1969, 1700 EST.

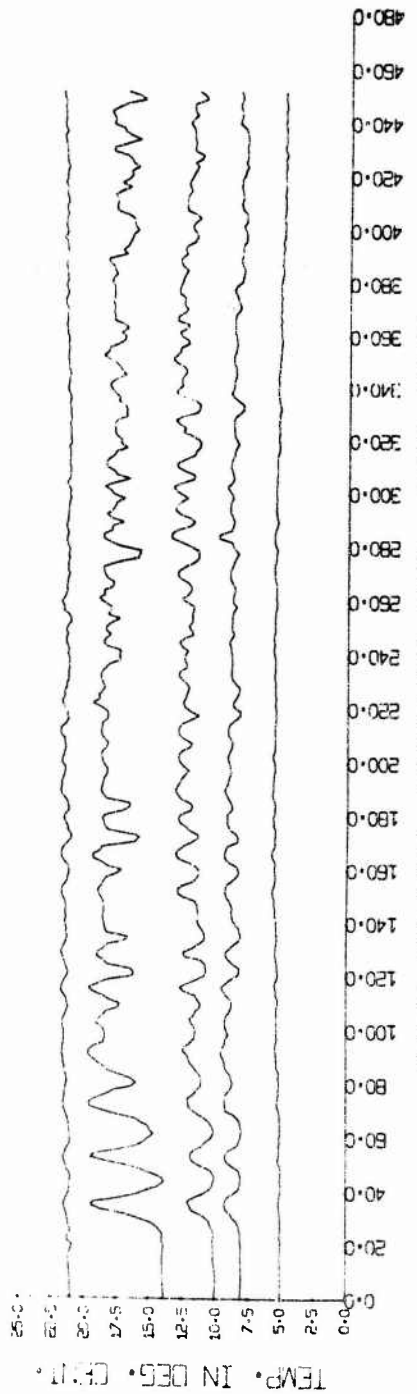

Figure 29. Temperatures recorded August 24, 1968 at barge site 1. The thermistor depths are 25, 50, 75, 100 and 150 feet.

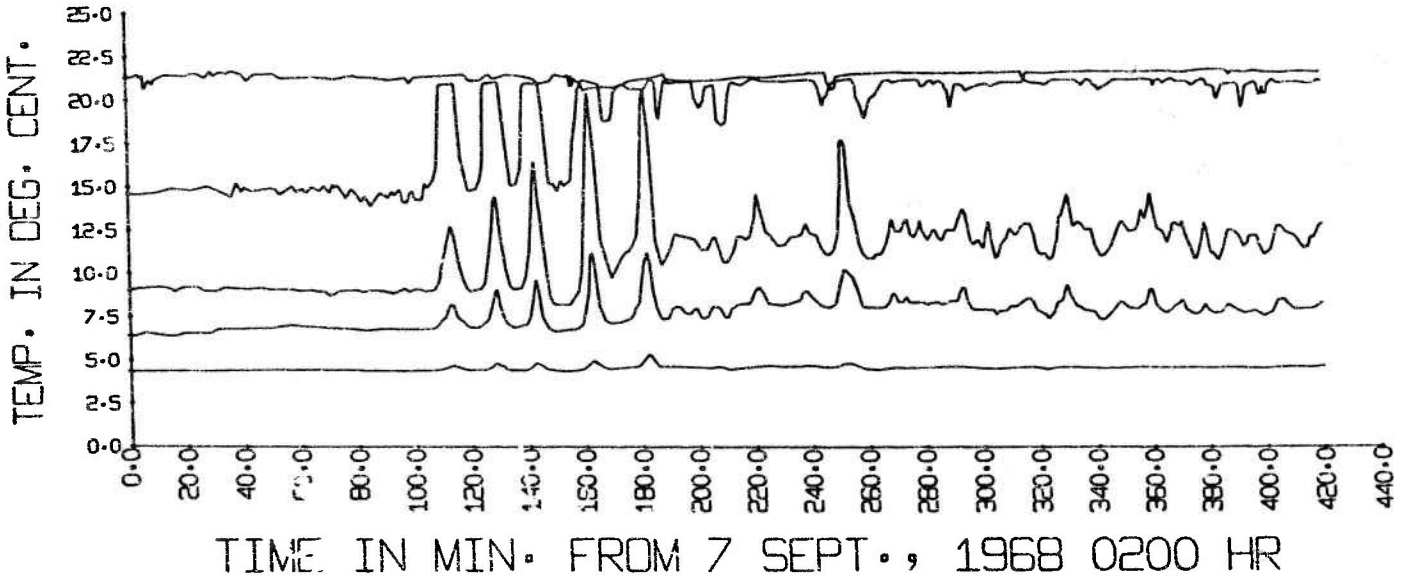

Figure 30. Similar to Figure 29 for September 7, 1968.

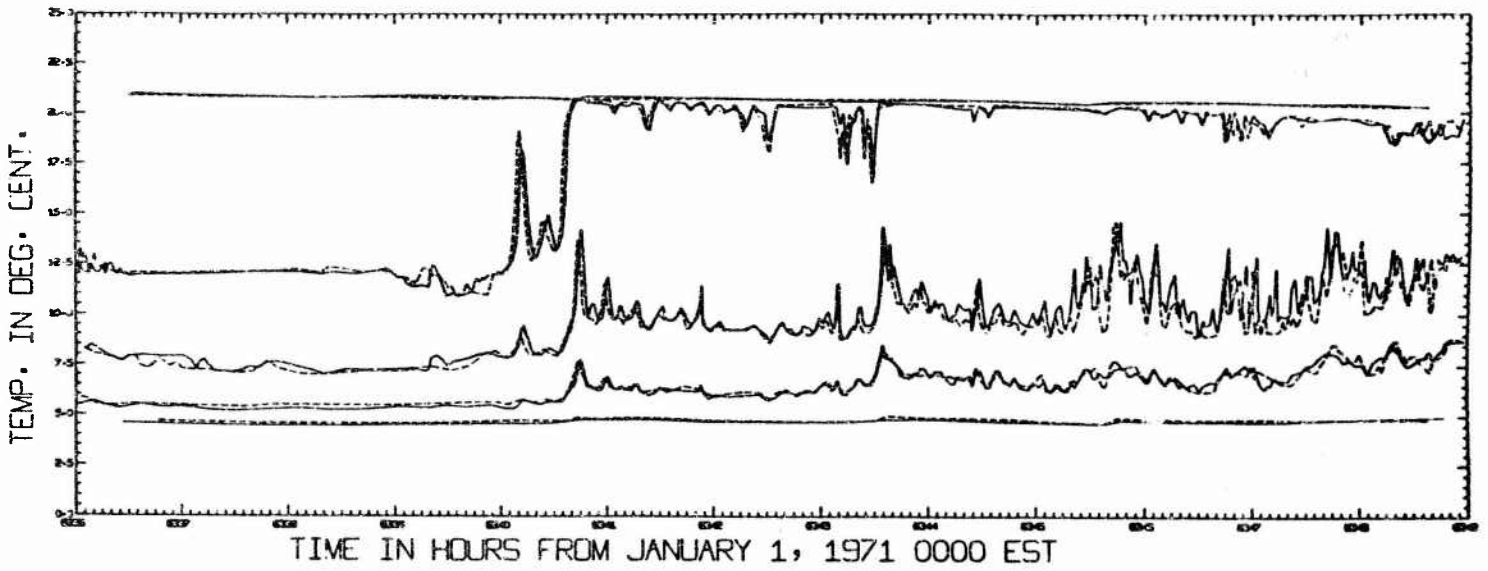

Figure 31. Similar to Figure 23. The left margin at 6336 hours is September 22, 1971, 0000 EST.

subdued. There is a peak seen at 50 feet following some low-amplitude activity. The maximum that brings the 50-foot level into the mixed layer is seen at 75 and 100 feet but there is not much activity thereafter for a few hours. The amplitude of this oscillation is about 30 feet at the 75-foot level.

The surge of September 24, 1971, shown in Figure 32, is unusual, there being much activity at the 50-foot level before the arrival of the surge. The amplitudes of the oscillations are low, water motions are considerably less than 25 feet.

The surge of October 2, 1969 is shown in Figure 33. Both the 25- and 50-foot levels are seen to be in the mixed layer. The 75-foot level experienced temperature oscillations of almost 10°C but these represent water motions of only about 25-foot amplitude. Commencing about 1830 EST and lasting for over two hours, oscillations with periods less than 5 minutes are seen at the 75-foot level. (The period of the Brunt-Vaisala frequency at this level is also just under 5 minutes.) The period of the initial oscillations associated with the surge front is about 16.4 minutes.

Figure 36 shows the surge of October 6, 1971. The amplitude is about 30 feet. The 50-foot level remains out of the mixed layer until a number of hours after the surge passes. This surge contains 11 fairly regular initial oscillations, the most seen. The period is about 17.6 minutes.

The surge of October 8, 1968 is seen in Figure 37. In many respects it is very similar to that of October 4, 1969. Both show vertical water motions of over 50 feet in amplitude

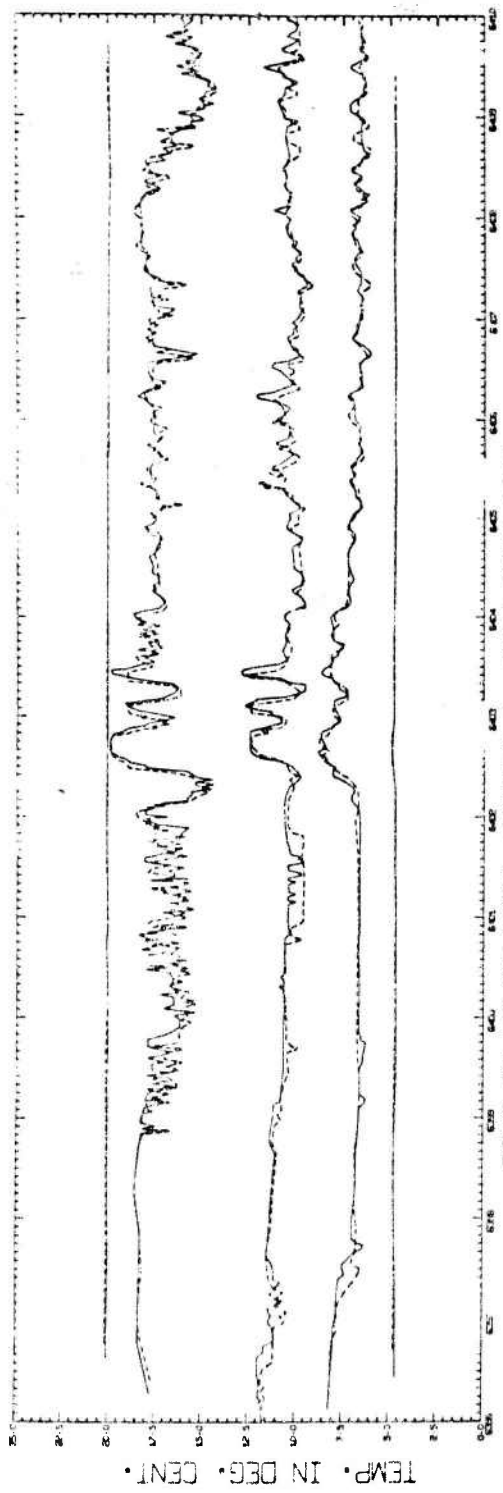

Figure 32. Similar to Figure 23. The left margin at 6396 hours is September 24, 1971, 1200 EST.

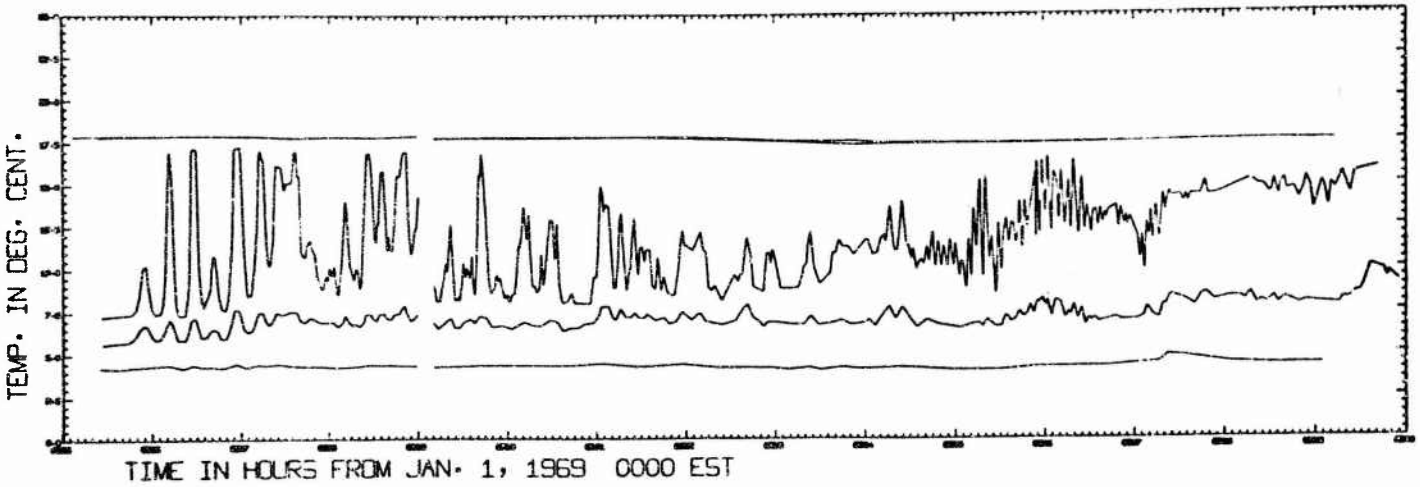

Figure 33. Similar to Figure 28. The left margin at 6585 hours is October 2, 1969, 0900 EST.

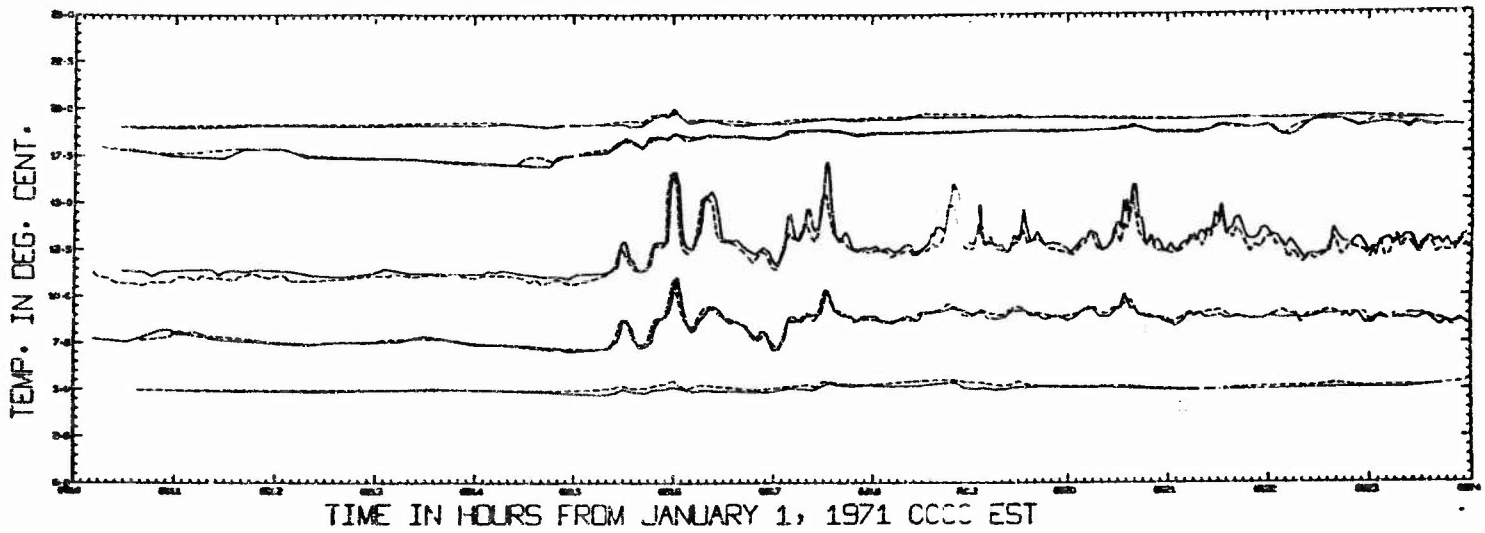

Figure 34. Similar to Figure 23. The left margin at 6610 hours is October 3, 1971, 1000 EST.

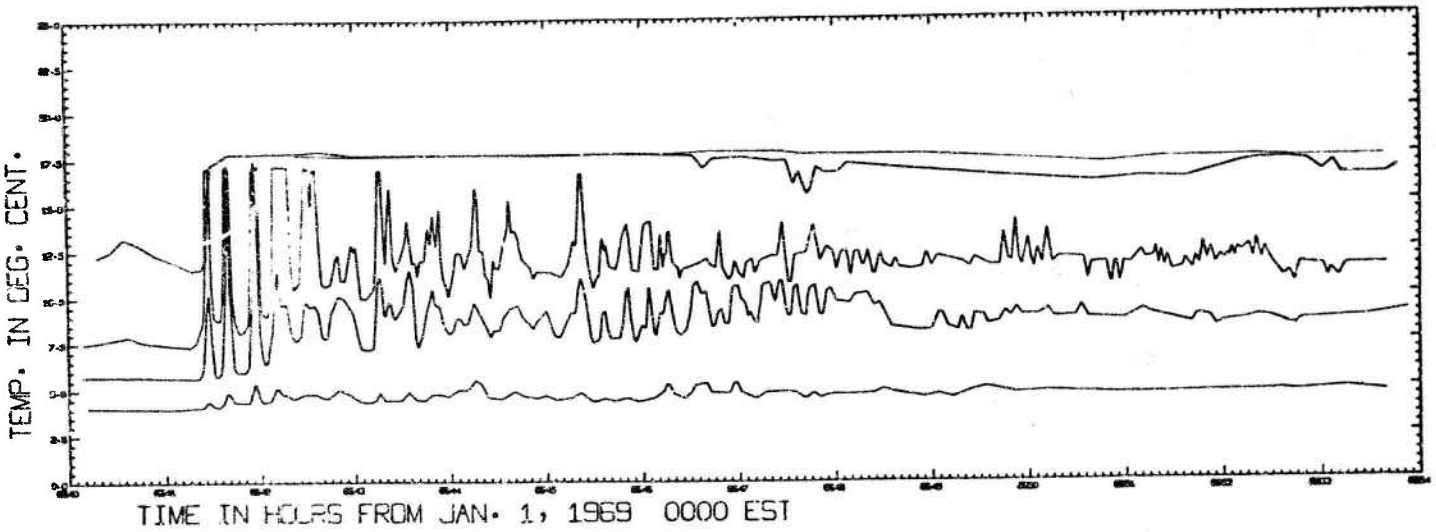

Figure 35. Similar to Figure 28. The left margin at 6640 hours is October 4, 1969, 1600 EST.

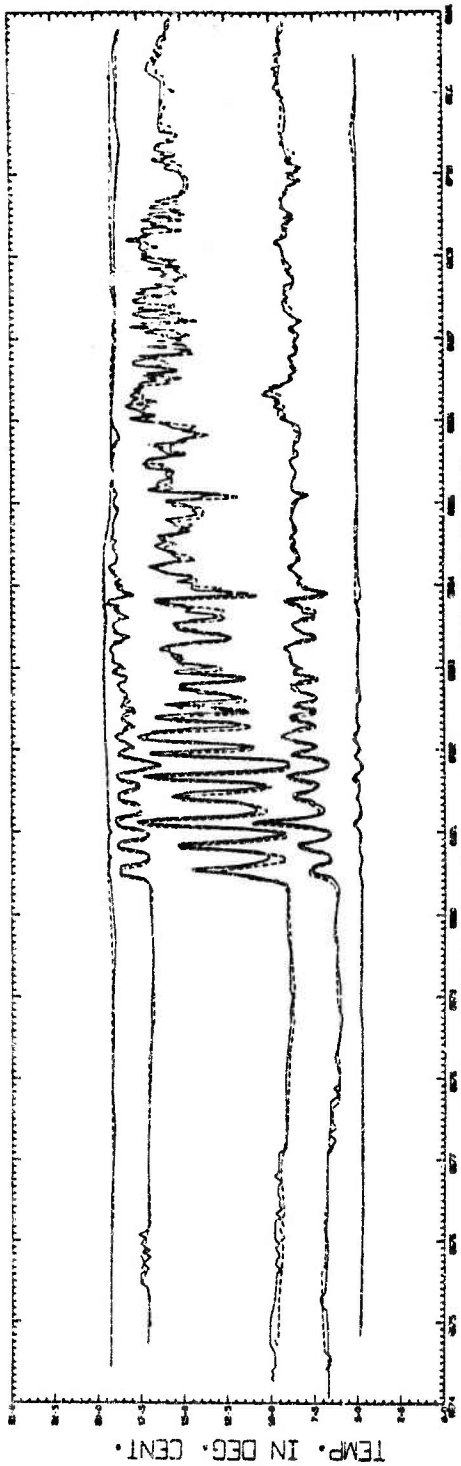

Figure 36. Similar to Figure 23. The left margin at 6674 hours is October 6, 1971, 0200 EST.

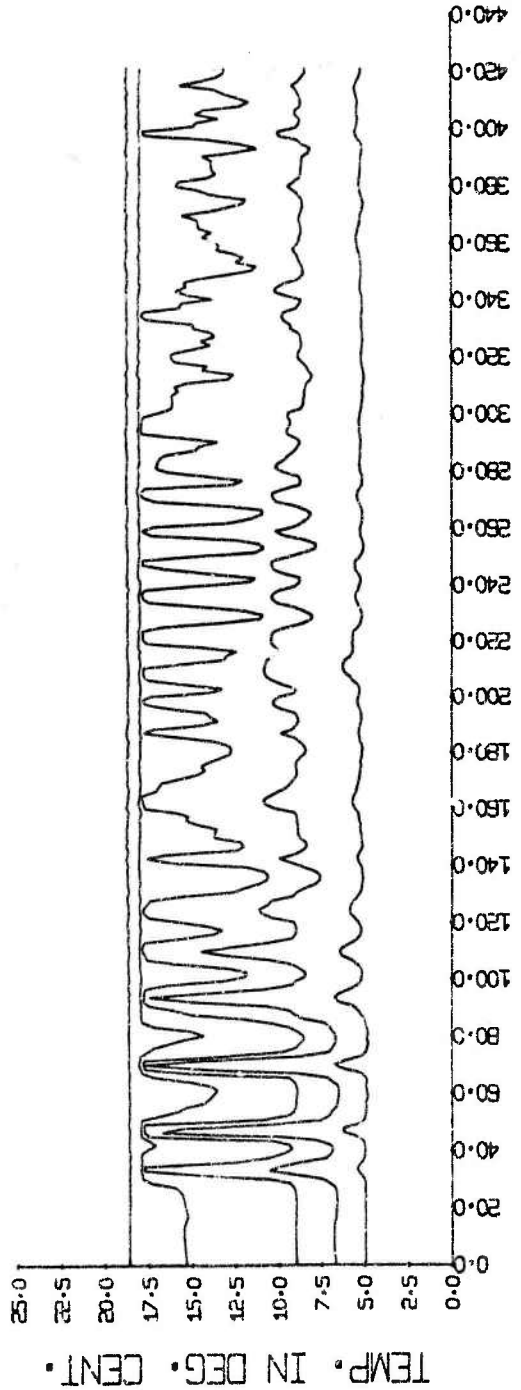

Figure 37. Similar to Figure 29 for October 8, 1968.

at the 100-foot level and in both surges the maximum amplitude is seen in the third temperature peak. This surge also shows regular oscillations at the 75-foot level beginning about 150 minutes after the front passes and continuing for about 90 minutes. The period of the initial oscillations is about 13.6 minutes and that of the later, regular ones varies from about 10 to 15 minutes.

The surge of October 13, 1969, shown in Figure 40, contains regular oscillations beginning about 4-1/2 hours after the front came through and lasting more than 1-1/2 hours, similar to that of October 8, 1968. The amplitude of the initial oscillations is only about 25 feet and the period about 22.5 minutes.

The surge of October 18, 1969, seen in Figure 42, is somewhat unusual in appearance. There are short-period oscillations at 75 feet similar to that seen on September 24, 1971. The 150-foot thermistor indicates a wave amplitude of over 50 feet at that depth, yet the 75-foot level is below the mixed layer throughout most of this record. The period of the initial oscillations is about 19.7 minutes.

The surge of October 22, 1969, seen in Figure 43, begins differently from the previous ones seen in October. The initial temperature rise is not as rapid and the first decline not as smooth nor as rapid as in previous surges. The 75-foot thermistor is probably above the base of the mixed layer for most of the record although from the figure it appears to be at a lower temperature than the 25- and 50-foot ones. This is

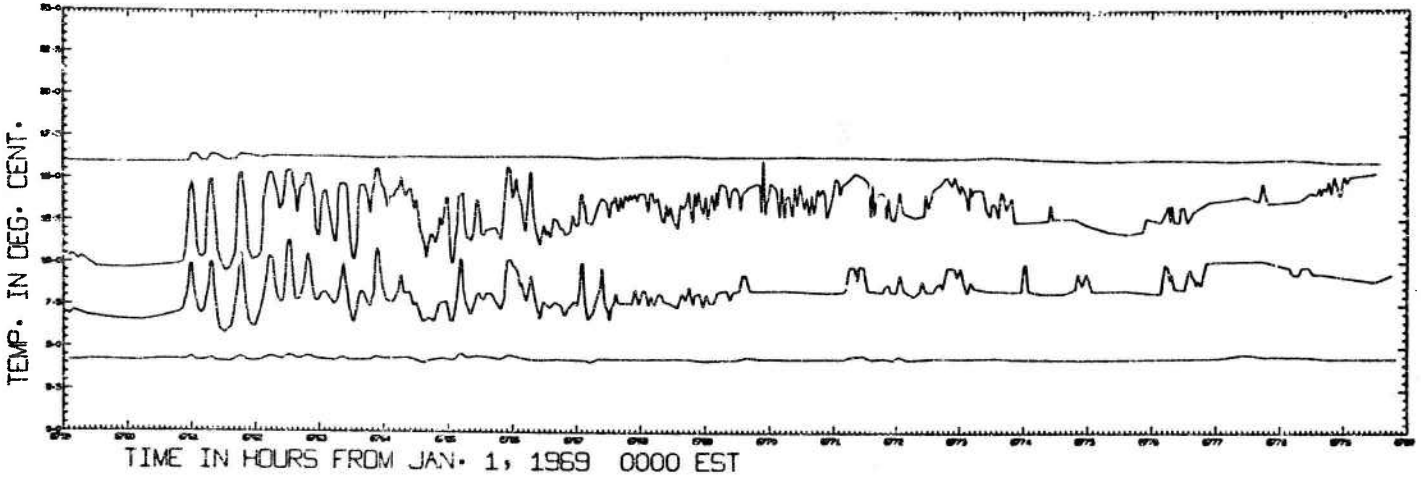

Figure 38. Similar to Figure 28. The left margin at 6759 hours is October 9, 1969, 1500 EST.

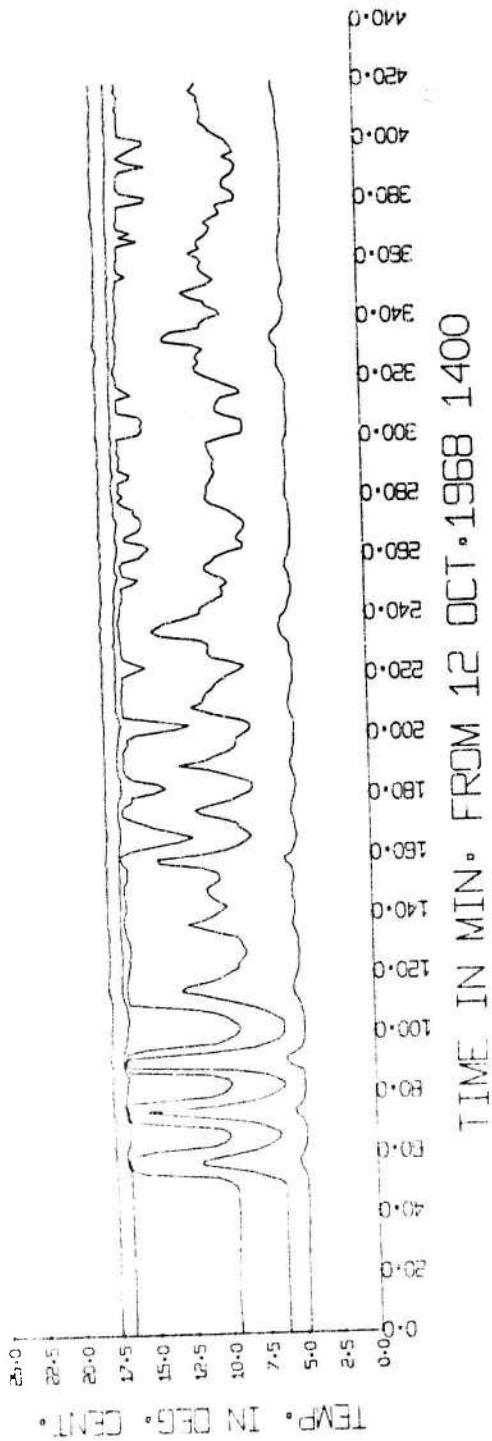

Figure 39. Similar to Figure 29 for October 12, 1968.

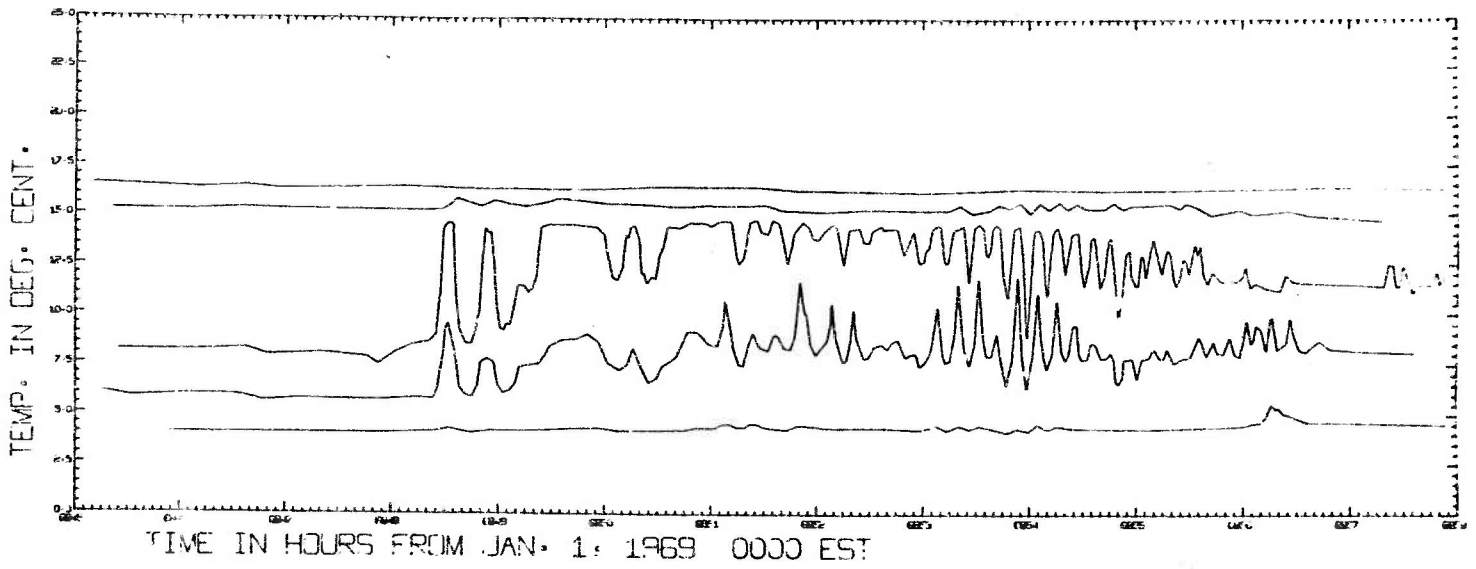

Figure 40. Similar to Figure 28. The left margin at 6845 hours is October 13, 1969, 0500 EST.

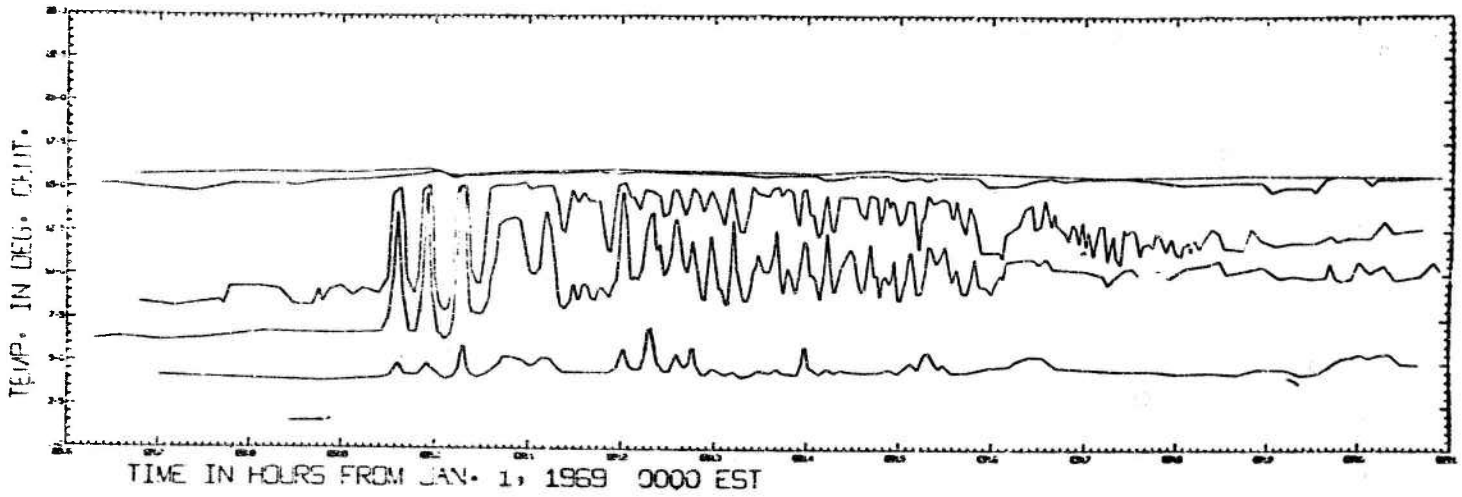

Figure 41. Similar to Figure 28. The left margin at 6906 hours is October 15, 1969, 1800 EST.

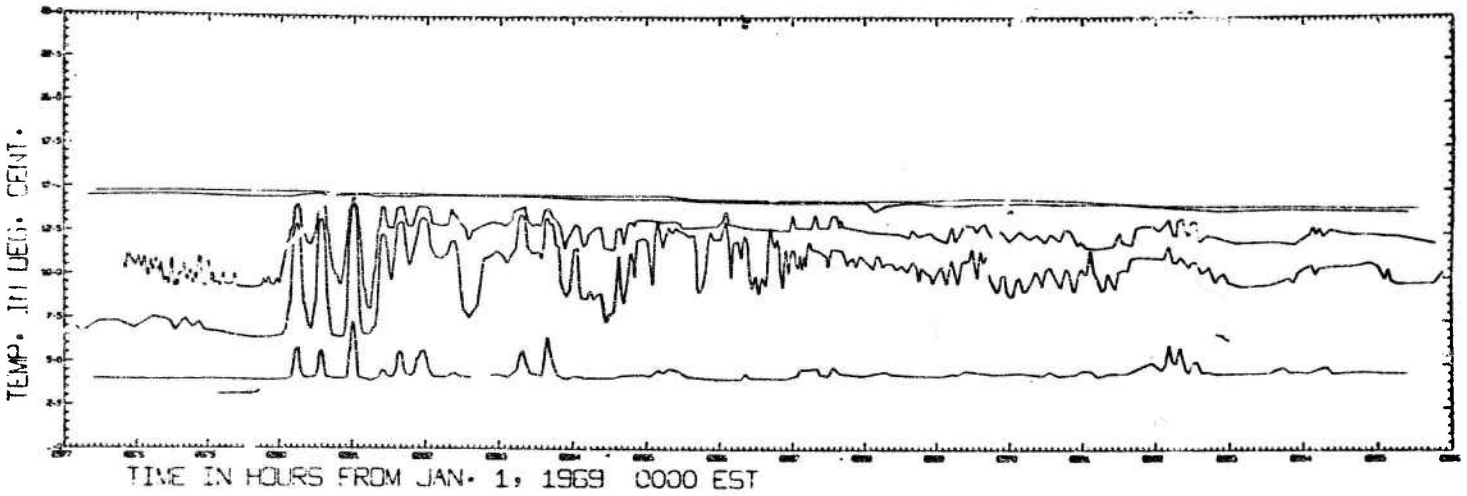

Figure 42. Similar to Figure 28. The left margin at 6977 hours is October 18, 1969, 1700 EST.

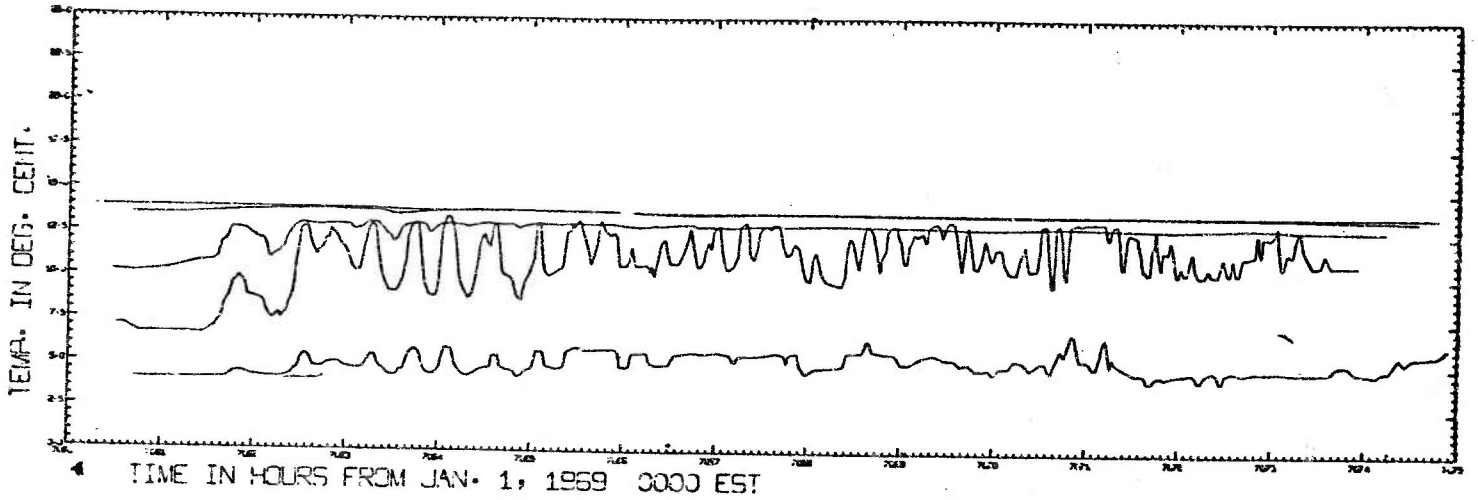

Figure 43. Similar to Figure 28. The left margin at 7060 hours is October 22, 1969, 0 ,0 EST.

probably due to the calibration difficulties experienced with the older thermistor chain.

Figure 47 shows the surge of October 30, 1968. Disregarding the fact that temperature peaks at the 100-foot level are higher than even the 25-foot temperatures (this is due to the calibration difficulties encountered with the old thermistor string), it is apparent that the flat temperature peaks at this level indicate that the mixed layer is oscillating to below 100 feet. This surge is unusual for the oscillations seen at 75 feet before the front arrives and because of the single temperature peak seen as the surge arrives.

The surge of November 4, 1969 is shown in Figure 48. The mixed layer is below 75 feet before the arrival of the surge and oscillates above and below 100 feet after the front comes through. Oscillations are close to 50 feet in amplitude at the 150-foot level and the period is the longest observed, about 40.3 minutes.

The oscillations associated with the surge front of November 16, 1968, shown in Figure 52, build up slowly in contrast to those seen earlier in the year. Fluctuations are seen at 50 feet which is very unusual for so late in the year.

Figure 53 shows the temperature data of November 22, 1971. It is questionable as to whether this represents a surge.

It is evident from the figures that, although exceptions can be found for almost any generalization made about the surges, there are a number of characteristics that are common to all or most of the surges seen in Seneca Lake. In all cases,

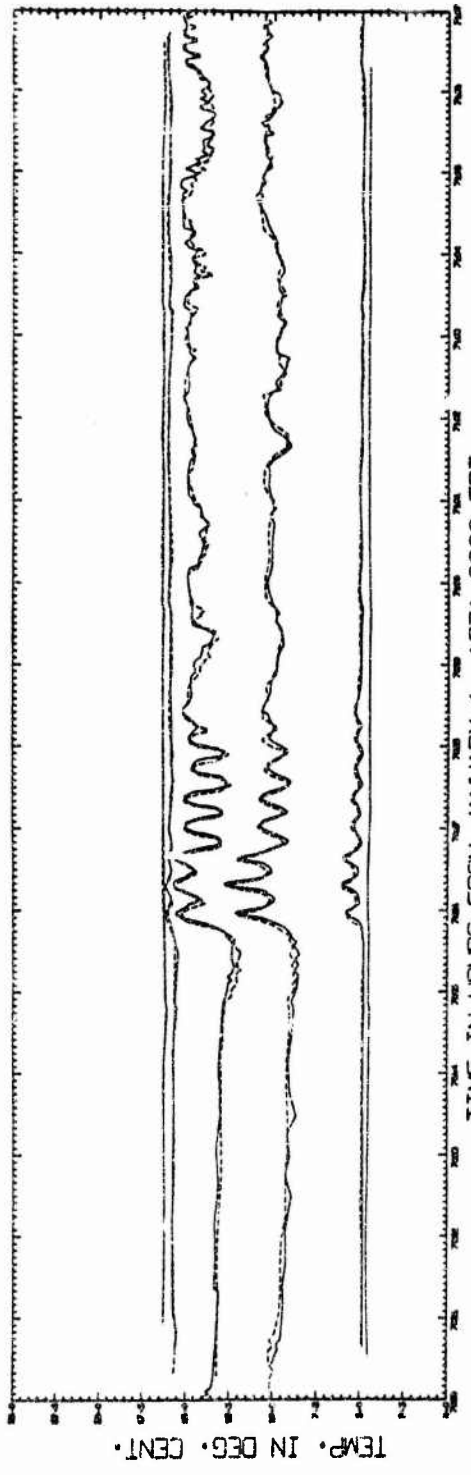

Figure 44. Similar to Figure 23. A thermistor at 225 feet has been added to the north string. The left margin at 7090 hours is October 23, 1971, 1000 EST.

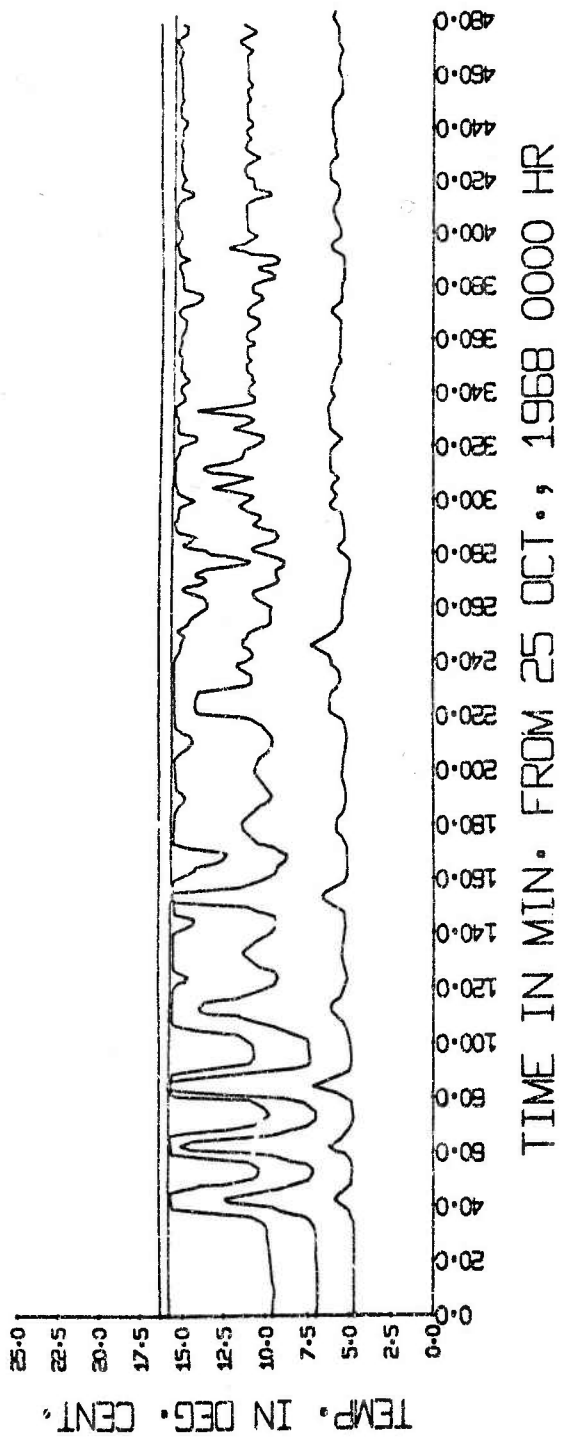

Figure 45. Similar to Figure 29 for October 25, 1968.

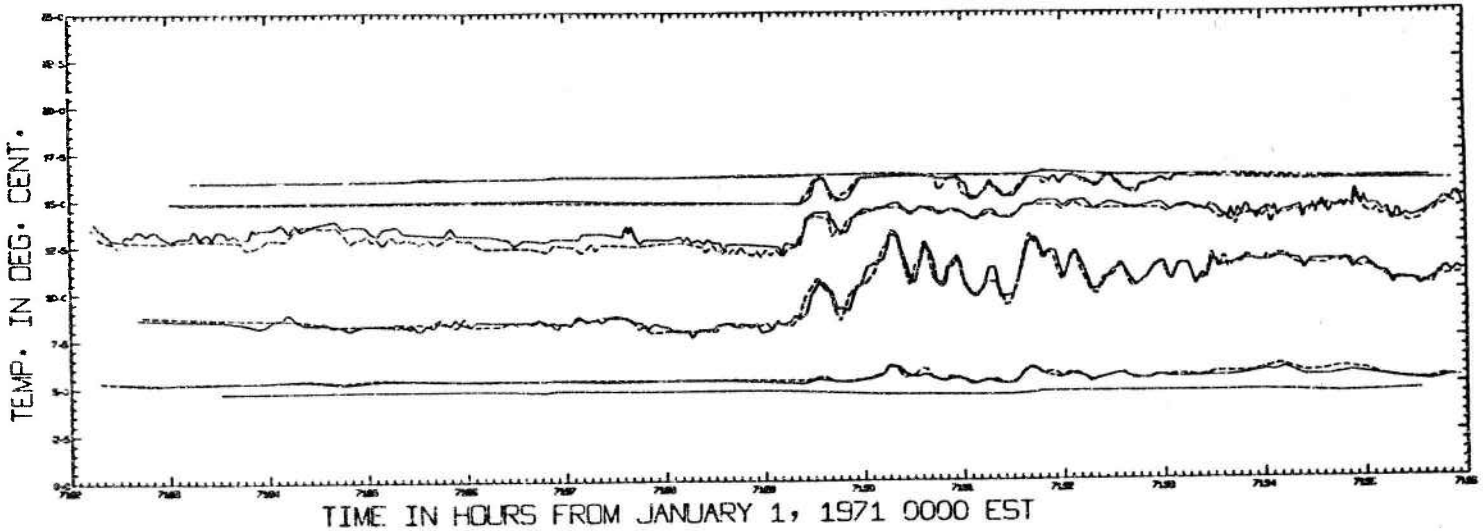

Figure 46. Similar to Figure 44. The left margin at 7182 hours is October 27, 1971, 0600 EST.

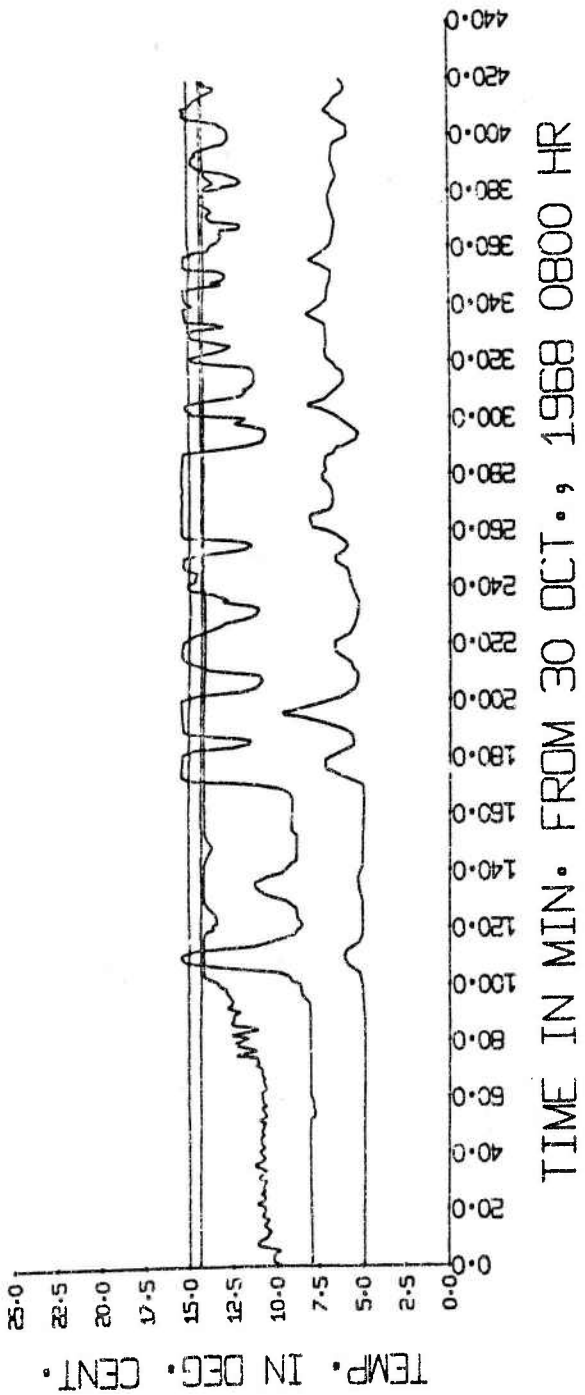

Figure 47. Similar to Figure 29 for October 30, 1968.

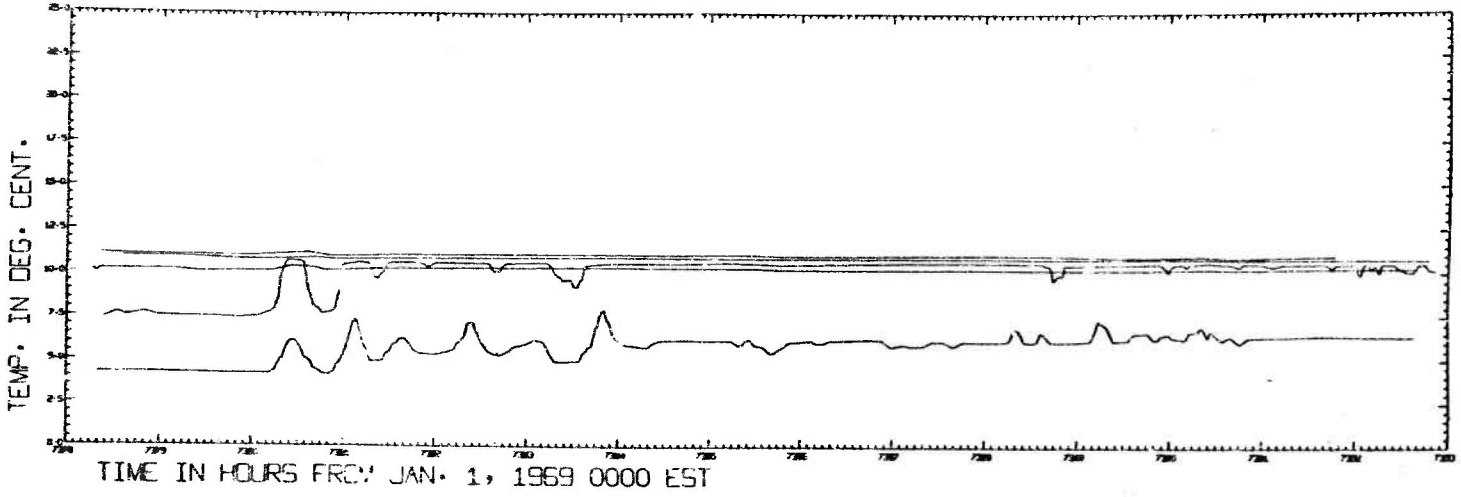

Figure 48. Similar to Figure 28. The left margin at 7378 hours is November 4, 1969, 1000 EST.

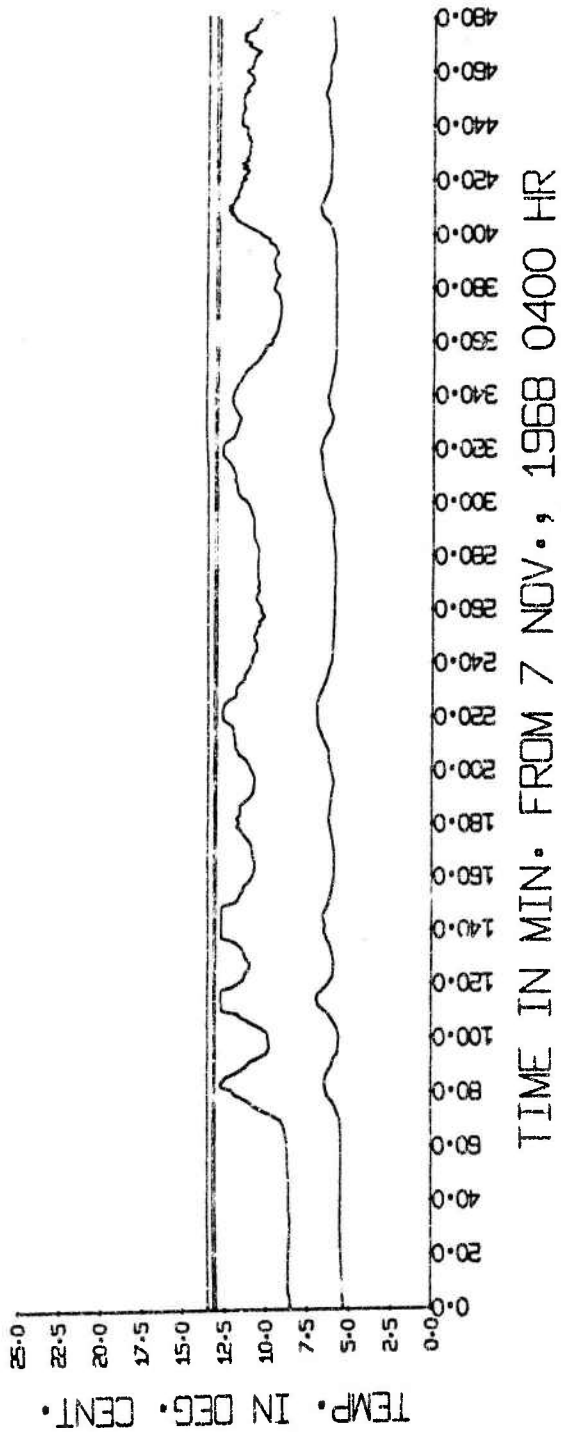

Figure 49. Similar to Figure 29 for November 7, 1968.

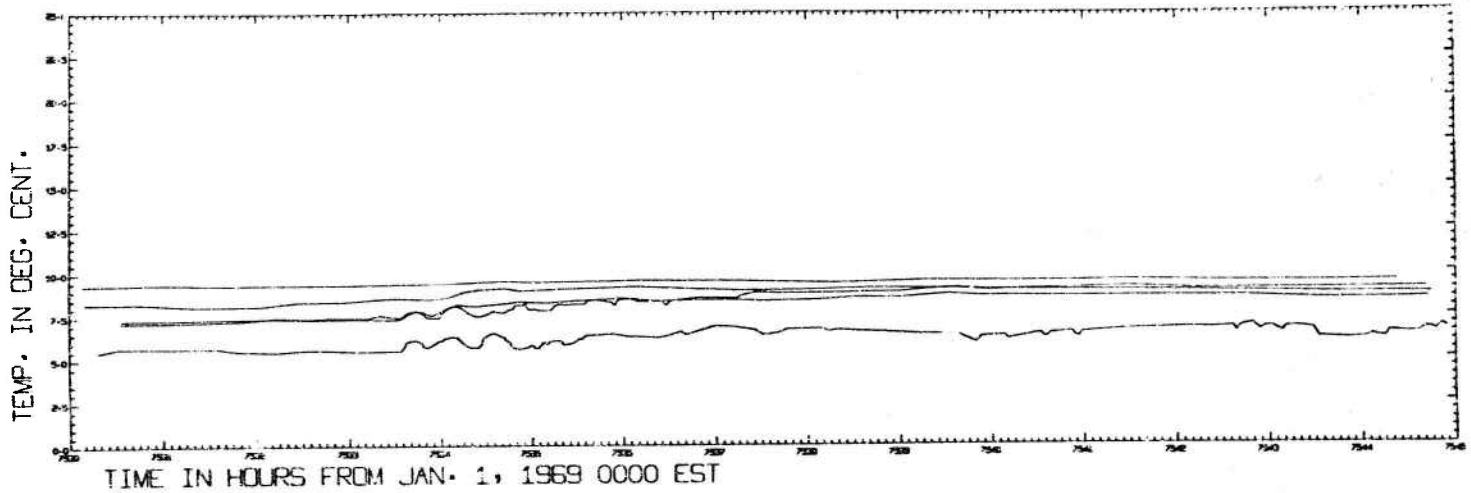

Figure 50. Similar to Figure 28. The left margin at 7530 hours is November 10, 1969, 1800 EST.

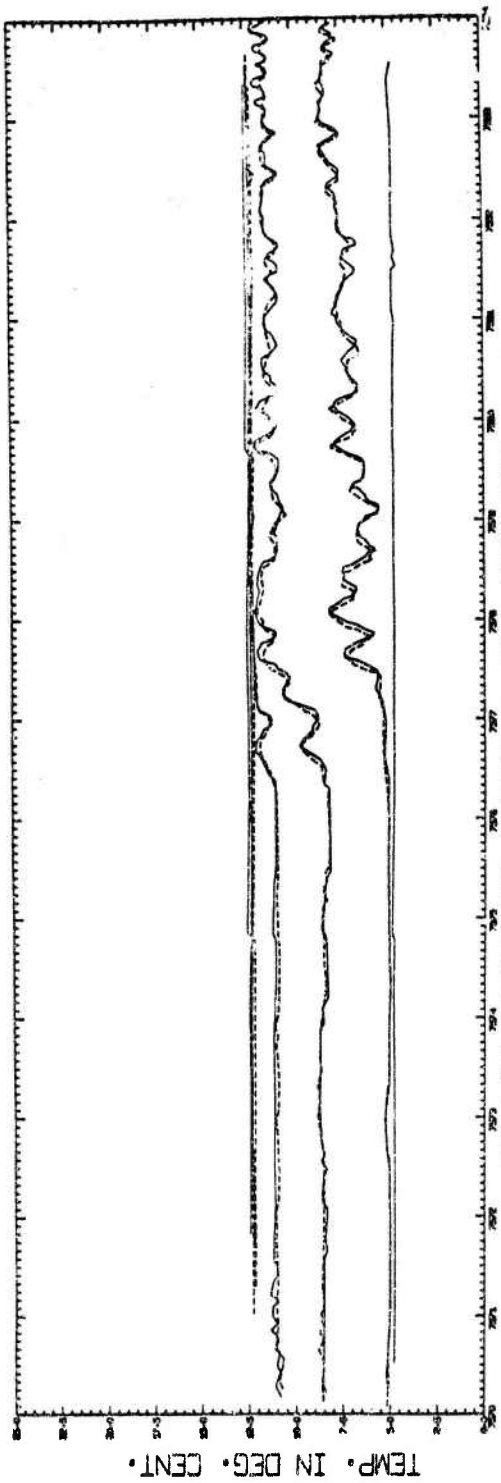

Figure 51. Similar to Figure 44. The left margin at 7570 hours is November 12, 1971, 1000 EST.

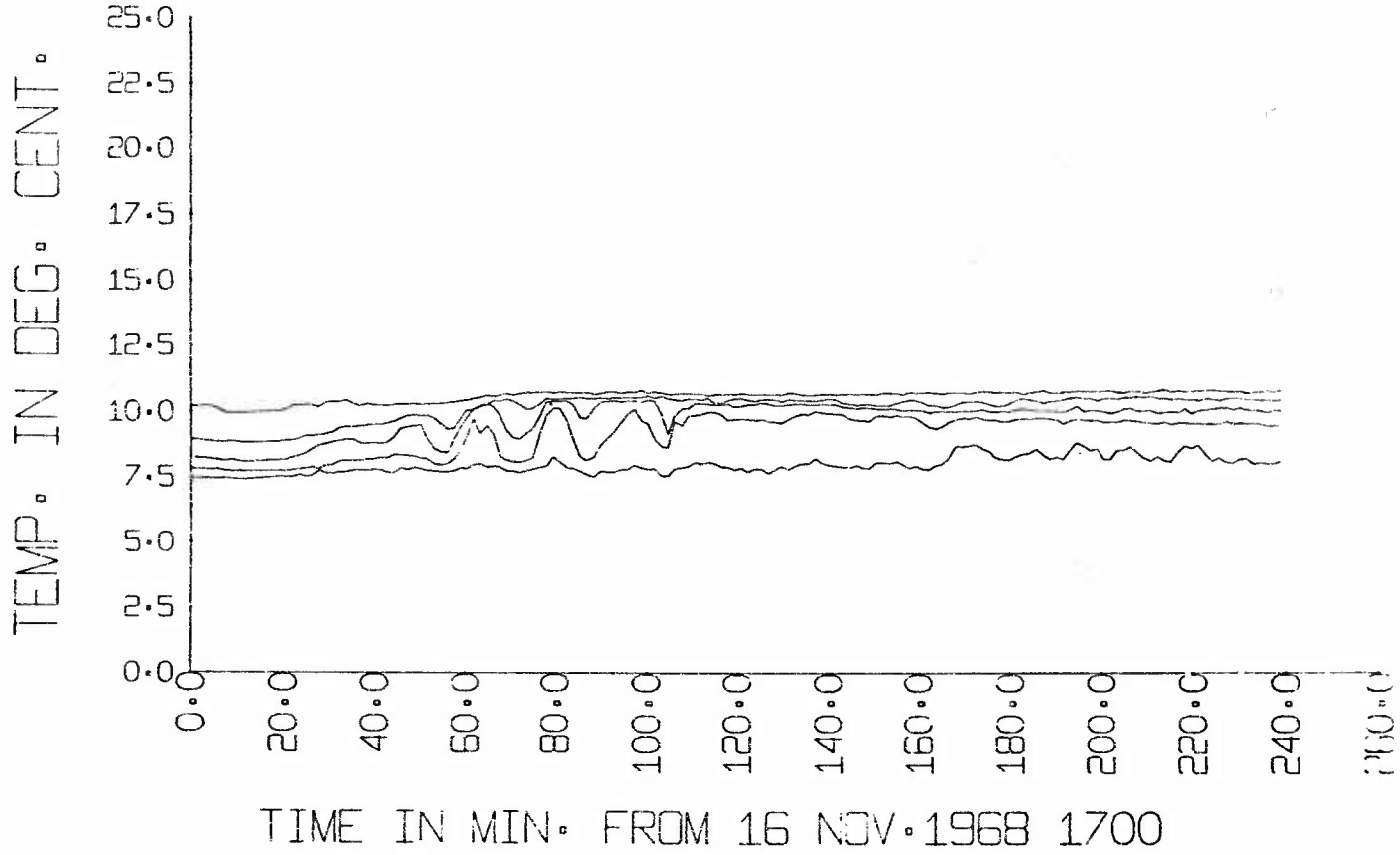

Figure 52. Similar to Figure 29 for November 16, 1968.

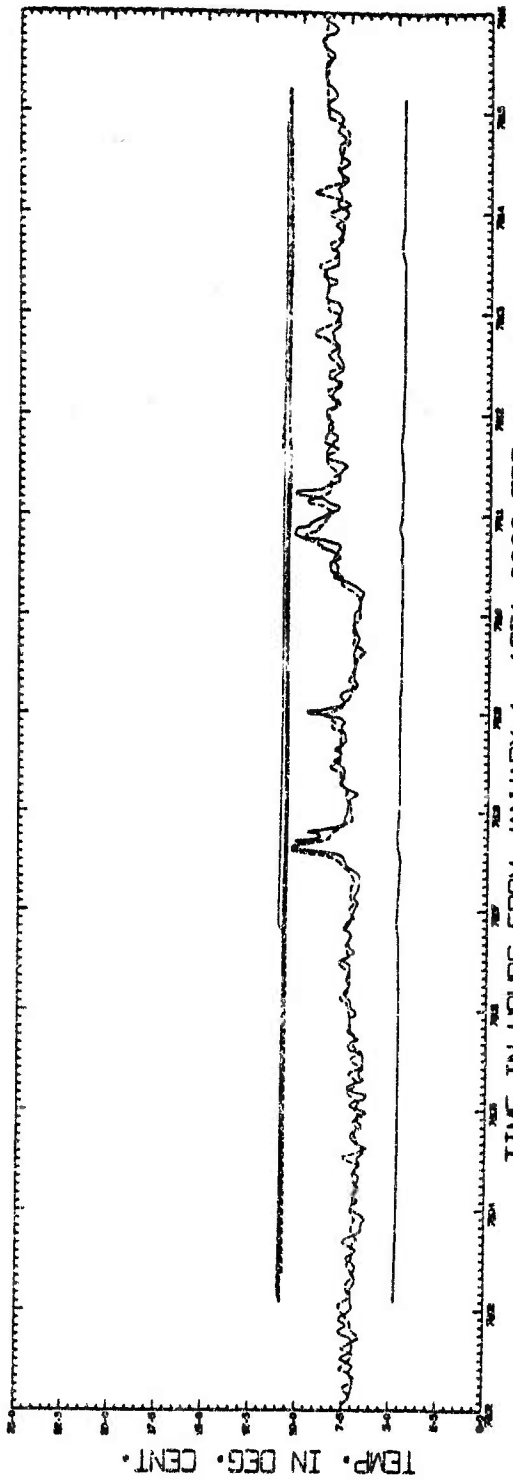

Figure 53. Similar to Figure 44. The left margin at 7802 hours is November 22, 1971, 0200 EST.

temperatures have been slowly dropping at all levels below the mixed layer (the temperature structure curve is shifting upward) for tens of hours before the surge is seen, indicating that the warm water of the epilimnion is moving away and is being replaced by colder water from below. In all cases, the first strong oscillation is a rise in temperature and when the wave train had passed, all levels showed either the same or a higher temperature than before the surge. This shows that the surge is always a fall in the level of isotherms, indicating warm water moving in and colder water being displaced downward. In most cases, the first oscillations start rather suddenly and the first few are smooth and regular. In all cases, the frequency of the initial oscillations are less than the Brunt-Vaisala frequency. The first few waves generally have the largest amplitudes and are very coherent over at least a few hundred feet; the following oscillations, which usually continue for hours and generally are irregular, are less coherent and contain more turbulence. The wave trains seen in 1971 were generally of smaller amplitude than those of 1968 and 1969 and their initial temperature rise was not as sudden. This may be due to the different location used in 1971. Table 2 contains a summary of the data for all of the short-period wave trains associated with surges seen in the years 1968, 1969 and 1971.

In Figure 54 the period of the initial oscillations of the wave train are plotted against the date of the surge. It can be seen that there is a definite increase in period from July through November. A straight line can be drawn through

TABLE 2: SUMMARY OF DATA FOR SHORT-PERIOD INTERNAL WAVES

Date	Initial period (min)	Mixed layer depth before (ft)	Mixed layer depth after (ft)	Max ampl. (ft)	Depth of max ampl (ft)
Jul 15/71	9.4±0.5	<25	<25	25	50
Jul 28/71		<25	<25	10	50
Jul 30/71	11.3±0.5	<25		25	50
Aug 18/71	13.0±0.5	<25	<25	20	50
Aug 18/69	14.1±0.5	25	35	15	50
Aug 24/68	17.8±0.5	30	40	20	50
Sep 7/68	15.9±0.5	25	35	50	75
Sep 22/71		30	45	30	75
Sep 24/71		30	40	10	75
Oct 2/69	16.4±0.5	55	70	25	75
Oct 3/71		30	40	20	75
Oct 4/69	11.7±0.5	30	50	60	100
Oct 6/71	17.6±0.5	30	50	30	75
Oct 8/68	13.6±0.5	30	65	65	100
Oct 9/69	18.8±0.5	45	55	25	100
Oct 12/68	16.9±0.5	60	70	65	100
Oct 13/69	22.5±0.5	40	50	25	100
Oct 15/69	19.2±0.5	35	50	50	100
Oct 18/69	19.7±0.5	50	60	60	150
Oct 22/69		50	70	40	100
Oct 23/71	21.1±0.5	45	60	20	100
Oct 25/68	19.7±0.5	50	75	50	100
Oct 27/71		35	55	20	100
Oct 30/68		60	85	25	100
Nov 4/69	40.3±0.5	75	100	40	150
Nov 7/68	31.1±1.5	80	90	30	100
Nov 10/69	26.3±1.0				
Nov 12/71	30.0±2.0	60	80	35	150
Nov 16/68					
Nov 22/71		110	120	30	150

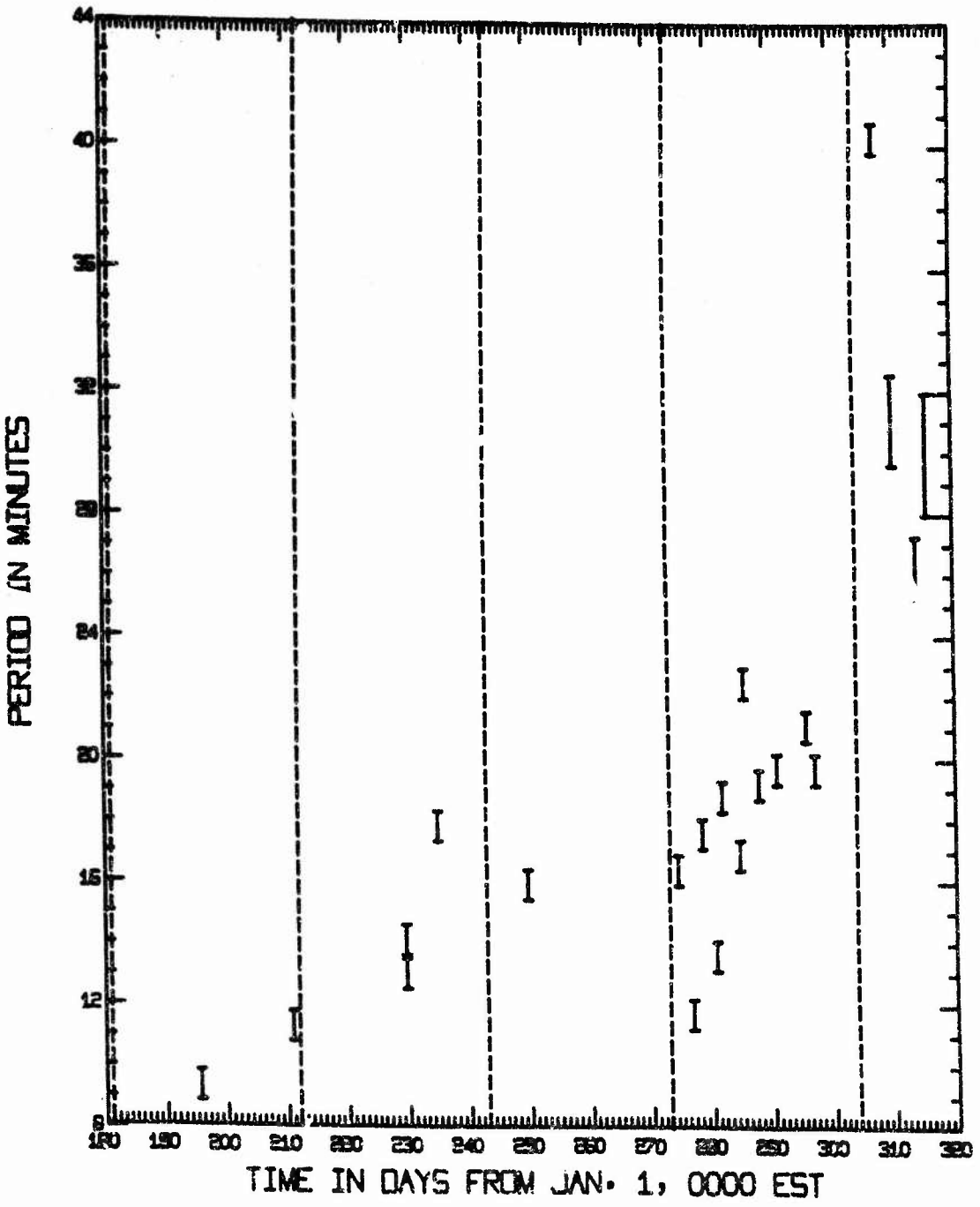

Figure 54. Period of the initial oscillations of the wave trains associated with internal surges seen in the years 1968, 1969 and 1971. The vertical broken lines delineate separate months beginning with July.

the points from July through October and it would show an increase in period of 1 minute about every 12 days. However, there would be a number of points, especially in October, that would not fit the line well. The periods measured in November were much higher than in previous months and do not fit a linear pattern. An exponential curve of initial period versus time of year would fit the total data better but there are not enough points to attempt a determination of the curve parameters. The initial period is probably a function of the thermal structure of the lake which also changes throughout the summer and fall (see Figure 3) although no simple relationship between the various parameters (densities, layer thicknesses) and the period has been found.

Another way to present the temperature data is to plot the depths of several isotherms as a function of time rather than plotting the original temperatures at specific depths versus time. This type of presentation is shown for four of the surges seen in 1968 in Figures 55 through 58. A linear interpolation was used to determine temperatures between thermistors. This distorts the isotherms drawn in the figures because the real temperature structure is more like an exponential function of depth than a linear one. Also, because of calibration difficulties, comparisons of temperatures between two thermistors at different depths cannot be done very accurately. Although only illustrative, Figures 55 through 58 show more clearly that the surges are, in all cases, a lowering of the isotherm levels. The figures also show that the short-period oscillations have sharp troughs and flat crests, in contrast to the waves seen

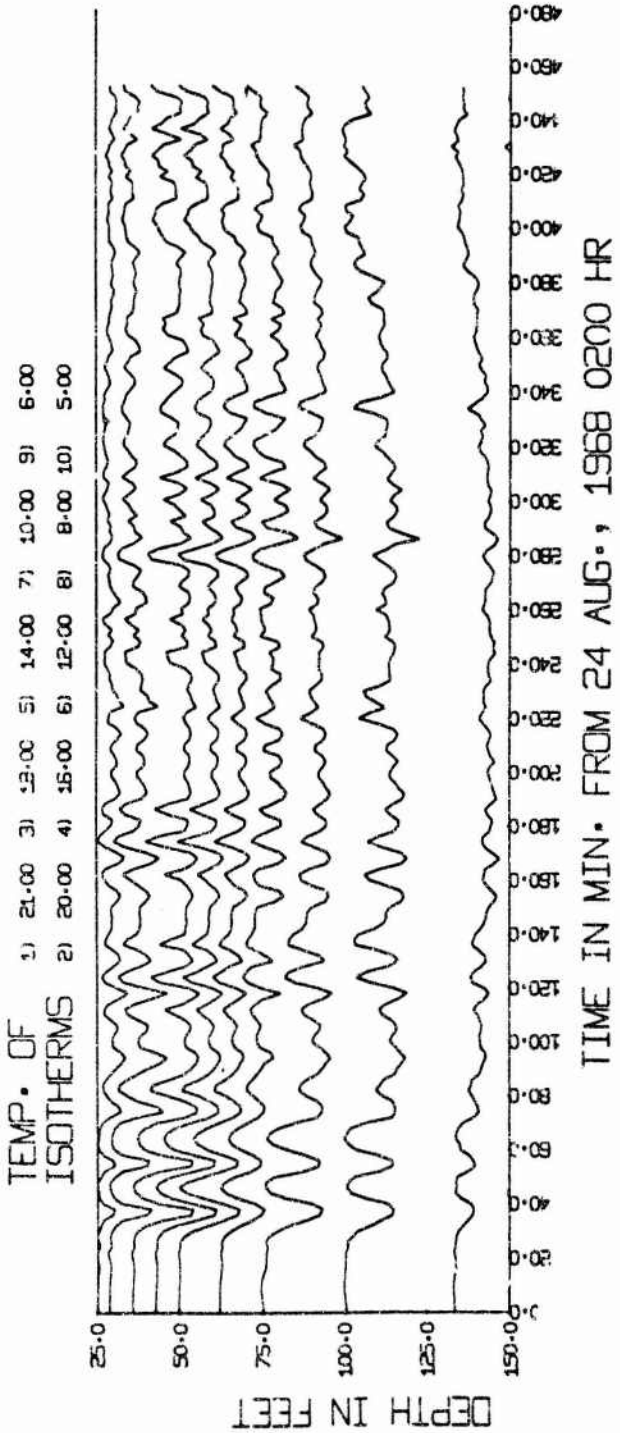

Figure 55. Isotherm depths for surge of August 24, 1968 (Figure 29).

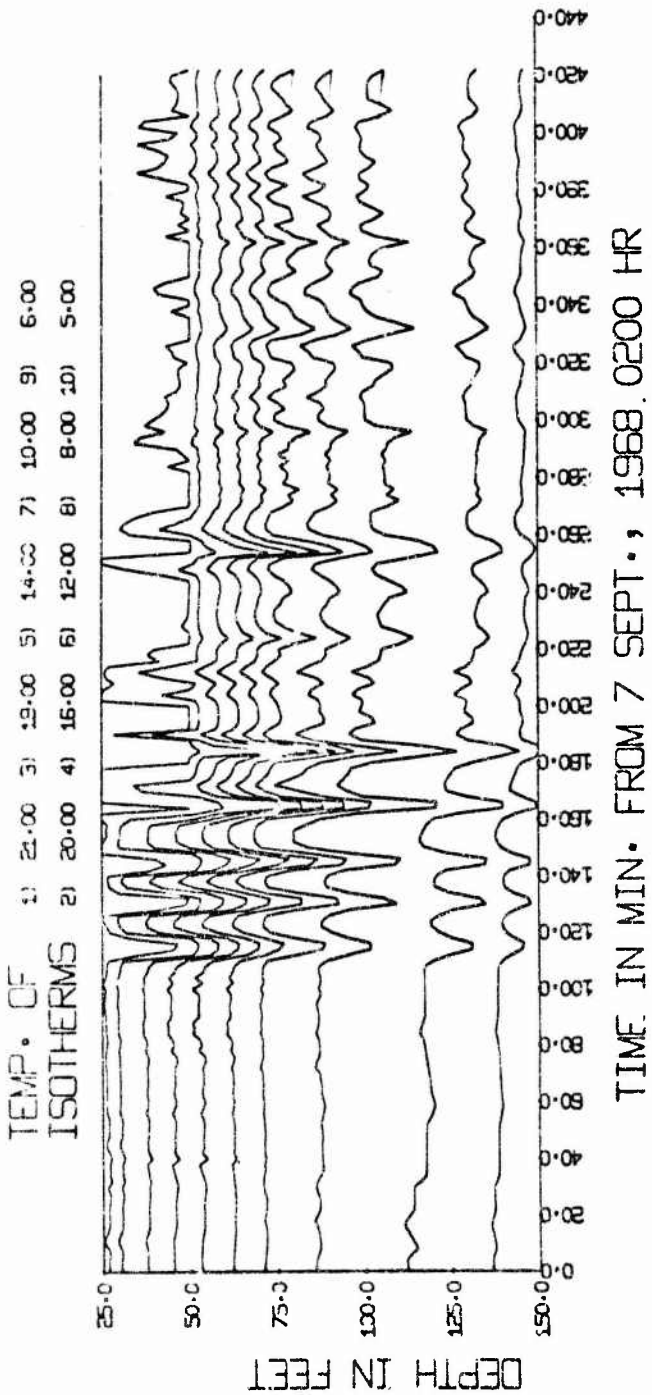

Figure 56. Isotherm depths for surge of September 7, 1968 (Figure 30).

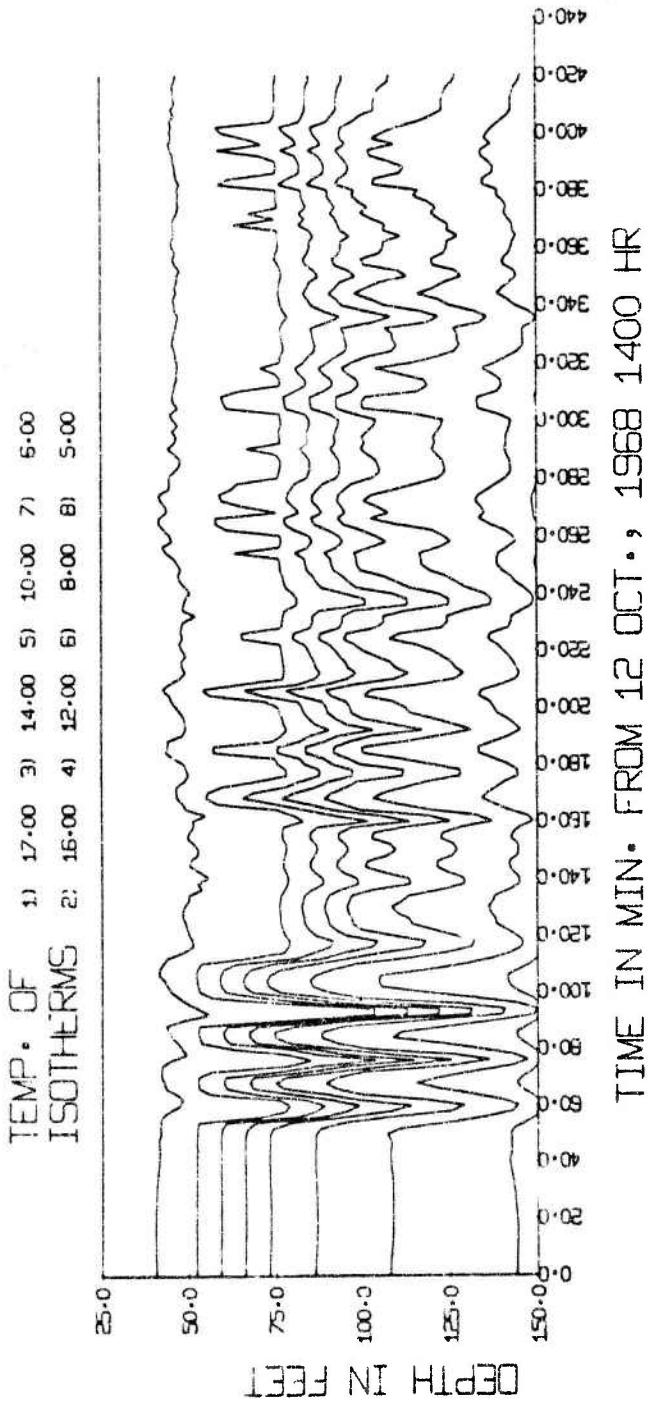

Figure 57. Isotherm depths for surge of October 12, 1968 (figure 39).

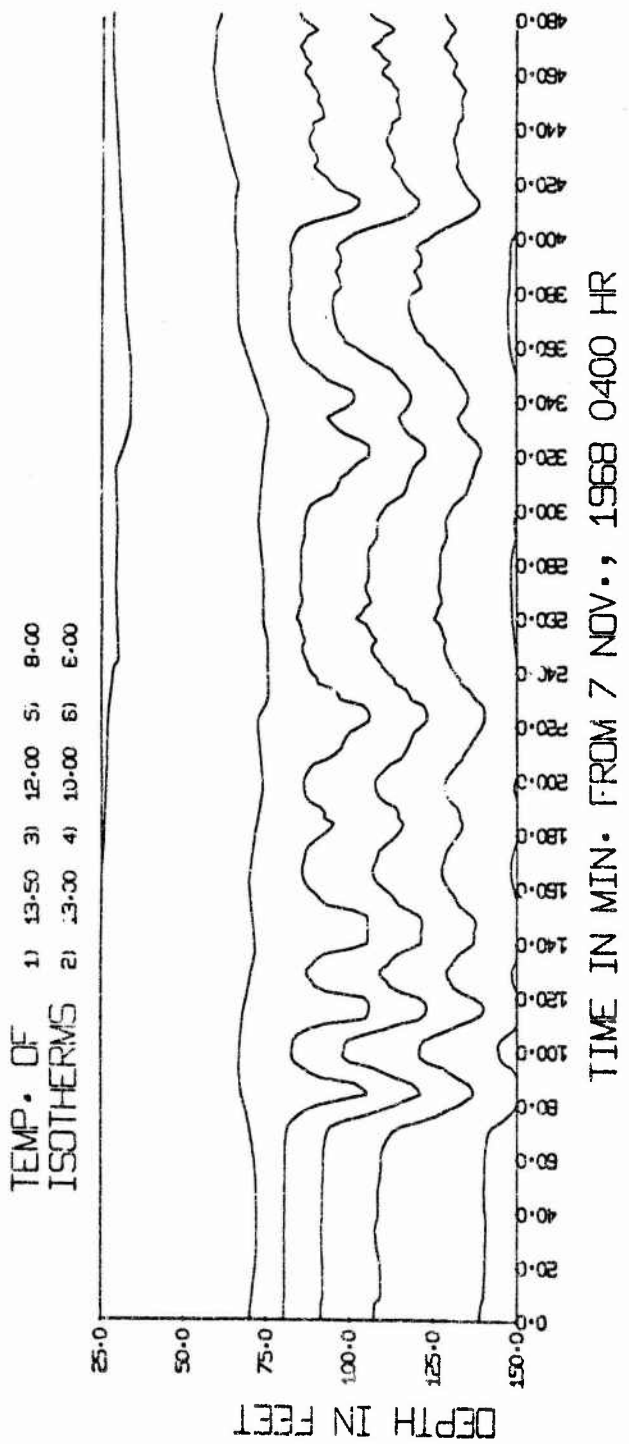

Figure 58. Isotherm depths for surge of November 7, 1968 (Figure 49).

in the tank model (Figure 17).

Power spectra of the short-period wave trains were obtained for three of the surges seen in 1969. Twenty hours of data at one-minute intervals, beginning shortly before the surge was seen, were used to obtain the spectra. Figure 59 shows the power spectrum of temperature at 50 feet for the surge of August 18, 1969 seen in Figure 28. There is a spectral peak at 15.0 minutes which is close to the period measured from the records, 14.1 minutes. The power spectrum of October 13, 1969 at 75 feet is shown in Figure 60. There are two peaks seen on this spectrum; the first at 26.67 minutes is close to that measured for the initial oscillations, while the second peak at 10.91 minutes corresponds to the period of the oscillations seen later during this surge (see Figure 40). The power spectrum at 150 feet of the surge of November 4, 1969 (Figure 48) is shown in Figure 61. There is a peak at 40.0 minutes, which corresponds well with the measured period of 40.3 minutes. In all three spectra the peaks discussed are not above the background by much more than the 90% confidence band.

The two thermistor chains used in 1971 at site 2 were used to determine the direction of travel of the surges. In all 12 surges seen that year, the initial oscillations were always seen at the south end of the SMP before they were seen at the north end (see Figures 23, 25, 26, 27, 31, 32, 34, 36, 44, 46, 51 and 53). The spacing of the two thermistor strings on the SMP, however, was not great enough to determine phase velocities accurately. Phase velocities were determined for

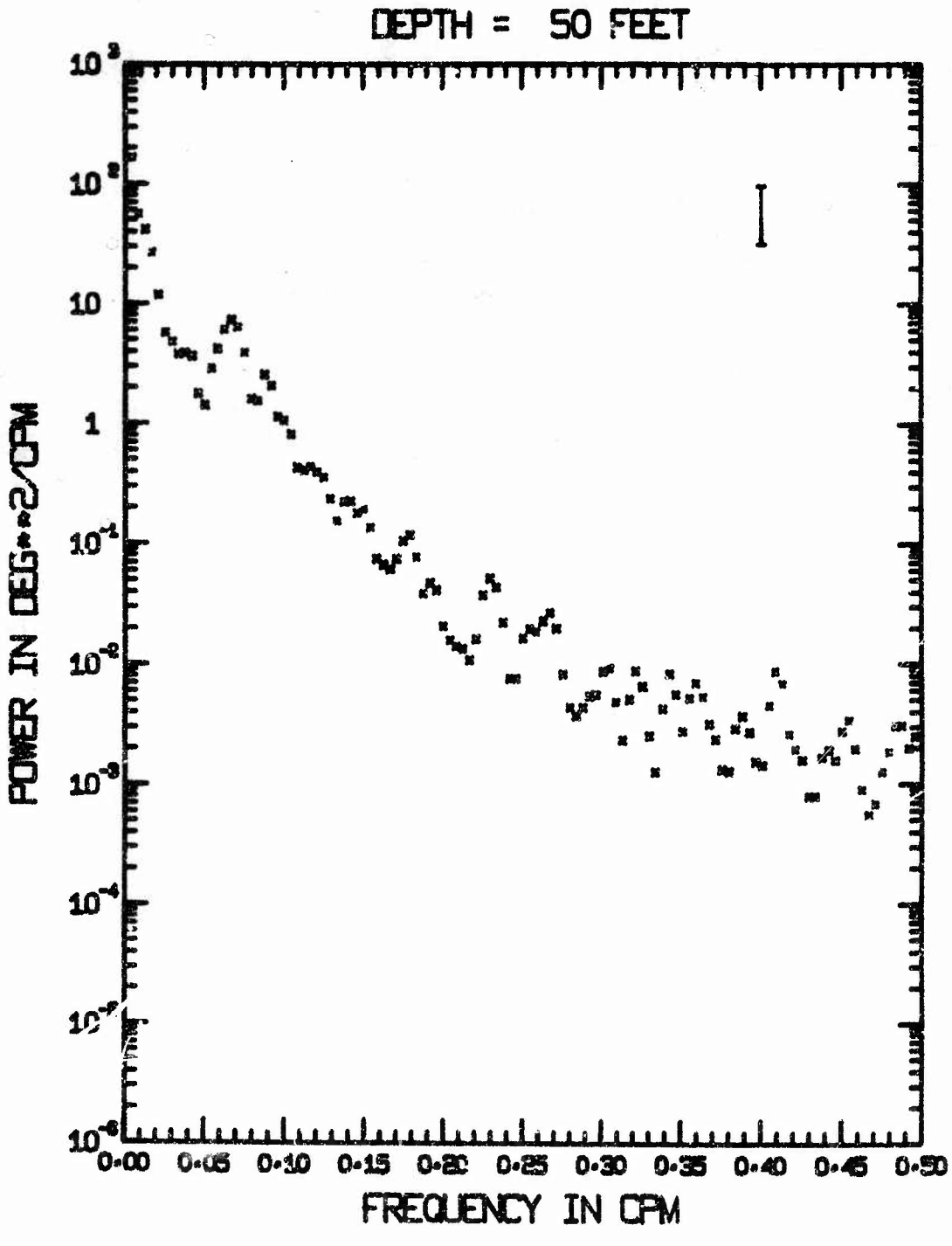

Figure 59. Power spectrum of 20 hours of data at one minute intervals beginning August 18, 1969, 1810 EST. Thermistor depth is 50 feet.

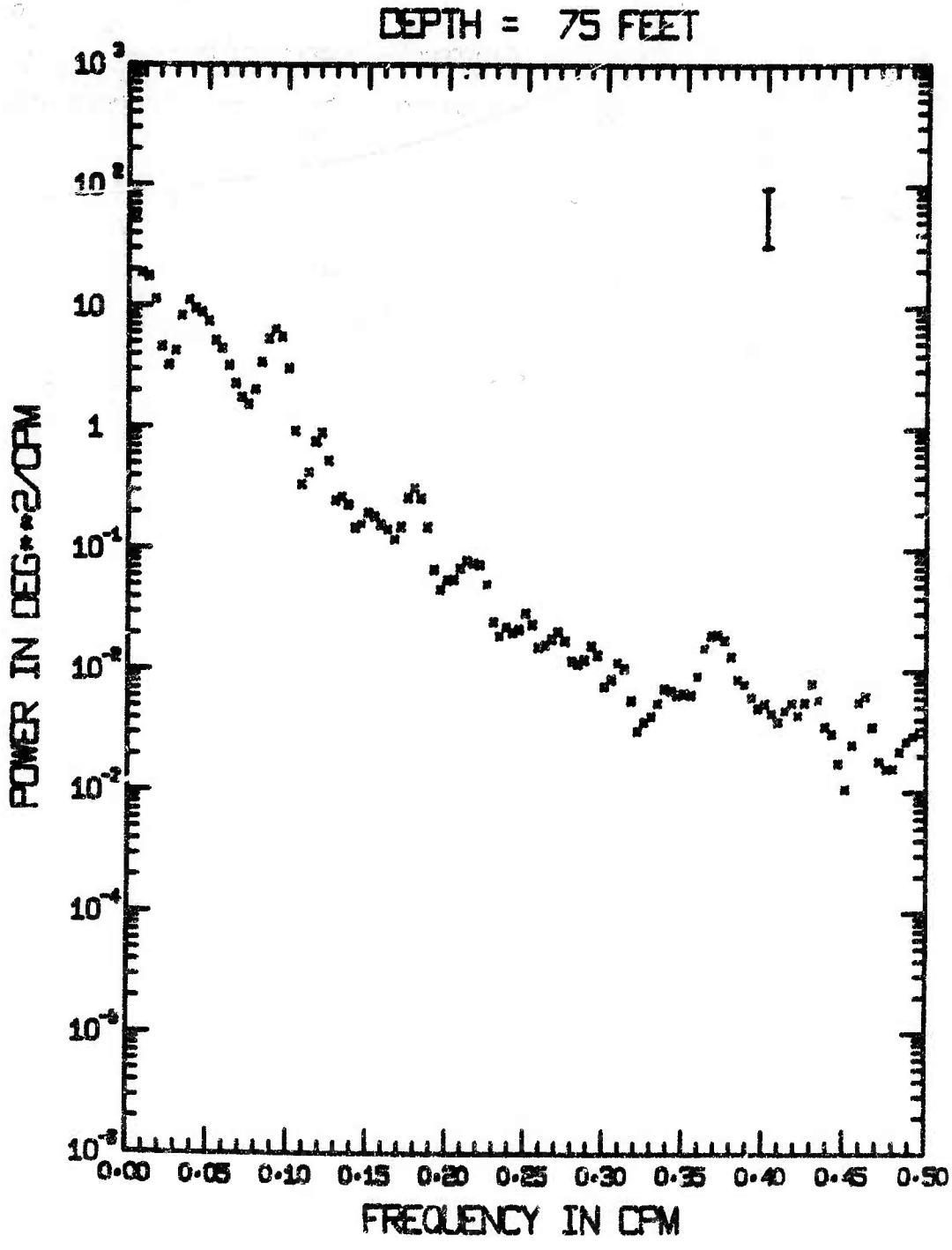

Figure 60. Power spectrum of 20 hours of data at one minute intervals beginning October 13, 1969, 0640 EST. Thermistor depth is 75 feet.

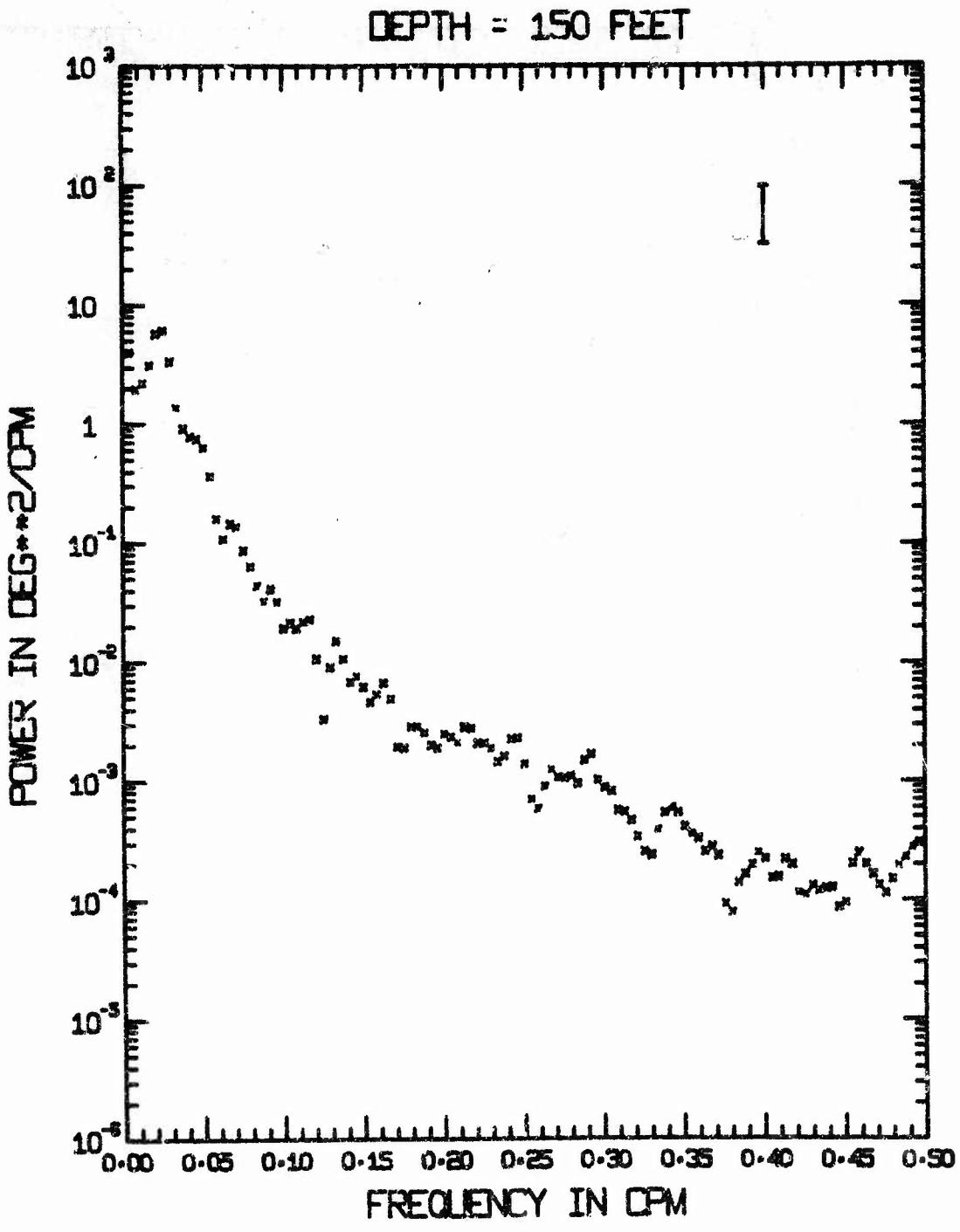

Figure 61. Power spectrum of 20 hours of data at one minute intervals beginning November 4, 1969, 1020 EST. Thermistor depth is 150 feet.

the five surges that were seen at both sites 1 and 2, and are listed in Table 3. The data for the surge of October 27, 1971 are puzzling at first glance because the arrival times of the first temperature peak give phase velocities considerably higher than those determined from the second and third peaks. Inspection of Figure 45 shows, however, that the first few oscillations of this surge are somewhat unusual. There are at least three possibilities: (1) A temperature peak is missing between the first two seen at the SMP. If this is the case, then the second peak seen at the SMP should be compared with the third at the TCP, yielding a travel time of 2 hours, 11 minutes and a phase velocity of 49.24 cm./sec. (2) The first peak seen at the SMP has emerged from the surge front during the time of travel between the TCP and SMP. If this is the case, then the second SMP peak should be compared with the first one seen at the TCP and the third SMP peak with the second TCP peak. This yields travel times ranging from 2 hours, 51 minutes to 2 hours, 57 minutes and phase velocities ranging from 36.44 to 37.72 cm./sec. (3) A combination of (1) and (2) above, i.e., a temperature peak is missing on the SMP and the first peak seen there has emerged after the surge passed the TCP. If this is the case, then the second SMP peak should be compared with the second TCP peak and the third with the third. This is listed in Table 3, the resulting phase velocities are between 42.16 and 43.25 cm./sec.

A comparison of the first three peaks seen on the records obtained at site 1 with those of site 2 suggests that the third hypothesis given above is correct, however, the compari-

TABLE 3: TRAVEL TIMES OF SURGES BETWEEN SITES 1 AND 2

Date		Arrival time (EST) Site 1	Site 2	Travel time	Speed (cm/sec) obs.	theor.
July 15, 1971	1st max	1408	1712	3 hr 04 m	35.05	
	1st min	1415	1717	3 hr 02 m	35.44	37.6
	2nd max	1422	1722	3 hr 00 m	35.83	
Oct. 23, 1971	1st max	1308	1550	2 hr 42 m	39.81	
	1st min	1318	1603	2 hr 45 m	39.09	41.2
	2nd max	1328	1612	2 hr 44 m	39.33	
Oct. 27, 1971	1st max	1121	1330	2 hr 09 m	50.00	
	1st min	1135	1345	2 hr 10 m	49.62	
	2nd max	1145	1418	2 hr 33 m	42.16	39.0
	2nd min	1156	1427	2 hr 31 m	42.72	
	3rd max	1207	1436	2 hr 29 m	43.25	
Nov. 12, 1971	1st max	1345	1645	3 hr 00 m	35.83	
	1st min	1400	1658	2 hr 58 m	36.24	
	2nd max	1415	1713	2 hr 58 m	36.24	
	2nd min	1426	1721	2 hr 55 m	36.86	30.1
	3rd max	1440	1738	2 hr 58 m	36.24	
	3rd min	1452	1750	2 hr 58 m	36.24	
Nov. 22, 1971	1st max	0200	0737	5 hr 37 m	19.16	29.1

son was not conclusive because the chart paper at the TCP ran out at the time of arrival of the fourth peak.

The observed speeds determined for the three other surges in which more than the first temperature maximum was used are internally consistent to within 1 cm./sec. Timing discrepancies between the two barges are known to be less than five minutes at the worst, so it is felt that the measured phase velocities listed in Table 3 are certainly accurate to better than ±2 cm/sec. In the last column of Table 3 are listed the theoretical travel times of the surges, calculated using linear theory and a multilayered lake model (see Appendix II). It is seen that the calculated and observed speeds are very close for the three cases (July 15, October 23 and November 12) in which the measured speeds are considered very reliable, but there does not seem to be a simple relationship between the two. In particular, the Froude number, which is the ratio of the surge speed to that of a linear wave and which theoretically is always greater than one, would be less than unity for two of those surges. A possible explanation of this discrepancy will be attempted in the following section.

Theoretical and experimental studies of non-linear waves

It has already been shown that the long-period internal waves seen in Figures 9 through 22 are non-linear surges and cannot be understood in terms of simple linear models. What of the short-period wave trains seen in Figures 23 through 53? Many of the initial oscillations seen, while not sinosoidal in shape, are symmetrical with respect to time. Many also have a period that can be measured (Table 2). A first attempt

was made to understand the wave trains as linear waves generated by the non-linear surge and coupled to it by the phase velocity. A matrix technique similar to that employed by Haskell (1951) for Rayleigh and Love waves was used to obtain dispersion curves for internal waves in many-layered fluids. In the course of the investigation, however, it became evident that the wave trains associated with the surges are non-linear and the matrix method developed did not apply. Because this method can be useful in other problems of internal waves, a summary of the technique is given in Appendix II.

As pointed out earlier in this report, a number of authors have seen short-period wave trains travelling with internal surges generated in tank models. Figure 17 is a photograph of one case. Several authors have theoretically investigated the evolution of an initial perturbation on the surface of a fluid using the Korteweg-de Vries equation (Korteweg and de Vries, 1895) and have shown that wave trains similar to those seen in laboratory experiments and in Seneca Lake develop from a surge in certain circumstances. Peregrine (1966) used a numerical technique to investigate the equations and shows figures illustrating the results. In particular, he shows the growth and development of undular bores under several initial conditions (see his Figures 3 through 6 which look very much like the surges seen in Seneca Lake).

Witting (1972) classified five types of surface bores. He shows photographs and illustrative figures of several types. The different types of bores occupy separate areas on a graph of bore strength (which is measured by the Froude number, F_1,

which is the ratio of the bore speed to that of a linear wave) versus the depth of water. A Froude number can be calculated for the three surges listed in Table 3 whose measured speeds are considered reliable, but two of them would be less than one. A possible explanation of the situation is suggested by the positions of the two observation sites in Figure 1. It is seen from the map that the sites are near a bend in the lake. A straight-line distance between the sites was used to obtain the phase velocities listed in Table 3. It is probable, however, that a surge does not follow a straight line ray path between the two barges. This is shown schematically in Figure 62. In the upper portion of the figure is shown the case in which the two barges are not on the same ray path, which is assumed to be straight. In this case, the true distance travelled by a wave front would be less than that measured by a factor of the cosine of the angle between the ray path and the direct path between the barges. This would reduce the measured speeds and worsen the situation. The lower portion of the figure shows the case in which the two barges are on the same ray path but it is curved (in the figure it is a 75 degree circular arc, which has enough curvature to result in Froude numbers greater than one for the three surges being considered). In this case, the distance between the barges along the ray path would be greater than the straight-line distance and the measured speeds would be increased. The actual ray path of a surge between the two sites might be a combination of both cases. If the second predominates, the problem of Froude numbers apparently less than unity would be resolved. It is

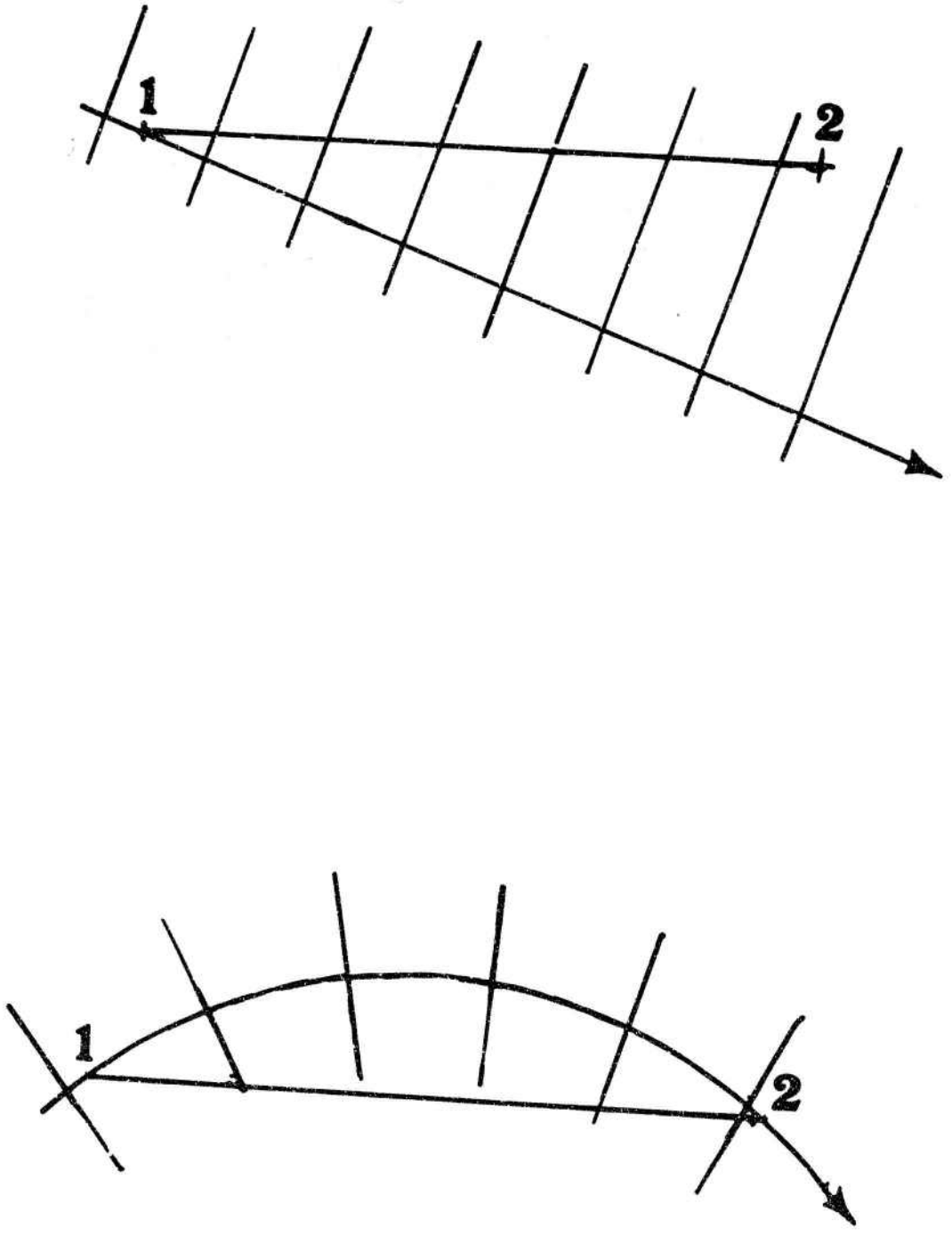

Figure 62. Two possible ray paths between the barge sites.

apparent though, that with the data obtained very little can be said about Froude numbers other than they are close to one.

Kadomtsev and Karpman (1971) discuss the evolution of an initial perturbation into a set of solitary waves or solitons. Their Figure 4, which was obtained by numerically solving the Korteweg-de Vries equation, looks much like the initial large-amplitude oscillations seen in the lake. When dissipation is included, the Korteweg-de Vries-Burgers equation results. Solutions of this equation, in addition to producing an initial train of large-amplitude waves, also result in a change in level behind the initial oscillations similar to the depression of isotherms following a surge seen in the lake. Although the evidence obtained thus far is only qualitative, it appears likely that the surges seen in Seneca Lake can be understood in terms of nonlinear waves governed by the Korteweg-de Vries equation.

In summary, the temperature data obtained in Seneca Lake, when filtered and sampled at periods of a few hours or more, look similar to that obtained from other lakes by many workers. The oscillations seen were explained as temperature seiches of the thermocline and this hypothesis seemed to explain most of the important features seen in the data. By 1953, with the publication of Mortimer's paper, the subject of long-period internal waves in long narrow lakes seemed to be well understood. However, in 1971, Thorpe showed that the internal seiche in Loch Ness appeared to be a nonlinear surge rather than a simple standing wave controlled by the dimensions of the lake.

The data obtained from Seneca Lake show conclusively that in this lake, at least, there are large-amplitude undular surges that appear to be the internal analogues of the surface bores investigated by several authors. It is therefore apparent that a whole new avenue of investigation is opening up.

Wind measurements

In the classic description of internal seiches in lakes, the wind plays a role of initially inclining the isotherms which then respond by rocking back and forth at the natural period of the lake. Briefly stated, the sequence of events is, according to this theory: (1) a wind blows roughly parallel to the long axis of the lake for a sufficient time to (2) blow a sizeable amount of the warm surface water to one end of the lake with the colder, deeper water replacing it at the other end. The thermocline is therefore tilted, the tilt maintained by the opposition of the pressure gradient which tends to restore the thermocline to the horizontal and the wind stress which tends to push even more warm water down the lake; (3) after a period of time, the wind dies down. The tilted thermocline is no longer a stable condition and (in most cases) it oscillates up and down at the ends of the lake with a node near the center. These simple harmonic oscillations die out owing to frictional effects. Although the internal waves seen in Seneca Lake have the character of internal surges travelling up the lake rather than a linear oscillations of the thermocline, wind stress would still appear to be the most likely cause of the initial imbalance that starts the surge going.

In order to test the theory, winds were monitored at site 1 (Figure 1) for 15 days in August, 1970, and for two periods in 1971, totalling 63 days. Wind speed and direction were recorded on strip charts and digitized at one-hour intervals. No surges were seen during the time wind data was collected in 1970 but the wind data itself is interesting. Regular oscillations, with a period of 24 hours are seen especially in the north-south component (see Figure 63). These are very prominent between the 11th and 16th (days 222 to 228 in the figure) of August. A close examination of the data reveals maximum north velocities in the afternoons (usually before 6 p.m.), maximum south velocities in the mornings (usually around 6 a.m.) with zero north-south velocities before noon and midnight. The geography of the region offers a reasonable explanation of the wind pattern. Seneca Lake is in a valley oriented north-south and is between the mountains of the Northern Appalachian Plateau to the south and the plain to the south of Lake Ontario to the north. In the afternoon, the north winds are coming from the direction of the plains and are blowing up the valley. In the early morning, the south winds are coming from the direction of the mountains and are blowing down the valley. This is just what is expected in the classic mountain and valley wind (see, for example, Defant, 1951) and it is therefore concluded that this is the normal wind pattern of the lake and is seen whenever it is not obscured by "meteorological" winds.

Figure 64 shows the wind data for 25 days beginning June 30, 1971. The mountain-valley wind is also seen at times in

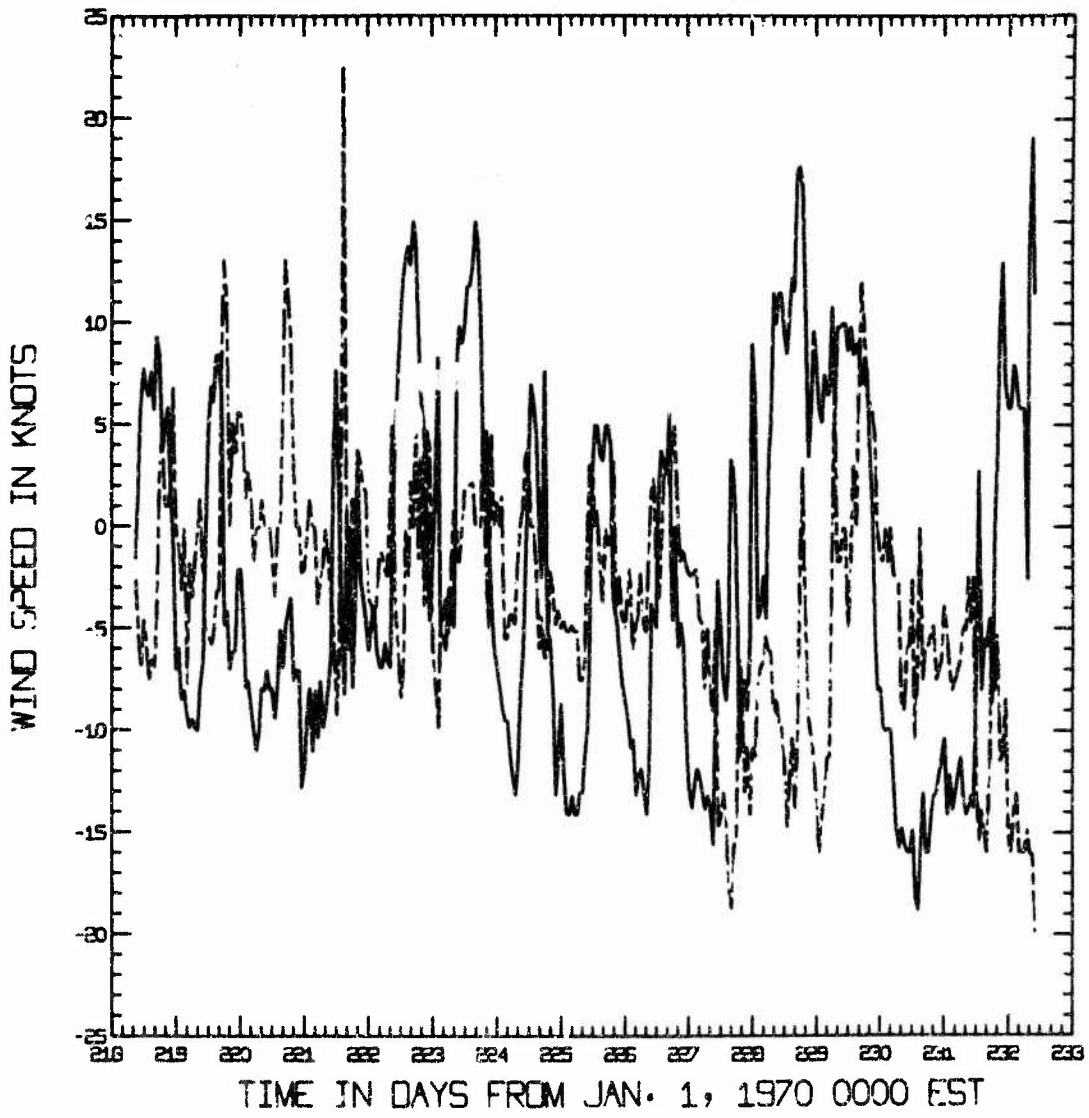

Figure 63. Wind speeds recorded at barge site 1 from August 7, 1970 through August 21, 1970. The north-south component is drawn in solid line, the east-west component in dashed line. Positive values are north and east.

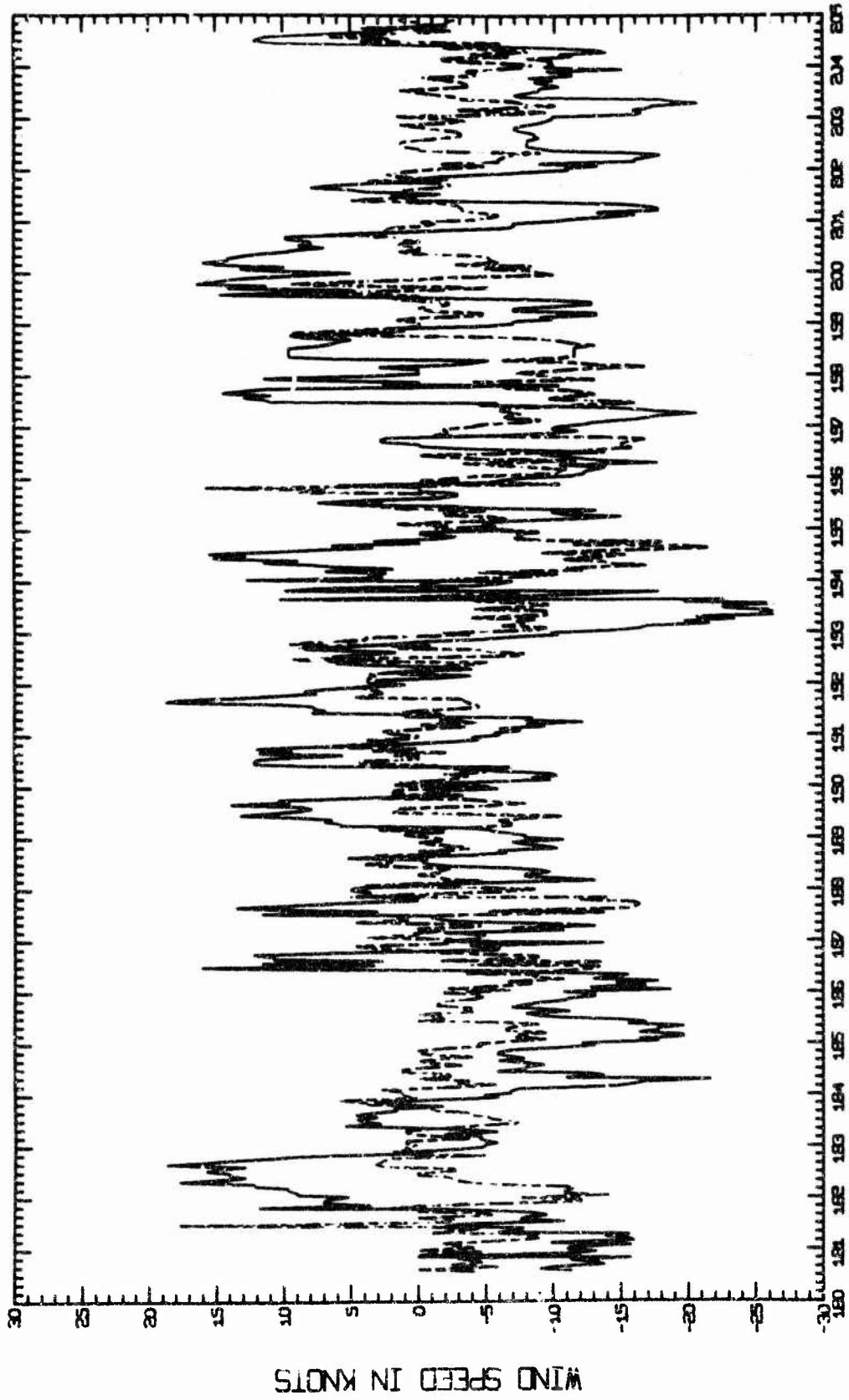

Figure 64. Wind speeds recorded at barge site 1 from June 30, 1971 through July 24, 1971. Symbols and conventions as per Figure 63.

this figure (e.g., from day 189 through 191). Only one surge was seen during the period shown in Figure 64; it passed site 2 on July 15 (day 195) at 1712 EST. Figure 65 shows the wind data for 38 days beginning October 21. Times when surges were seen are marked with arrows; solid ones for those seen at both sites and dashed arrows for surges seen only at site 1 (of the four surges seen only at site 1, three were probably seen at site 2 but could not be definitely correlated because difficulties with the chart drive of the recorder at site 2 made it impossible to determine arrival times at that site).

It is apparent that a simple relationship between the wind and the internal surges does not exist. Some surges occur after strong wind activity, others after weak activity, while some strong winds do not produce surges at all.

Another possible mechanism for piling up warm water at one end of the lake is the atmospheric pressure gradient. A pressure difference of one millibar between the ends of the lake would produce an equilibrium difference in surface level of about one centimeter. Because the density difference between the epilimnion and the hypolimnion is on the order of 10^{-3} times the density of water, a difference of about 10 meters in the depth of the thermocline at the two ends of the lake could be produced. While the usual atmospheric pressure differences along the lake is less than one millibar, differences of that magnitude are not uncommon. However, as with wind speeds, no relationship was found between the pressure gradient and surge generation.

It is interesting that all the surges for which a direc-

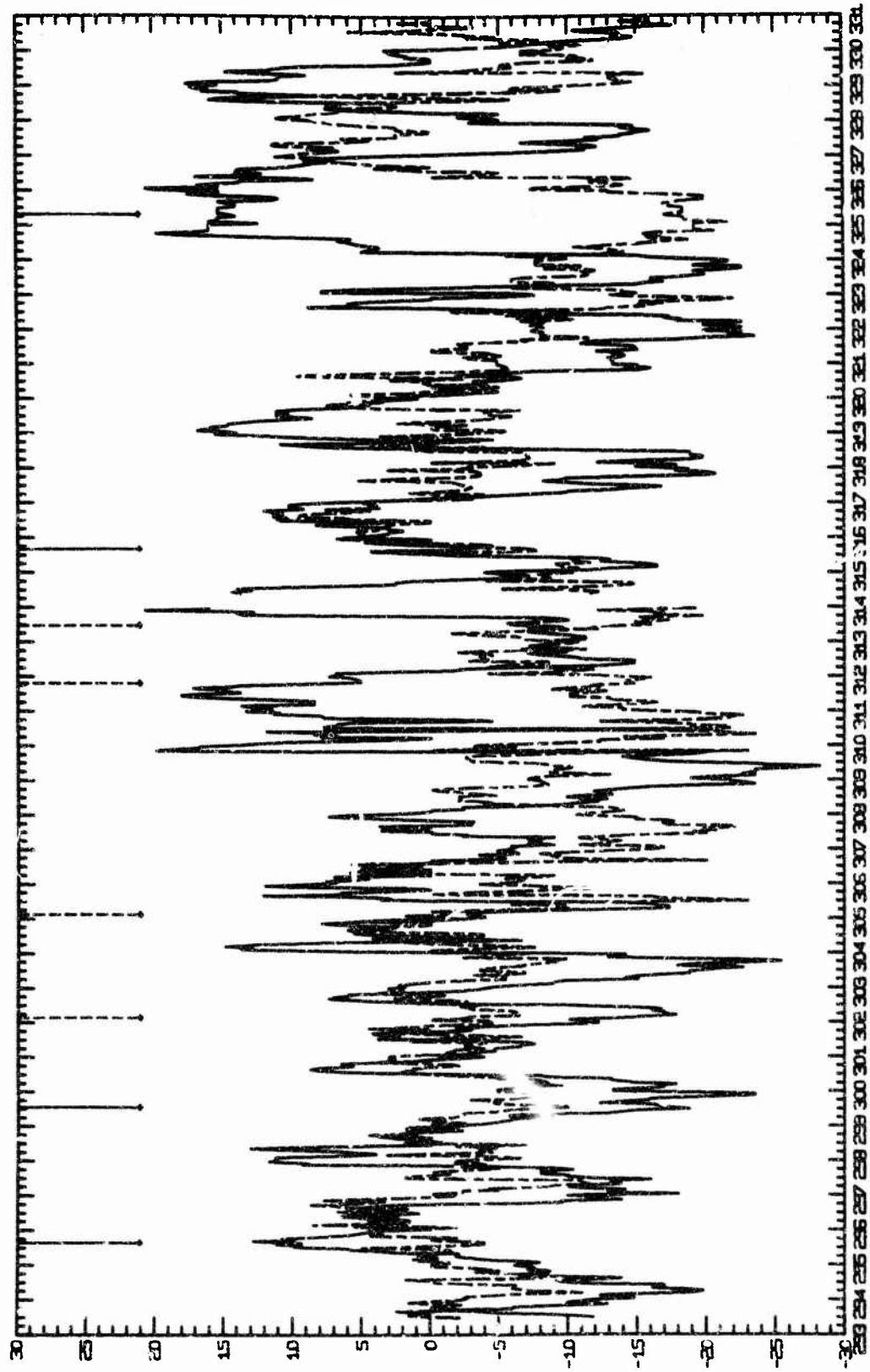

Figure 65. Wind speeds recorded at barge site 1 from October 21, 1971 through November 27, 1971. Symbols and conventions as per Figure 63. Times when surges were seen are shown by arrows; those seen at site 1 only are dashed, those seen at both sites are solid.

tion of travel has been determined were found to be moving north. The thermocline is in continuous motion (see Figures 9 through 11 and 18 through 22). It is possible that the undular surges only develop at the southern end of the lake when the wind re-enforces a weak surge already travelling the lake. The topography of the lake bottom is very different at the two ends (Figure 66). The southern part is deeper than the northern and the slope is much steeper. Less than 0.6 miles from the south end of the lake, the water is over 200 feet deep and depths over 400 feet are encountered about 1.75 miles from the southern end. The slope is much gentler at the northern end; 0.6 miles from shore the water is less than 25 feet deep. Water depths in excess of 200 feet are not encountered until about 3.7 miles from the northern end and 400 foot depths about 7.8 miles. Thus, a weak surge travelling north encounters gradually shoalling water, while one travelling to the south practically hits a wall. It might take the proper combination of the strength of a weak surge, its reflection at the southern end of the lake, re-enforced by proper winds to produce the large-amplitude undular surges seen near the center of the lake.

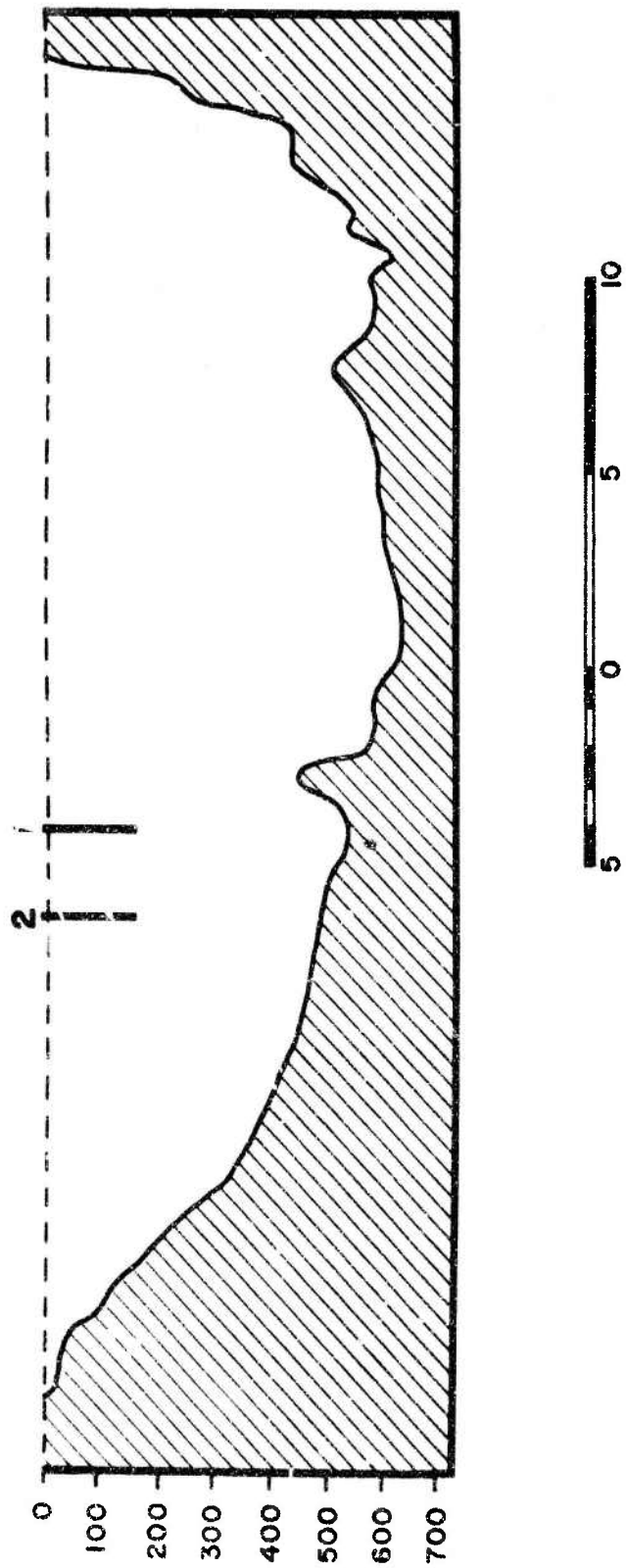

Figure 66. Longitudinal section of Seneca Lake. North is to the left. Sites 1 and 2 as per Figure 1. Depths are in feet, distance in miles.

CONCLUSION

Temperature measurements obtained during the course of four years have shed considerable light on the behavior of Seneca Lake. Bathythermograph records have been used to reconstruct the yearly temperature cycle. These records indicate that the lake is probably freely circulating throughout much of the winter although the temperature is below that of maximum density water. These records have also been used to calculate heat budgets. The heat budget curves (Figures 4 through 8) indicate that as the upper layers of the lake lose heat in autumn, lower layers are warming. This transfer of heat downward may by accomplished to a large extent by the large-amplitude internal surges seen in late summer and early fall.

These large-amplitude internal waves are the most striking feature of the temperature data seen. Although similar in amplitude to the internal "temperature" seiches seen in long, narrow lakes since the beginning of this century, the internal waves seen in Seneca Lake are non-linear and have large-amplitude, short-period wave trains associated with them. They closely resemble undular surges that have recently been investigated both theoretically and with tank models. It is concluded that the internal waves seen in the lake are internal analogues of these surface non-linear waves and are called internal undular surges.

The consequences of these internal surges have not been investigated but they could be of major importance. There is

probably much turbulent motion in the wave train associated with a surge. This turbulence may play an important role in the downward transport of heat seen in late summer and early autumn. It may also bring nutrients from the lower layers into the upper mixed layer, renew oxygen, etc. The consequences to the life forms in the lake of the large and rapid oscillations of isothermal surfaces could be profound.

The wind data collected in 1971 do not reveal a simple mechanism for the generation of the internal surges. Because all of the surges whose direction could be determined were travelling north, bottom topography (which is very different at the two ends of the lake) must play an important role.

The non-linear internal undular surges seen in Seneca Lake reopen an area of investigation that for many years limnologists felt was solved except for minor details. Are the surges seen in this lake an unusual occurrence or are they the general rule for narrow lakes? Thorpe (1971) has identified non-linear surges in Loch Ness but has not seen wave trains, either because his instruments were not sensitive enough or because they do not exist in that lake. Other lakes must be investigated.

Work should also continue in Seneca Lake. Because of the two barge sites near the center of the lake, data collection there is relatively easy. This should be augmented by data collected at other points in the lake so that surges could be followed as they travel through it. Investigators have been using small tanks to model nature. In Seneca Lake, nature has given us a large tank in a convenient location to

play with. Advantage should be taken of this.

Appendix I. Tables of Heat Budget Data

TABLE I.1: HEAT BUDGET DATA - 1968

Date	Total heat in calories x 10^{15} (layer depths in meters) 0-20	20-40	40-70	70-188.4	Total	Lake temp (°C)	Heat/area (cal/cm^2x10^3)
Feb 16	10.411	8.961	11.189	24.180	54.741	3.522	31.211
May 13	17.619	13.445	15.931	26.352	73.347	4.720	41.819
May 23	24.247	16.669	16.937	28.185	86.038	5.536	49.056
Jun 3	27.415	16.672	16.898	26.032	87.016	5.599	49.613
Jun 13	28.767	16.782	15.973	25.937	87.459	5.628	49.866
Jun 25	39.615	18.302	16.188	27.681	101.786	6.550	58.035
Jul 1	46.320	20.540	16.101	27.259	110.221	7.092	62.844
Jul 11	48.257	20.806	17.426	28.715	115.205	7.413	65.686
Aug 1	57.342	23.188	15.531	27.532	124.192	7.992	70.810
Aug 15	60.714	19.569	16.285	27.606	124.174	7.990	70.799
Sep 3	60.851	22.785	17.297	27.996	128.930	8.296	73.51[illegible]
Sep 18	59.720	25.297	16.653	28.556	130.227	8.380	74.250
Sep 27	60.446	30.667	16.225	27.450	134.788	8.673	76.851
Oct 15	50.286	31.920	18.267	27.899	128.372	8.261	73.193
Nov 1	39.911	31.329	18.888	28.744	118.872	7.649	67.776
Nov 12	34.997	27.645	18.321	28.130	109.093	7.020	62.200
Nov 19	26.896	22.977	23.148	31.520	104.542	6.727	59.606
Dec 13	18.311	15.612	19.232	33.070	86.224	5.548	49.162

TABLE I.2: HEAT BUDGET DATA - 1969

Date	Total heat in calories x 10^{15} (layer depths in meters) 0-20	20-40	40-70	70-188.4	Total	Lake temp (°C)	Heat/area (cal/cm^2x10^3)
Apr 17	10.411	8.961	11.189	21.356	51.917	3.340	29.601
Jun 11	32.933	15.024	14.484	22.785	85.226	5.484	48.592
Jun 19	40.234	18.981	16.934	26.313	102.402	6.589	58.385
Jun 23	38.589	16.970	15.242	26.163	96.964	6.239	55.285
Jul 28	54.713	20.476	17.433	27.123	119.746	7.705	68.274
Aug 12	59.547	20.813	17.067	27.415	124.843	8.033	71.180
Aug 19	62.044	17.175	14.800	25.029	119.048	7.661	67.877
Sep 2	60.390	21.895	16.147	27.555	131.987	8.493	75.254
Sep 10	64.167	24.155	15.741	27.449	131.512	8.463	74.983
Sep 22	57.944	20.565	16.538	28.113	123.161	7.925	70.222
Oct 1	51.547	27.608	17.493	26.672	123.320	7.935	70.312
Oct 20	41.230	31.924	21.066	26.890	121.110	7.793	69.052
Nov 5	31.581	25.674	21.577	27.649	106.481	6.852	60.711
Nov 20	26.029	22.403	27.955	35.296	111.682	7.186	63.677
Dec 31	13.882	11.948	14.918	28.475	69.223	4.454	39.468

TABLE I.3: HEAT BUDGET DATA - 1971

Date	Total heat in calories x 10^{15} (layer depths in meters) 0-20	20-40	40-70	70-188.4	Total	Lake temp (°C)	Heat/area (cal/cm^{2}x10^3)
May 12	16.202	11.794	13.656	24.916	66.569	4.283	37.955
Jun 3	24.574	17.109	17.390	28.623	87.696	5.643	50.001
Jun 16	32.755	17.072	16.557	27.170	93.573	6.021	53.352
Jun 30	40.014	15.732	15.676	26.557	97.979	6.305	55.864
Jul 14	56.449	24.577	17.359	26.946	125.332	8.065	71.459
Jul 30	45.433	15.578	15.454	27.072	103.537	6.662	59.033
Aug 13	53.704	20.196	15.615	28.080	117.597	7.567	67.049
Sep 2	52.386	22.011	15.517	26.322	116.236	7.480	66.273
Sep 10	54.438	17.972	15.657	26.900	114.967	7.398	65.550
Sep 23	58.122	23.685	15.414	26.702	123.924	7.974	70.656
Oct 1	54.339	22.810	15.306	27.630	120.084	7.727	68.467
Oct 13	46.392	18.186	15.094	27.325	106.997	6.885	61.005
Oct 22	46.676	23.947	15.494	26.944	113.060	7.275	64.462
Nov 1	47.539	34.469	17.619	25.996	125.624	8.084	71.626
Nov 10	38.175	32.629	27.812	25.542	124.159	7.989	70.790
Nov 20	34.088	28.168	24.161	26.462	112.878	7.263	64.359
Dec 1	24.952	21.296	21.583	26.155	93.985	6.048	53.587

Appendix II. Linear Internal Waves in Multilayered Fluids - A Matrix Technique of Obtain Dispersion Curves

The first attempt to understand the short-period wave trains seen in Seneca Lake used a linear theory. A matrix method similar to that of Haskell (1951) was developed and a Fortran program was written to obtain dispersion curves for internal waves in a many-layered fluid. As work progressed on the Seneca Lake data it became increasingly evident that the wave trains seen could not be treated as linear waves, so this approach was abandoned. It is felt, however, that the techniques that were developed, especially the Fortran program, can be of use in other problems and are presented below.

II.a. To derive a differential equation for internal waves

The derivation of the differential equation used to get a period equation can be found in a number of textbooks (e.g., Phillips, 1966). Starting with a fluid in an unperturbed state, the hydrostatic equation is:

$$\frac{\partial p_0}{\partial z} + g\rho_0 = 0$$

$$p_0 = p_0(z) \qquad \rho_0 = \rho_0(z) \tag{II.a.1}$$

The linearized, frictionless equations of motion are (neglecting second order terms):

$$\frac{\partial u}{\partial t} - fv = -\frac{1}{\rho_0}\frac{\partial p}{\partial x} \qquad \text{(II.a.2)}$$

$$\frac{\partial v}{\partial t} + fu = -\frac{1}{\rho_0}\frac{\partial p}{\partial y} \qquad \text{(II.a.3)}$$

$$\frac{\partial w}{\partial t} + \frac{g}{\rho_0}\rho = -\frac{1}{\rho_0}\frac{\partial p}{\partial z} \qquad \text{(II.a.4)}$$

with $f = 2\,\Omega \sin\lambda$ (Ω the angular velocity of rotation of the earth and λ the latitude).

The fluid is assumed to be incompressible:

$$\frac{D\rho}{Dt} = 0 = \frac{\partial \rho}{\partial t} + \frac{\partial \rho_0}{\partial z} w \qquad \text{(II.a.5)}$$

The equation of continuity is:

$$\frac{\partial u}{\partial x} + \frac{\partial v}{\partial y} + \frac{\partial w}{\partial z} = 0 \qquad \text{(II.a.6)}$$

When the fluid is in a perturbed state the density and pressure will be:

$$p = p_0 + p' \qquad p' = p'(t,x,y,z)$$

$$\rho = \rho_0 + \rho' \qquad \rho' = \rho'(t,x.y,z)$$

Equations (II.a.2) through (II.a.5) become:

$$\frac{\partial u}{\partial t} - fv = -\frac{1}{\rho_0}\frac{\partial p'}{\partial x} \qquad \text{(II.a.2a)}$$

$$\frac{\partial v}{\partial t} + fu = -\frac{1}{\rho_0}\frac{\partial p'}{\partial y} \qquad \text{(II.a.3a)}$$

$$\frac{\partial w}{\partial t} + g\frac{\rho'}{\rho_0} = -\frac{1}{\rho_0}\frac{\partial p'}{\partial z} \qquad \text{(II.a.4a)}$$

$$\frac{\partial \rho'}{\partial t} + \frac{\partial \rho_0}{\partial z} w = 0 \qquad \text{(II.a.5a)}$$

Equations (II.a.4a) and II.a.5a) are used to eliminate :

$$\frac{\rho_0}{g}\frac{\partial^2 w}{\partial t^2} = \frac{\partial \rho_0}{\partial z} w - \frac{1}{g}\frac{\partial^2 p'}{\partial z \partial t} \qquad \text{(II.a.7)}$$

By combining equations (II.a.2a) with (II.a.7) and (II.a.3a) with (II.a.7) two equations can be obtained:

$$\frac{\partial^3 w}{\partial t^2 \partial x} - \frac{\partial^3 u}{\partial t^2 \partial z} + f\frac{\partial^2 v}{\partial t \partial z} + N^2\frac{\partial w}{\partial x} = 0 \qquad \text{(II.a.8)}$$

$$\frac{\partial^3 w}{\partial t^2 \partial y} - \frac{\partial^3 v}{\partial t^2 \partial z} - f\frac{\partial^2 u}{\partial t \partial z} + N^2\frac{\partial w}{\partial y} = 0 \qquad \text{(II.a.9)}$$

with $N^2 = -\frac{g}{\rho_0}\frac{\partial \rho_0}{\partial z}$

N is a function of z only, has the dimensions of seconds^{-1} and is called the Brunt-Vaisala frequency.

With the equation of continuity, both u and v can be eliminated from equations (II.a.8) and (II.a.9) to yield:

$$\frac{\partial}{\partial t^2}\left[\frac{\partial^2 w}{\partial x^2} + \frac{\partial^2 w}{\partial y^2} + \frac{\partial^2 w}{\partial z^2}\right] + N^2\left[\frac{\partial^2 w}{\partial x^2} + \frac{\partial^2 w}{\partial y^2}\right] \qquad \text{(II.a.10)}$$

$$+ f^2\frac{\partial^2 w}{\partial z^2} = 0$$

It is assumed that a wave solution for the vertical velocity w in the horizontal plane exists:

$$w(x,y,z,t) = e^{i(\omega t - k_x x - k_y y)}\phi(z)$$

with k_x and k_y the wave numbers in the x and y directions. Equation (II.a.10) then reduces to:

$$(\omega^2 - N^2)(k_x^2 + k_y^2)\phi + (f^2 - \omega^2)\frac{\partial^2 \phi}{\partial z^2} = 0 \qquad \text{(II.a.11)}$$

Rearranging terms and calling the wave number in the direction of travel, k, the differential equation is obtained:

$$\frac{\partial^2 \phi}{\partial z^2} + k^2\frac{\omega^2 - N^2}{f^2 - \omega^2}\phi = 0 \qquad \text{(II.a.12)}$$

with $k^2 = k_x^2 + k_y^2$

II.b. To obtain a period equation for the many-layered model

using a matrix method

The derivation of a period equation for internal waves in a fluid of many layers using a matrix method is similar to a method developed by Haskell (1951) for surface seismic waves. We start with a fluid of finite depth with a rigid bottom and take the z axis pointing positively down. In general, N, the Brunt-Vaisala frequency will be a continuous function of the depth, z. This will be approximated by assuming the fluid to contain n layers, each with a constant Vaisala frequency and a discontinuity of the Vaisala frequency across layers. We wish to solve the differential equation:

$$\frac{d^2\phi}{dz^2} + k^2 \phi \left(\frac{\omega^2-N^2}{f^2-\omega^2}\right) = 0 \qquad \text{(II.b.1)}$$

with N constant.

In layer p we have:

$$\frac{d^2\phi}{dz^2} + k^2 \phi \left(\frac{\omega^2- N_p^2}{f^2- \omega^2}\right) = 0 \qquad \text{(II.b.2)}$$

whose solution is:

$$\phi = A_p e^{m_p z} + B_p e^{-m_p z} \qquad \text{(II.b.3)}$$

with

$$m_p = k \left(\frac{\omega^2-N_p^2}{f^2-\omega^2}\right)^{\frac{1}{2}} \qquad \text{(II.b.4)}$$

For $\omega > f$, m_p will be real for $\omega > N_p$ and imaginary for $\omega < N_p$. Taking the derivative of ϕ with respect to z, which will be denoted $\dot{\phi}$, we obtain:

$$\frac{d\phi}{dz} = \dot{\phi} = m_p A_p e^{m_p z} - m_p B_p e^{-m_p z} \qquad \text{(II.b.5)}$$

Layer p with thickness h_p is bounded by the (p-1) interface on top and the p interface on the bottom. Coordinates can be translated so that the origin of the z axis is on the (p-1) interface (this only changes the constants A_p and B_p which will drop out of the results). At the (p-1) interface we have:

$$\phi_{p-1} = A_p + B_p \tag{II.b.6}$$

$$\dot{\phi}_{p-1} = m_p A_p - m_p B_p \tag{II.b.7}$$

This can be written in matrix form as:

$$(\phi_{p-1}, \dot{\phi}_{p-1}) = E_p(A_p, B_p) \tag{II.b.8}$$

with E_p the matrix:

$$E_p = \begin{bmatrix} 1 & 1 \\ m_p & -m_p \end{bmatrix} \tag{II.b.9}$$

Written out, equation (II.b.8) is:

$$\begin{bmatrix} \phi_{p-1} \\ \dot{\phi}_{p-1} \end{bmatrix} = \begin{bmatrix} 1 & 1 \\ m_p & -m_p \end{bmatrix} \begin{bmatrix} A_p \\ B_p \end{bmatrix} \tag{II.b.8a}$$

At the p interface, $z=h_p$ and:

$$\phi_p = A_p e^{m_p h_p} + B_p e^{-m_p h_p} \tag{II.b.10}$$

$$\dot{\phi}_p = m_p A_p e^{m_p h_p} - m_p B_p e^{-m_p h_p} \tag{II.b.11}$$

or in matrix form:

$$(\phi_p, \dot{\phi}_p) = D_p(A_p, B_p) \tag{II.b.12}$$

with D_p the matrix:

$$D_p = \begin{bmatrix} e^{m_p h_p} & e^{-m_p h_p} \\ m_p e^{m_p h_p} & -m_p e^{-m_p h_p} \end{bmatrix} \qquad \text{(II.b.13)}$$

Combining equations (II.b.8) and (II.b.12) to eliminate A_p and B_p results in:

$$(A_p, B_p) = E_p^{-1} (\phi_{p-1}, \dot{\phi}_{p-1}) = D_p^{-1} (\phi_p, \dot{\phi}_p) \qquad \text{(II.b.14)}$$

or

$$(\phi_p, \dot{\phi}_p) = D_p E_p^{-1} (\phi_{p-1}, \dot{\phi}_{p-1}) \qquad \text{(II.b.15)}$$

with:

$$E_p^{-1} = \begin{bmatrix} \frac{1}{2} & \frac{1}{2m_p} \\ \frac{1}{2} & -\frac{1}{2m_p} \end{bmatrix} \qquad \text{(II.b.16)}$$

We define a new quantity, $a_p = D_p E_p^{-1}$:

$$a_p = \begin{bmatrix} a_{p_{11}} & a_{p_{12}} \\ a_{p_{21}} & a_{p_{22}} \end{bmatrix} \qquad \text{(II.b.17)}$$

The terms of the matrix a_p will be hyperbolic sines and cosines when m_p is real and trigonometric sines and cosines when m_p is imaginary. As an illustration, consider the matrix element $(a_p)_{11}$:

$$(a_p)_{11} = \frac{1}{2}(e^{m_p h_p} + e^{-m_p h_p}) \qquad \text{(II.b.18)}$$

For m_p real:

$$(a_p)_{11} = \cosh(m_p h_p) \qquad \text{(II.b.19)}$$

For m_p imaginary:

$$(a_p)_{11} = \cos(m_p' h_p) \qquad \text{(II.b.20)}$$

with

$$m_p' = -im_p = k\left(\frac{N^2-\omega^2}{\omega^2-f^2}\right)^{\frac{1}{2}} \qquad \text{(II.b.21)}$$

We therefore have the equation:

$$(\phi_p, \dot{\phi}_p) = a_p(\phi_{p-1}, \dot{\phi}_{p-1}) \qquad \text{(II.b.22)}$$

In a similar manner we can obtain for the (p-1) layer, of thickness h_{p-1} and Vaisala frequency N_{p-1} and bounded by the (p-2) and (p-1) interfaces, the equation:

$$(\phi_{p-1}, \dot{\phi}_{p-1}) = a_{p-1}\,(\phi_{p-2}, \dot{\phi}_{p-2}) \qquad \text{(II.b.23)}$$

In equation (II.b.22), ϕ_{p-1} and $\dot{\phi}_{p-1}$ refer to the values of ϕ and $\dot{\phi}$ of <u>layer p</u> at interface (p-1), while in equation (II.b.23) they refer to the values of ϕ and $\dot{\phi}$ of <u>layer (p-1)</u> at interface (p-1). Because we want (as boundary conditions) both ϕ and $\dot{\phi}$ to be continuous across interfaces between layers, the values of ϕ_{p-1} and $\dot{\phi}_{p-1}$ are the same for equations (II.b.22) and (II.b.23) and we do not have to denote which layer they refer to, as long as we use their values at the interfaces only. Equations (II.b.22) and (II.b.23) can be combined to obtain:

$$(\phi_p, \dot{\phi}_p) = a_p a_{p-1}\,(\phi_{p-2}, \dot{\phi}_{p-2}) \qquad \text{(II.b.24)}$$

with:

$$a_p a_{p-1} = \begin{bmatrix} (a_p)_{11} & (a_p)_{12} \\ (a_p)_{21} & (a_p)_{22} \end{bmatrix} \begin{bmatrix} (a_{p-1})_{11} & (a_{p-1})_{12} \\ a_{p-1})_{21} & (a_{p-1})_{22} \end{bmatrix} = b \qquad \text{(II.b.25)}$$

If this process is continued upward to the first layer, bounded by the 0 and 1 interfaces, and downward to the last (n) layer, bounded by the (n-1) and n interfaces, the resulting equation is:

$$(\phi_n, \dot{\phi}_n) = a_n a_{n-1} \cdots a_{p+1} a_p a_{p-1} \cdots a_2 a_1 (\phi_0, \dot{\phi}_0) \qquad \text{(II.b.26)}$$

Call the matrix product of a_i, F, i.e.:

$$F = a_n a_{n-1} \cdots a_2 a_1 = \begin{bmatrix} F_{11} & F_{12} \\ F_{21} & F_{22} \end{bmatrix} \qquad \text{(II.b.27)}$$

Using the matrix F, we have:

$$(\phi_n, \dot{\phi}_n) = F(\phi_0, \dot{\phi}_0) \qquad \text{(II.b.28)}$$

ϕ_n and ϕ_0 are the values of ϕ at the bottom and surface, respectively. ϕ_n is set equal to zero because of the rigid bottom. ϕ_0 is assumed to be zero because we are dealing with internal waves, whose surface motions are very small.

$$\phi_n = \phi_0 = 0$$

$$(0, \dot{\phi}_n) = F(0, \dot{\phi}_0) \qquad \text{(II.b.29)}$$

Equation (II.b.29) can be written out:

$$0 = 0\ F_{11} + F_{12}\ \dot{\phi}_0 \qquad \text{(II.b.30)}$$

$$\dot{\phi}_n = 0\ F_{21} + F_{22}\ \dot{\phi}_0 \qquad \text{(II.b.31)}$$

Either of the two equations can be used as a period equation. Equation (II.b.30) is chosen because it yields the simpler one:

$$F_{12} = 0 \qquad \text{(II.b.32)}$$

II.c. Fortran program

```
      IMPLICIT REAL*8 (A-H,O-Z),REAL*4 (W-Z)
      REAL*4 SOL(5,200,4),ALNG(200,4),C,PER,PERM
      DIMENSION DENS(51),ZEN(50),THKFT(50),ENPRMN(50),DATE(3)
      COMMON EN(50),THKNS(50),NLAY
      COMMON/FIXUP/FCOR,RTS(50),ABRT(50)
      DATA PI,GRAV/3.1415926536 D 0,0.980 D 3/

C     READ INPUT DATA
  200 READ(5,1) IEND,NPTS,NMODE,NLAY,IFT
C         IEND=NO. TIMES THRU LOOP IN SLVPE   NPTS=NO. OF PTS. TO CALCULATE
C     BETWEEN OMEGA=FCOR AND ENMAX   NMODE=NO. OF MODES TO BE CALCULATED
C     NLAY=NO. OF LAYERS   IFT= 1 FOR THKNS IN FT., 0 IF IN CM.
    1 FORMAT(5I5)
      READ(5,2) TF,DKK,OMGST,AKAST,AKFSH,AKPMN,DENSB
C         TF=TOLERENCE OF DEL IN SLVPE  DKK=DELTA KAPPA USED IN DELPE
C     OMGZ=LOWEST OMEGA (PROG WILL CALCULATE A KAPPA FOR OMEGA BETWEEN OMGZ AND
C     MAX VAISALA FREQ (ENMAX). IF OMGZ .LT. FCOR WILL SET OMGZ=FCOR).
C                              AKAST=STARTING (LOWEST) KAPPA   AKFSH=HIGHEST KAPPA
C     TO TEST WITH OMGST     AKPMN=MINIMUM CHANGE IN KAPPA FOR NEW MODE
C     DENSB=DENS. AT BOTTOM OF LAST (NLAY) LAYER
    2 FORMAT(7F10.5)
      READ(5,3) (DENS(I),THKNS(I),I=1,NLAY)
C         DENS(I)=DENS. AT TOP OF LAYER   THKNS(I)=THICKNESS OF LAYER, FT O  C
    3 FORMAT(5F10.5)
      READ(5,99) DATE
C     DATE IS IN FORM  (1)=YR  (2)=MO  (3)=DAY  (4)=HR  (5)=MIN
   99 FORMAT(5F10.3)

C     LADITUDE AND CORIOLIS PARAM.
      READ(5,3) ALTDG,ALTMN,ALNDG,ALNMN
      ALATDG=ALTDG+ALTMN/60.0
      FCOR=(PI/(12.0 D 0*3.6 D 3))*DSIN(ALATDG*PI/180.0 D 0)*2.0 D 0

      IF (NLAY) 1000,1000,20
   20 NLAY1=NLAY+1
      DENS(NLAY1)=DENSB
      IF (IFT) 24,24,22
   22 DO 23 I=1,NLAY
   23 THKNS(I)=12.0 D 0*2.54000D 0 0*THKNS(I)

C     CALCULATE VAISALA FREQS, FIND HIGHEST, SET SOLUTION ARRAY TO ZERO
   24 DO 124 I=1,NLAY
  124 EN(I)=DSQRT(GRAV*DLOG(DENS(I+1)/DENS(I))/THKNS(I))
      CALL MAX(ENMAX,EN,NLAY)
      JN=NPTS+1
      DO 21 I=1,5
      DO 21 J=1,JN
      DO 21 K=1,4
   21 SOL(I,J,K)=0.0 D 0

C     FIND OMGST (OMEGA HALF WAY BETWEEN OMGZ AND ENMAX ON LOG SCALE).  USES THIS
C     TO FIND THE FIRST KAPPA
```

```
      IF (FCOR .GT. OMGZ)   OMGZ=FCOR
      DLOMG=DABS(DLOG(ENMAX/OMGZ))
      DOMG=DLOMG/NPTS
      OMGL=DLOG(OMGZ)+NPTS*DOMG/2.0 D 0
      OMGST=DEXP(OMGL)

C     PRINT AND PUNCH INPUT DATA
      WRITE(6,4)
    4 FORMAT('1',15X,'**INTERNAL WAVE DISPERSION IN FLUID OF MANY LAYERS
     1, EACH WITH CONSTANT VAISALA FREQUENCY**',//,25X,'USES MATRIX M TH
     2OD SIMILAR TO THAT OF HASKELL TO SET UP PERIOD EQUATION',/,40X,
     3 'SOLVES BY ITERATION OF KAPPA FOR A GIVEN OMEGA',//)
      WRITE(6,98) DATE,ALTDG,ALTMN,ALNDG,ALNMN
   98 FORMAT(T45,'*DATE AND POSITION OF MODEL*',/,T10,'YEAR',F6.0,3X,
     1 'MONTH',F4.0,3X,'DAY',F4.0,10X,'LATITUDE',F7.0,' DEG',F4.0,' MIN'
     6 ,10X,'LONGITUDE',F7.0,' DEG',F4.0,' MIN',//)
      WRITE(6,5) FCOR,OMGST,AKAST,NLAY,NMODE
    5 FORMAT(/,10X,'CORIOLIS PARAMETER =',D12.5,5X,'STARTING OMEGA =',
     1 D12.5,5X,'STARTING KAPPA =',D12.5,/,20X,'NUMBER OF LAYERS USED IN
     2 MODEL =',I3,5X,'NUMBER OF MODES TO BE CALCULATED =',I2,/)
      ZFCOR=FCOR
      ZDNSB=DENSB
      ZLAY=NLAY
      WRITE(7,97) DATE,ALTDG,ALNDG,ZFCOR,ZDNSB,ZLAY
   97 FORMAT(5F6.1,3E13.6)
      WRITE(6,6)
    6 FORMAT(/,T20,'THICKNESS OF LAYER',T69,'TOP DENS. OF LAYER',T100,
     1 'LAYER VAISALA',/,T2,'LAYER NO.',T19,'IN CM.',T37,'IN FT.',T73,
     2 'IN GM./C.C.',T91,'FREQ. IN 1/SEC.',T108,'PER. IN MIN.')
      DO 223 I=1,NLAY
      THKFT(I)=THKNS(I)/(12.0 D 0*2.540005 D 0)
      ZEN(I)=EN(I)
  223 ENPRMN(I)=2.0 D 0*PI/(EN(I)*60.0 D 0)
      WRITE(6,7) (I,THKNS(I),THKFT(I),DENS(I),EN(I),ENPRMN(I),I=1,NLAY)
    7 FORMAT(T4,I3,T14,D13.6,T32,D13.6,T70,D17.10,T91,D13.6,T108,D13.6)
      WRITE(6,107) DENS(NLAY1)
  107 FORMAT(T70,D17.10)
      WRITE(7,94) (THKNS(I),DENS(I),ZEN(I),I=1,NLAY)
   94 FORMAT(2(F12.2,F12.7,E16.8))

      MODE=1
      NPTN=0

C     FIND KAPPA FOR OMGST    MP=1 FOR SOLUTIONS .GT. OMGST
   25 OMG=OMGST
      NPTN=0
      MP=1
      CALL ROOTS(NLAY,OMG,FCOR,RTS,ABRT,EN)
      CALL FRSTK(AKAST,AKPMN,AKAP,OMG,AKFSH,TF,DKK,IER,IEND,F)
      IF (IER) 154,26,154
  154 WRITE(6,155) IER
  155 FORMAT(/,T50,'**ERROR RETURN**',/,T55,'IER=',I2,/)
      GO TO 54

C     GET SOLUTIONS ALONG DISPERSION CURVE
   26 OMG1=OMG
      AKAST=AKAP
   27 AKAP1=AKAP
      F1=F
      OMGL2=DLOG(OMG1)+DOMG*0.C5 D 0
      OMG2=DEXP(OMGL2)
```

```
      IF (OMG2-ENMAX) 127,30,30
  127 CALL ROOTS(NLAY,OMG2,FCOR,RTS,ABRT,EN)
      CALL SLVPE(OMG2,AKAP,TF,DKK,IER,IEND,F)
      IF (IER) 37,28,37
   28 AKAP2=AKAP
      F2=F
      OMG=(OMG1+OMG2)/2.0 D 0
      AKAP=(AKAP1+AKAP2)/2.0 D 0
      U=(OMG1-OMG2)/(AKAP1-AKAP2)
      NPTN=NPTN+1
      IF (NPTM .LT. NPTN) NPTM=NPTN
      SOL(MODE,NPTN,1)=OMG
      SOL(MODE,NPTN,2)=AKAP
      SOL(MODE,NPTN,3)=U
      SOL(MODE,NPTN,4)=(F1+F2)/2.0 D 0
      OMGNL=DLOG(OMG)+MP*DOMG
      OMG1=DEXP(OMGNL)
C     IF OMEGA=ENMAX, FIND SOLUTIONS .LT. OMGST
      IF (OMG1-ENMAX) 32,30,30

C     MP=-1 FOR SOLUTIONS .LT. OMGST
   30 MP=-1
      NPTA=NPTN
      OMG=OMGST
      OMGNL=DLOG(OMG)+MP*DOMG
      OMG1=DEXP(OMGNL)
      U=SOL(MODE,1,3)
      AKAP=AKAST

C     USE SLOPE OF DISPERSION CURVE TO GUESS KAPPA OF NEXT OMEGA
   32 IF (OMG1-FCOR) 38,38,34
   34 AKAP=AKAP+(OMG1-OMG)/U
      CALL ROOTS(NLAY,OMG1,FCOR,RTS,ABRT,EN)
      CALL SLVPE(OMG1,AKAP,TF,DKK,IER,IEND,F)
      IF (IER) 37,27,37
   37 IF (MP) 38,54,30

C     REARRANGE SOLUTION IN ORDER OF INCREASING OMEGA
   38 NPTB=NPTN-NPTA
      DO 42 I=1,NPTB
      J=NPTN-I+1
      DO 42 K=1,4
   42 ARNG(I,K)=SOL(MODE,J,K)
      DO 44 I=1,NPTA
      J=NPTB+I
      DO 44 K=1,4
   44 ARNG(J,K)=SOL(MODE,I,K)
      DO 46 I=1,NPTN
      DO 46 J=1,4
   46 SOL(MODE,I,J)=ARNG(I,J)

C     PRINT SOLUTION
      WRITE(6,8) MODE
    8 FORMAT(/////,50X,'* MODE NUMBER',I3,' *',//,T6,'OMEGA',T19,'KAPPA'
     1,T29,'GROUP VEL U',T42,'PHASE VEL C',T57,'PERIOD',T70,'PERIOD',T81
     2,'WAVE LENGTH',T94,'WAVE LENGTH',T111,'F12',/,T5,'(1/SEC)',T17,
     3 '(1/CM)',T30,'(CM/SEC)',T43,'(CM/SEC)',T58,'(SEC)',T71,'(MIN)',
     4 T85,'(CM)',T98,'(FT)',/)
      DO 50 I=1,NPTN
      C=SOL(MODE,I,1)/SOL(MODE,I,2)
      PER=2.0 D 0*PI/SOL(MODE,I,1)
```

```
      PERM=PER/60.0 D 0
      WL=2.0 D 0*PI/SOL(MODE,I,2)
      WLFT=WL/(2.540005 D 0*12.0 D 0)
   50 WRITE(6,10) (SOL(MODE,I,J),J=1,3),C,PER,PERM,WL,WLFT,SOL(MODE,I,4)
   10 FORMAT(9E13.5)

C     TEST IF MORE MODES WANTED
      IF (MODE-NMODE) 52,54,54
   52 MODE=MODE+1
      AKPMN=AKPMN+AKAST
      GO TO 25

C     PUNCH SOLUTION ON CARDS
   54 NPTSS=NPTS+1
      WRITE (7,93) ((SOL(I,J,K),K=1,3),I=1,NMODE),J=1,NPTSS)
   93 FORMAT(3E13.6,2X,3E13.6)
      GO TO 200
 1000 CALL EXIT
      END
```

```
      SUBROUTINE FRSTK(AKAST,AKPMN,AKAP,OMG,AKFSH,TF,DKK,IER,IEND,F)
C        FINDS SMALLEST KAPPA GREATER THAN THAT SPECIFIED THAT SOLVES PERIOD EQ.
      IMPLICIT REAL*8 (A-H,O-Z)
    1 AKAP=AKAST
      CALL SLVPE(OMG,AKAP,TF,DKK,IER,IEND,F)
      IF (IER) 4,2,4
    2 IF (AKAP-AKPMN) 4,4,8
    4 AKAST=5.0 D 0*AKAST
      IF (AKAST-AKFSH) 1,1,17
    8 AKAST=AKPMN+0.2 D 0*(AKAST-AKPMN)
      DO 15 I=1,5
      AKAP=I*AKAST
      CALL SLVPE(OMG,AKAP,TF,DKK,IER,IEND,F)
      IF (IER) 15,10,15
   10 IF (AKAP-AKPMN) 15,15,17
   15 CONTINUE
   17 IER=2
   18 RETURN
      END
```

```
      SUBROUTINE MAX(AMAX,A,N)
      REAL*8 AMAX,B,A(1)
      AMAX=A(1)
      DO 10 I=2,N
      B=A(I)
      IF (AMAX .LT. B) AMAX=B
   10 CONTINUE
      RETURN
      END
```

```
      SUBROUTINE SLVPE(OMG,AKAP,TF,DKK,IER,IEND,DEL)
C     FINDS A KAPPA FOR GIVEN OMEGA THAT SOLVES PERIOD EQ.  USES DELPE TO TEST
C     KAPPA
      IMPLICIT REAL*8 (A-H,O-Z)
      IER=0
      HDKK=DKK
      TOL=TF/1.0 D 3
      CALL DELPE(OMG,AKAP,DEL,DF,DKK,IER)
      IF (IER .GT. 0E GO TO 20
      DO 10 I=1,IEND
      IF (DF) 5,2,5
    2 DKK=2.0 D 0 *DKK
      GO TO 35.
    5 DK=2.0 D 0 *DKK*AKAP*DEL/DF
      IF (DABS(DEL)-DABS(DF/2.0 D 0)) 12,15,15
   12 DKK=DKK/5.0 D 0
      IF (DKK-0.5 D-15) 40,32,32
   15 DK=0.8 D 0*DK
      DKA=DABS(0.5 D 0*DK/AKAP)
      IF (DKA .LT. DKK) DKK=DKA
      IF (DKK-0.15 D-14) 40,22,22
   22 IF (DABS(DK/AKAP)-1.0 D 0) 32,25,25
   25 IF (DK) 30,30,27
   27 AKAP = AKAP/3.0 D 0
      GO TO 35
   30 AKAP=2.0 D 0*AKAP
      GO TO 35
   32 AKAP=AKAP-DK
   35 CALL DELPE(OMG,AKAP,DEL,DF,DKK,IER)
      IF (IER .GT. 0E GO TO 20
      TOLF=TOL*AKAP
      IF (DKK-1.0 D-10) 38,38,10
   38 IF (DABS(DEL)-TOLF) 20,20,10
   10 CONTINUE
C     ERROR RETURN  NO SOLUTION WITHIN TOLERENCES AFTER IEND TIMES THRU LOOP
      IER=1
      GO TO 20
   40 TOLR=TF*AKAP
      IF (DABS(DEL)-TOLR) 20,20,45
C     ERROR RETURN  SOLUTION NOT WITHIN TOLERENCES
   45 IER=3
   20 DKK=HDKK
      RETURN
      END
```

```
      SUBROUTINE DELPE(OMG,AKAP,DEL,DF,DKK,IER)
C        FINDS DELTA FOR PERIOD EQ.  F(1,2)=DELTA, WHICH WE WANT =0
C   F=A(N)A(N-1)...A(1), A= 2 BY 2 MATRIX
      IMPLICIT REAL*8 (A-H,O-Z)
      DIMENSION A(2,2),B(2,2),F(2,2),F12(2)
      COMMON EN(50),D(50),NLAY
      COMMON/FIXUP/FCOR,RTS(50),ABRT(50)
      ROOT=RTS(NLAY)
      SROOT=ABRT(NLAY)
      DJ=D(NLAY)
      AKAP=AKAP*(1.0 D 0-DKK)
      DO 100 II=1,2
      CALL AMTRX(ROOT,AKAP,DJ,F,SROOT,IER)
      N=NLAY-1
      DO 15 I=1,N
      J=NLAY-I
      DI=D(J)
      RJOT=RTS(J)
      SRJOT=ABRT(J)
      CALL AMTRX(RJOT,AKAP,DI,A,SRJOT,IER)
      DO 10 K=1,2
      DO 10 L=1,2
   10 B(K,L)=F(K,L)
      DO 15 K=1,2
      DO 15 L=1,2
   15 F(K,L)=B(K,1)*A(1,L)+B(K,2)*A(2,L)
      F12(II)=F(1,2)
  100 AKAP=AKAP*(1.0 D 0+DKK)/(1.0 D 0-DKK)
      DEL=(F12(1)+F12(2))/2.0 D 0
      AKAP=AKAP*(1.0 D 0-DKK)/((1.0 D 0+DKK)*(1.0 D 0+DKK))
      DF=(F12(2)-F12(1))
      RETURN
      END
```

```
      SUBROUTINE ROOTS(NLAY,OMG,FCOR,RTS,ABRT,EN)
C   CALCULATES ROOTS IN EACH LAYER
      REAL*8 OMG,FCOR,RTS(1),ABRT(1),EN(1)
      DO 10 I=1,NLAY
      RTS(I)=(OMG*OMG-EN(I)*EN(I))/(OMG*OMG-FCOR*FCOR)
   10 ABRT(I)=DSQRT(DABS(RTS(I)))
      RETURN
      END
```

```
      SUBROUTINE ANTRX(ROOT,AKAP,D,A,SROOT,IER)
C        FINDS MATRIX ELEMENTS FOR INTERNAL WAVES IN LAYERED FLUID USING HASKEL
C    METHOD
      REAL*8 ROOT,AKAP,D,SROOT,EM,EMD,ET,A(2,2)
      EM=AKAP*SROOT
      EMD=EM*D
      IF (ROOT) 10,10,15
   10 A(1,1)=DCOS(EMD)
      A(1,2)=DSIN(EMD)/EM
      A(2,1)=-EM*EM*A(1,2)
      GO TO 20
   15 IF (EMD .GT. 1.74 D 2) GO TO 25
      ET=DEXP(EMD)
      A(1,1)=(ET+1.0 D 0/ET)/2.0 D 0
      A(1,2)=(ET-1.0 D 0/ET)/(2.0 D 0*EM)
      A(2,1)=EM*EM*A(1,2)
   20 A(2,2)=A(1,1)
      RETURN
   25 IER=5
      RETURN
      END
```

REFERENCES

Berg, C.O., Middle Atlantic states, in Limnology in North America, edited by D.G. Frey, 191-237, University of Wisconsin Press, Madison, 1963.

Birge, E.A. and C. Juday, A limnological study of the Finger Lakes of New York, Bull. U.S. Bur. Fish., 32, 525-609, 1914.

Birge, E.A. and C. Juday, Further limnological observations on the Finger Lakes of New York, Bull. U.S. Bur. Fish., 37, 209-252, 1922.

Defant, F., Local winds, in Compendium of Meteorology, edited by T.F. Malone, 655-672, Waverly Press, Baltimore, 1951.

Haskell, N.A., The dispersion of surface waves on multilayered media, Bull. Seism. Soc. Am., 43, 17-34, 1951.

Henson, E.B., Evidence of internal wave activity in Cayuga Lake, New York, Limnol. Oceanogr., 4, 441-447, 1959.

Henson, E.B., A.S. Bradshaw and D.C. Chandler, The physical limnology of Cayuga Lake, New York, Cornell Univ. Agr. Expt. Sta., Mem. No. 378, 1-63, 1961.

Hutchison, G.E. A Treatise on Limnology, Volume 1 - Geography, Physics, and Chemistry, John Wiley and Sons, New York, 1957.

Kadomtsev, B.B. and V.I. Karpman, Nonlinear waves, Soviet Physics Uspekhi, 14, 40-60, 1971.

Korteweg, D.J. and G. de Vries, On the change of form on a new type of long stationary wave, Phil. Mag. (V), 39, 422-443, 1895.

Mortimer, C.H., The response of stratified lakes to wind, Schweiz. Zeitschr. Hydrol., 15, 94-151, 1953.

Mortimer, C.H., Some effects of the earth's rotation on water movements in stratified lakes. Proc. Intern. Assoc. Theor. Appl. Limnol., 12, 66-77, 1955.

Neumann, G. and W.J. Pierson, Jr., Principles of Physical Oceanography, Prentice-Hall, Englewood Cliffs, New Jersey, 1966.

Peregrine, D.H., Calculations of the development of an undular bore, J. Fluid Mech., 25, 321-330, 1966.

Phillips, O.M., The Dynamics of the Upper Ocean, Cambridge University Press, Cambridge, 1966.

Thorpe, S.A., On standing internal gravity waves of finite amplitude, J. Fluid Mech., 32, 489-528, 1968A.

Thorpe, S.A., A method of producing a shear flow in a stratified fluid, J. Fluid Mech., 32, 693-704, 1968B.

Thorpe, S.A., Asymmetry of the internal seiche in Loch Ness, Nature, 231, 306-308, 1971.

Von Engeln, O.D., The Finger Lakes Region: Its Origin and Nature, Cornell University Press, Ithaca, New York, 1961.

Watson, E.R., Movements of the waters of Loch Ness as indicated by temperature observations, Geogr. Jour., 24, 430-437, 1904.

Wedderburn, E.M., The temperature of the fresh-water lochs of Scotland with special reference to Loch Ness, Trans. Roy. Soc. Edinburgh, 45, 407-489, 1907.

Wedderburn, E.M., Temperature observations in Loch Garry (Invernesshire), Proc. Roy. Soc. Edinburgh, 29, 98-135, 1909.

Wedderburn, E.M., The temperature seiche, I: Temperature observations in Madüsee, Pomerania, II: Hydrodynamical theory of temperature oscillations in lakes, III: Calculation of the period of the temperature seiche in the Madüsee, Trans. Roy. Soc. Edinburgh, 47, 619-636, 1911.

Wedderburn, E.M., Temperature observations in Loch Earn, with a further contribution to the hydrodynamical theory of the temperature seiche, Trans. Roy. Soc. Edinburgh, 48, 629-695, 1912.

Wedderburn, E.M. and A.M. Williams, The temperature seiche, IV: Experimental verification of the hydrodynamical theory of temperature seiches, Trans. Roy. Soc. Edinburgh, 47, 636-642, 1911.

Witting, J., Fairly-long water waves, CRC Critical Reviews in Solid State Sciences, 2, 555-581, 1972.

ACKNOWLEDGEMENTS

This investigation was supported by the Office of Naval Research under contract N00014-67-A-0108-0016. The facilities on Seneca Lake were maintained by the Naval Underwater Systems Center, Systems Measurement Branch in Dresden, New York. The assistance, freely given by the personnel of NUSC,SMB, especially Gordon Hanson, the director, and Carl Schadt, is greatly appreciated. Werner Tiemann was of help in the digitization of the 1968 data. Barry Allen was of great help in the installation and maintenance of the expanded system employed in 1971. It was Dr. James Witting who directed the author to non-linear wave theory and special thanks is hereby given. The author specifically thanks Dr. Kenneth Hunkins, under whose supervision this study was undertaken, for his early recognition of the importance of the phenomena observed in Seneca Lake and his determination to complete the study with the limited amount of funds available.